Strategies to Improve Solid Phase Microextraction Sensitivity: Temperature, Geometry and Sorbent Effects

by

Ruifen Jiang

A thesis

presented to the University of Waterloo

in fulfillment of the

thesis requirement for the degree of

Doctor of Philosophy

in

Chemistry

Waterloo, Ontario, Canada, 2013

AUTHOR'S DECLARATION

I hereby declare that I am the sole author of this thesis. This is a true copy of the thesis, including any required final revisions, as accepted by my examiners.

I understand that my thesis may be made electronically available to the public.

Abstract

Solid phase microextraction (SPME) has been widely used in a variety of sample matrices and proven to be a simple, fast and solvent-free sample preparation technique. A challenging limitation in the further development of this technique has been the insufficient sensitivity for some trace applications. This limitation lies mainly in the small volume of the extraction phase. According to the fundamentals of SPME, different strategies can be employed to achieve higher sensitivity for SPME sampling. These include cooling down the extraction phase, preparing a high capacity particle-loading extraction phase, as well as using a thin film with high surface area-to-volume ratio as the extraction phase. In this thesis, four sampling approaches were developed for high sensitivity sampling by employing cold fiber, thin film, cooling membrane and particle loading membrane as sampling tools. These proposed methods were applied to liquid, solid and particularly trace gas analysis.

First, a fully automated cold fiber device that improves the sensitivity of the technique by cooling down the extraction phase was developed. This device was coupled to a GERSTEL® MultiPurpose Sampler (MPS 2), and applied to the analysis of volatiles and semi-volatiles in aqueous and solid matrices. The proposed device was thoroughly evaluated for its extraction performance, robustness, reproducibility and reliability by gas chromatograph/mass spectrometer (GC/MS). The evaluation of the automated cold fiber device was carried out using a group of compounds characterized by different volatilities and polarities. Extraction efficiency and analytical figures of merit were compared to commercial SPME fibers. In the analysis of aqueous standard samples, the automated cold fiber device showed a significant improvement in extraction efficiency when compared to commercial polydimethylsiloxane (PDMS) and non-cooled cold fiber. This was achieved due to the low temperature of the coating during sampling.

Results from the cold fiber and commercial divinylbenzene/carboxen/polydimethylsiloxane (DVB/CAR/PDMS) fiber analysis of solid sample matrices were obtained and compared. Results demonstrated that the temperature gap between the sample matrix and the coating significantly improved the distribution coefficient, and consequently, the extraction amount. The newly automated cold fiber device presents a platform for headspace analysis of volatiles and semi-volatiles for a large number of samples, with improved throughput and sensitivity.

Thin film microextraction (TFME) improves the sensitivity by employing a membrane with a high surface area-to-volume ratio as the extraction phase. In Chapter 3, a simple non-invasive sample preparation method using TFME is proposed for sampling volatile skin emissions. Evaluation experiments were conducted to test the reproducibility of the sampling device, the effect of the membrane size, and the method for storage. Results supported the reproducibility of multi-membrane sampling, and demonstrated that sampling efficiency can be improved using a larger membrane. However, ability to control the sampling environment and time was proved to be critical in order to obtain reliable information; the *in vivo* skin emission sampling was also influenced by skin metabolism and environmental conditions. Next, the method of storage was fully investigated for the membrane device before and after sampling. This investigation of storage permitted the sampling and instrument analysis to be conducted at different locations. Finally, the developed skin sampling device was applied in the identification of dietary biomarkers after garlic and alcohol ingestion. In this experiment, the previously reported potential biomarkers dimethyl sulphone, allyl methyl sulfide and allyl mercaptan were detected after garlic intake, and ethanol was detected after the ingestion of alcohol. Experiments were also conducted in the analysis of volatile organic compounds (VOCs) from upper back, forearm and back thigh of the body on the same individual. Results showed that 27 compounds can be

detected from all of the 3 locations. However, these compounds were quantitatively different. In addition, sampling of the upper back, where the density of sebaceous glands is relatively high, detected more compounds than the other regions.

In Chapter 4, a novel sample preparation method that combines the advantages of cold fiber and thin film was developed to achieve the high extraction efficiency necessary for high sensitivity gas sampling. A cooling sampling device was developed for the thin film microextraction. Method development for this sampling approach included evaluation of membrane temperature effect, membrane size effect, air flow rate and humidity effect. Results showed that high sensitivity for equilibrium sampling can be achieved by either cooling down the membrane and/or using a large volume extraction phase. On the other hand, for pre-equilibrium extraction, in which the extracted amount was mainly determined by membrane surface area and diffusion coefficient, high sensitivity was obtained by thin membranes with a large surface area and/or high sampling flow rate. In addition, humidity evaluations showed no significant effect on extraction efficiency due to the absorption property of the liquid extraction phase. Next, the limit of detection (LOD) and reproducibility of the developed cooling membrane gas sampling method were evaluated. LOD with a membrane radius of 1 cm at room temperature sampling were 9.24 ng/L, 0.12 ng/L, 0.10 ng/L for limonene, cinnamaldehyde and 2-pentadecanone, respectively. Intra- and inter-membrane sampling reproducibility had a relative standard deviation (RSD%) lower than 8% and 13%, respectively. Results uniformly demonstrated that the proposed cooling membrane device could serve as a powerful tool for gas in trace analysis.

In Chapter 5, a particle-loading membrane was developed to combine advantages of high distribution coefficient and high surface area geometry, and applied in trace gas sampling. Bar

coating, a simple and easy preparation method was applied in the preparation of the DVB/PDMS membrane. Membrane morphology, particle ratio, membrane size and extraction efficiency were fully evaluated for the prepared membrane. Results show that the DVB particles are uniformly distributed in the PDMS base. The addition of a DVB particle enhanced the stiffness of the membrane to some extent, and improved the extraction capacity of the membrane. Extraction capacity for benzene was enhanced by a factor of 100 when the membrane DVB particle ratio increased from 0% to 30%. Additionally, the prepared DVB/PDMS membrane provided higher extraction efficiency than pure PDMS membrane and DVB/PDMS fiber, especially for highly volatile and polar compounds. The high reproducibility of the prepared DVB/PDMS membrane in air sampling demonstrated the advantage of the bar coating preparation method, and also permitted quantitative analysis. Last, the prepared particle-loading membrane was applied to semi-quantitative and quantitative analysis of indoor and outdoor air, respectively. Both the equilibrium calibration method and diffusion-based calibration method were proposed for the quantitative analysis. Results showed that the high capacity particle-loading membrane can be used for monitoring trace analytes such as perfume components and air pollutants.

Acknowledgements

I would like to thank my supervisor, Professor Janusz Pawliszyn, for this research opportunity and his on-going support during my studies.

I would also like to thank my committee members, Professors Mike Chong, Wojciech Gabryelski, Tadeusz Gorecki for their time and helpful guidance in preparation of this thesis. I would like to extend my sincere gratitude to my external examiner, Dr. Zoltan Mester, and my internal examiner Professor Mark Servos for their invaluable time and commitment to serve on my examination committee.

I extend a sincere thank you to all my colleagues and collaborators throughout the years.

This thesis would never have been possible without support of my family and friends. Thank you for your love and understanding.

Dedication

To my parents and sisters, for their love, support and encouragement.

Table of contents

AUTHOR'S DECLARATION ii

Abstract iii

Acknowledgements vii

Dedication viii

List of figures xiv

List of tables xviii

List of abbreviations xix

List of symbols xxi

Preamble xxiii

Chapter 1 Introduction of Solid Phase Microextraction 1

1.1 Analytical process 1

1.2 Sample preparation 2

1.3 Solid phase microextraction (SPME) 6

1.3.1 The configuration of commercial SPME 6

1.3.2 The principles of SPME 8

1.3.3 The application of SPME 10

1.3.3.1 SPME for gas sampling 10

1.3.3.2 SPME for solid sampling 15

1.3.3.3 SPME for aqueous sampling 16

1.3.4 Strategies on improvement of SPME sensitivity 17

1.3.4.1 Increase of the distribution coefficient (Kes) 17

1.3.4.2 Increase of the volume of the extraction phase (Ve) 21

1.3.4.3 Increase of both Kes and Ve simultaneously 26

1.3.5 The calibration methods of SPME 26

1.4 The objectives of the thesis 32

Chapter 2 Fully Automated Cold Fiber Device for High Throughput Sample Preparation 34

2.1 Introduction 34

2.1.1 Miniaturization of the cold fiber device 34

2.1.2 Principle of cold fiber SPME 36

2.1.3 Limitations of the previous automated cold fiber 37

2.1.4 The objective of this project 38

2.2 Experimental 38

2.2.1 Reagents and supplies 38

2.2.2 Instrumentation 40

2.2.3 Experimental procedure 41

2.3 Results and discussion 43

2.3.1 Modification of the automated cold fiber device 43

2.3.2 Evaluation of the new automated cold fiber device 45

2.3.3 Analyzing factors that affect cold fiber extractions 48

2.3.4 Comparison of extraction efficiency of cold fiber device with commercial PDMS fiber 51

2.3.5 Extraction of analytes from solid matrices using the automated cold fiber device 53

2.3.6 Analytical figures of merit 55

2.4 Summary 56

Chapter 3 Development of a Non-invasive and Convenient Method for Skin Volatile Compounds Sampling 58

3.1 Introduction 58

3.1.1 Significance of skin volatile compounds sampling 58

3.1.2 Traditional methods for skin volatiles sampling and their limitation 58

3.1.3 Advantages of TFME for skin volatiles sampling 60
3.1.4 The motivation and objective of the current work 62
3.2 Experimental 62
3.2.1 Reagents and supplies 62
3.2.2 Instrumentation 63
3.2.3 In vivo set-up for thin film sampling of skin volatiles 65
3.2.4 In vial sampling set-up for evaluation of thin film skin volatiles sampling 66
3.3 Results and discussion 67
3.3.1 Reproducibility of the sampling of skin volatile compounds 67
3.3.2 Comparison between headspace and direct contact sampling 70
3.3.3 Effect of membrane size 72
3.3.4 Storage method evaluation 73
3.3.5 Dietary biomarker for garlic and alcohol intake 75
3.3.6 Comparison of the skin emissions from different areas of the body 78
3.4 Summary 81
Chapter 4 Development of a Cooling Membrane Approach for High Sensitivity Gas Sampling 82
4.1 Introduction 82
4.2 Experimental 86
4.2.1 Reagents and supplies. 86
4.2.2 Instrumentation 86
4.2.3 Standard gas generator 88
4.2.4 Construction of the cooling membrane device 92
4.3 Results and discussion 94
4.3.1 Evaluation of the cooling membrane device 94

4.3.2 Extraction time profile for the cooling membrane sampling 96
4.3.3 Effect of membrane size and temperature 97
4.3.4 Effect of sampling flow rate 99
4.3.5 Effect of sampling gas humidity 101
4.3.6 The limit of detection 102
4.3.7 Real sample analysis 103
4.4 Summary 103
Chapter 5 Preparation of a Particle Loading Membrane for Trace Gas Sampling 106
5.1 Introduction 106
5.2 Experimental 111
5.2.1 Reagents and supplies 111
5.2.2 Instrumentation 111
5.2.3 Standard gas generator 112
5.2.4 Particle loading membrane preparation 114
5.2.5 Experimental procedure 117
5.3 Results and discussion 118
5.3.1 Evaluation of the prepared DVB/PDMS membrane 118
5.3.1.1 Morphology of the prepared membrane 118
5.3.1.2 Effect of particle ratio on extraction efficiency 119
5.3.1.3 The analytical figures of merit 120
5.3.1.4 Effect of membrane size 122
5.3.1.5 Comparison of the extraction efficiency of the DVB/PDMS membrane with PDMS membrane and DVB/PDMS fiber 123
5.3.2 Semi-quantitative air sampling 126
5.3.3 Quantitative air sampling 130

5.3.3.1 Loss and storage evaluation 131
5.3.3.2 The extraction time profiles for the target compounds 132
5.3.3.3 The equilibrium calibration method for volatile compounds 133
5.3.3.4 The Pre-equilibrium calibration methods for semi-volatile compounds 134
5.3.3.5 Real sample anlaysis 138
5.4 Summary 140
Chapter 6 Summary and Future Perspectives 142
References 146
Appendix 154

List of figures

Figure 1.1 Classification of extraction techniques. 6

Figure 1.2 The configuration of the commercial SPME fiber 7

Figure 1.3 The SPME operation modes: (a) DI-SPME; (b) HS-SPME; and (c) HM-SPME [16]. Figure reprinted from reference with permission of publisher. 8

Figure 1.4 Universal extraction time profile for agitated sample of infinite volume, when the boundary layer controls the extraction rate. 10

Figure 1.5 Schematic of sampling with exposed (for spot sampling) and retracted (for TWA sampling) SPME fibers [24]. Figure reprinted from reference with permission of publisher. 11

Figure 1.6 Comparison of the extraction time profiles of toluene at 1 ppb with the use of 65 μm PDMS/DVB and 100 μm PDMS fibers [32]. Figure reprinted from reference with permission of publisher. 12

Figure 1.7 The temperature profiles of headspace sampling naphthalene-spiked silica gel using (a) DVB/CAR/PDMS fiber, (b) cold fiber with coating temperature of 40 ℃. The sample matrix was prepared by spiking 100 ng naphthalene into 2 g silica gel. 16

Figure 1.8 Coating selection guide 19

Figure 1.9 Comparison of cold fiber with and without cooling for vial seal air sampling [54]. Figure reprinted from reference with permission of publisher. 21

Figure 1.10 The time profiles of fluoranthene by thin film and Twister sampling [62]. Figure reprinted from reference with permission of publisher. 23

Figure 1.11 Various application of TFME. (A) Breath analysis [59]; (B) Active water sampling [69]; (C) Thin film passive sampler [60]; (D) Skin sampling. 25

Figure 2.1 The configuration of cold fiber [54]. Figure reprinted from reference with permission of publisher. 35

Figure 2.2 The configuration of the automated cold fiber device [30]. Figure reprinted from reference with permission of publisher. 36

Figure 2.3 The configuration of GERSTEL SLH injector. (Picture from Gersetel® website) 41

Figure 2.4 Comparison of cold fiber SLH and conventional SLH. 44

Figure 2.5 The stability of SLH for cold fiber injection 45

Figure 2.6 The cold fiber extraction time profiles of 2-heptanone with three different combinations of sampling temperatures. Aqueous solution: 1 µL working solution #1 was spiked into 3 mL ultrapure water. 2-heptanone total spiked amount was 145.3 ng 49

Figure 2.7 Extraction temperature profile of (A) cold fiber and (B) DVB/CAR/PDMS fiber for aqueous sampling. Cold fiber coating temperature, 35 ℃. Aqueous solution: 1 µL working solution #2 was spiked into 3 mL ultrapure water. 51

Figure 2.8 Comparison of extraction amount of cold fiber, cold fiber without cooling and commercial PDMS fiber for 14 compounds under the optimized conditions for each fiber. These extractions were performed with a solution spiked with 1 µL working solution #2 into 3 mL ultrapure water. 53

Figure 2.9: Extraction temperature profile of 7 PAHs in silica gel samples using (A) cold fiber device and (B) DVB/CAR/PDMS fiber. Extraction time for cold fiber, 20 min; for DVB/CAR/PDMS, 30 min. Cold fiber coating temperature: 40 ℃ 55

Figure 3.1 The reported headspace sampling holder for skin volatile compounds sampling [146] [85]. Figure reprinted from reference with permission of publisher. 61

Figure 3.2 The diagram of thin film TDU injection, (Figure from GERSTEL® website)..... 64

Figure 3.3 Schematic diagram of the membrane *in vivo* sampling device used for skin volatiles sampling 66

Figure 3.4 The in vial sampling set-up for evaluation of the proposed skin volatiles thin film sampling approach. 67

Figure 3.5 The comparison of the HS (solid line) and direct sampling (dash line) chromatogram from the same area of the skin. 1. octanal; 2. nonanal; 3. decanal; 4. 1-tetradecanol; 5. isopropyl palmitate; 6. 1-octadecanol; 7. squalene. 72

Figure 3.6 Comparison of different storage methods of the sampled membrane. 1. toluene; 2. ethylbenzene; 3. p-xylene; 4. o-xylene; 5. decane; 6. octanal; 7. D-limonene. 74

Figure 3.7 The trends of alcohol amount detected from skin before and after drinking. 77

Figure 4.1 SPME sampling using a gas sampling bulb. 88

Figure 4.2 The syringe pump standard gas generator [35]. 89

Figure 4.3 The configuration of the permeation tube. 89

Figure 4.4 Configuration of the standard gas generator 90

Figure 4.5 The configuration of the cooling membrane device. 93

Figure 4.6 (A) The extraction time profile for three compounds sampled by the cooling membrane device with membrane temperature at 21 ± 0.5 ℃. (B) Comparison of the extraction time profile of limonene at different membrane temperatures. The concentrations of the target compounds in the sampling gas are 635 ng/L, 132 ng/L, 80 ng/L for limonene, cinnamaldehyde and 2-pentadecanone respectively. GC injector, solvent vent/split, 20 mL/min. 97

Figure 4.7 The membrane size effect. The concentrations of the target compounds in the sampling gas are 635 ng/L, 132 ng/L, 80 ng/L for limonene, cinnamaldehyde and 2-pentadecanone respectively. GC injector, solvent vent/split, 20 mL/min. 98

Figure 4.8 The effect of the membrane temperature. The concentrations of the target compounds in the sampling gas are 635 ng/L, 132 ng/L, 80 ng/L for limonene, cinnamaldehyde and 2-pentadecanone respectively. GC injector, solvent vent/split, 50 mL/min 99

Figure 4.9 The gas velocity effect. The concentrations of the target compounds in the sampling gas are 374 ng/L, 27 ng/L, 23 ng/L for limonene, cinnamaldehyde and 2-pentadecanone respectively. GC injector, solvent vent/split, 50 mL/min. 100

Figure 4.10 The effect of gas humidity. The concentrations of the target compounds in the sampling gas are 442 ng/L, 32 ng/L, 41 ng/L for limonene, cinnamaldehyde and 2-pentadecanone respectively. GC injector, solvent vent/split, 50 mL/min. 102

Figure 4.11 Comparison of extraction efficiency of cooling and without cooling for real sample analysis using the cooling membrane device. The sampling time, 3 hours. 1. trichloroethylene; 2. toluene; 3. o-xylene; 4. nonane; 5. decane; 6. limonene; 7. undecane; 8. nonanal; 9. decanal ; 10. undecanal. 105

Figure 5.1 The configuration of the standard gas generator 113

Figure 5.2 Comparison of the particle morphology before and after sonication 115

Figure 5.3 Chromatograms of the membrane blanks prepared by different PDMS 116

Figure 5.4 The home-made air sampling device..... 118

Figure 5.5 The morphology of the prepared particle loading membrane (DVB/PDMS, w/w, 30/100) 119

Figure 5.6 Comparison of the extraction amount of benzene for different particle ratio membranes 120

Figure 5.7 The effect of membrane size on the particle loading membrane..... 123

Figure 5.8 Comparison of the extraction efficiency for three types of extraction phase for outdoor air sampling. (Compounds shown in Table 5.2) 125

Figure 5.9 The desorption profile of benzene and naphthalene. (a) desorbed in standard gas generator with flow rate of 10.6 cm/s; (b) exposed in the environmental air 132

Figure 5.10 Extraction time profiles for benzene and naphthalene from standard gas generator 133

Figure 5.11 The relationship of the adsorption and desorption profiles of benzene and naphthalene 136

Figure 5.12 Monitoring the benzene and naphthalene concentration in traffic air 140

List of tables

Table 1.1 Some applications of SPME for air sampling..... 13

Table 1.2 Physical properties of adsorbents used in SPME fibers 18

Table 1.3 Summary of the literature on TFME [78]..... 25

Table 2.1 Data for 14 analyzed compounds and their standard solutions 39

Table 2.2 Comparison of the peak area repeatability and retention time deviation using different fibers 46

Table 2.3 Comparison of cold fiber aqueous sampling calibration curve linear range and LOD with commercial PDMS and DVB/CAR/PDMS fiber..... 56

Table 3.1 The reproducibility of the skin sampling set-up. 68

Table 3.2 Comparison of the reproducibility of two *in vivo* sampling designs 70

Table 3.3 Compounds detected from three locations of the same individual. 78

Table 4.1 The GC conditions for different experiment..... 87

Table 4.2 The analytical figure of merits of the cooling membrane sampling. 95

Table 4.3 Comparison of the calculated and experimental data 95

Table 5.1 The analytical figures of merit for DVB/PDMS membrane benzene air sampling.... 122

Table 5.2 Compounds detected from the outdoor air 125

Table 5.3 Compounds detected from the chemical storage room..... 128

Table 5.4 Fragrance compounds detected from the indoor air 130

Table 5.5 The log$KC_{e\,max}$ of benzene on 20% DVB/PDMS membrane obtained from different matrices. 134

Table 5.6 Comparison of calculations with experimental results 137

List of abbreviations

AMDIS	Automated Mass Spectral Deconvolution and Identification System
BAC	Blood alcohol concentration
BTEX	Benzene, Toluene, Ethylbenzene , Xylene
C18-PAN	Octadecyl-Polyacrylonitrile
CIS	Cooled injection system
DI	Direct immersion
DVB/CAR/PDMS	Divinylbenzene/carboxen/polydimethylsiloxane
EPA	Environmental Protection Agency
FID	Flame ionization detector
GC/MS	Gas chromatograph
HM	Hollow membrane
HPLC	High performance liquid chromatography
HS	Headspace
IMS	Ion mobility spectrometer
LLE	Liquid liquid extraction
LLME	Liquid liquid microextraction
LOD	Limit of detection
MAE	Microwave-assisted extraction
MIP	molecularly-imprinted polymer
MPS2	MultiPurpose Sampler
MS	Mass spectrometer
NIOSH	National Institution of Occupational Safety and Health
OSHA	Occupational Safety & Health Administration
P&T	Purge & trap
PA	Polyacrylate
PAHs	Poly aromatic hydrocarbon
PCB	Polychlorinated biphenyl

PDMS	Polydimethylsiloxane
PDMS/DVB	Polydimethylsiloxane/divinylbenzene
PFE	Pressured fluid extraction
PTFE	Polytetrafluoroethylene
QC	Quality control
RAM	Restricted access material
RSD%	Percentage of relative standard deviation
SBSE	Stir bar sorptive extraction
SCCM	Standard cubic centimeter per minute
SDME	Single drop microextraction
SEM	Scanning electron microscope
SFE	Supercritical fluid extraction
SLH	Septumless head
SPE	Solid phase extraction
SPME	Solid phase microextraction
TDU	Twister desorption unit
TEC	Thermoelectric cooler
TFME	Thin film microextraction
TWA	Time weighed average
VOCs	Volatile organic compounds

List of symbols

n	Equilibrium extraction amount
$\bar{h}$	Average mass-transfer coefficient
$C_{e\,max}$	Maximum concentration of the active sites on the coating
C_e	Equilibrium concentration of the analyte on the solid coating
C_e^{∞}	Equilibrium concentrations of analyte in the coating
C_p	Constant pressure heat capacity of the analyte
C_s	Concentration of sample matrix
C_s^{∞}	Equilibrium concentration of analyte in the sample matrix
K_{es}	Distribution coefficient
$\overline{Nu}$	Average Nusselt number
P_r	Prandtl number
R_e	Reynolds number
T_f	Fiber temperature
T_s	Sample matrix temperature
V_e	Volume of the extraction phase
V_s	Volume of the sample matrix
$\frac{dn}{dt}$	Initial extraction rate
q_0	Amount of preloaded standard on the extraction phase
$t_{95\%}$ or t_e	Equilibrium extraction time
$b-a$	Thickness of the coating
A	Surface area of the extraction phase
D	Diffusion coefficient
K	Adsorption equilibrium constant (affinity constant) of the analyte

L	Length of the coating;
Q	Amount of the standard remaining on the extraction phase
R	Gas constant
t	Sampling time
u	Linear air velocity
v	Kinetic viscosity for air
δ	Thickness of the boundary layer

Preamble

Two published papers are included in this thesis: (1). R. Jiang, E. Carasek, S. Risticevic, E. Cudjoe, J. Warren, J. Pawliszyn; Evaluation of a completely automated cold fiber device using compounds with varying volatility and polarity; Anal. Chim. Acta. 742 (2012) 22. (2). R. Jiang, J. Pawliszyn; Thin film microextraction --- Another geometry of solid phase microextraction; Trends Anal. Chem. 39 (2012) 245. The articles are reprinted with the permission of Elsevier (see Appendix). The co-authors, Eduardo Carasek, Sanja. Risticevic, Erasmus. Cudjoe, Jamie. Warren authorized Ruifen Jiang to use the material in her thesis.

In addition, figure 1.3, figure 1.5, figure 1.6, figure 1.10, figure 2.2, and figure 3.1 in this thesis were reprinted from the reference with permission of the publishers (see Appendix).

Chapter 1 **Introduction of Solid Phase Microextraction**

1.1 Analytical process

The purpose of an analytical study is to obtain information about a given system. The analytical procedures for complex sample analysis consist of sampling, sample preparation, quantification, statistical evaluation and decision making steps. The sampling step consists of obtaining samples that properly define the object or the problem being characterized, and determining the size of said sample. The second step is sample preparation, which involves sample clean-up and enrichment. Due to the complexity of the matrix, or the low concentration of the substance being studied, original samples often are not ready for direct introduction into the measuring instruments. Thus, the main objectives of the sample preparation step are to isolate the components of interest from the sample matrix, and obtain a suitable preconcentration of the component under study for analysis. Once the sample preparation is complete, the analysis can then be carried out by the instrument of choice, which is chosen depending on the particular information being acquired.

Each analytical step is critical for gathering of precise and informative results, and must be followed in order. Because a new step cannot begin until the preceding one is completed, the slowest step determines the overall speed of the analytical process. It has been found that over two-thirds of analysis time is spent on the sampling and sample preparation steps [1-3]. One of the reasons for slow progress in the sample preparation step is that most of the traditional extraction processes involve multi-step proedures such as homogenization, clean-up, extraction, washing and preconcentration. These steps are difficult to be automated due to the large size of the sample required for analysis; this is particularly true for trace analystes being analyzed.

1.2 Sample preparation

Classical sample preparation techniques can be classified as either exhaustive or non-exhaustive extraction techniques [4]. A breakdown of different techniques available can be found in Figure 1.1. In principle, exhaustive extraction approaches utilize an overwhelming amount of extraction phase to extract all the analytes from the sample matrix. In this way, quantification of the sample matrix concentration can be determined by simply dividing the extracted amount over the sample volume. In order to ensure the complete transfer of analytes into the extraction phase, a large amount of organic solvent or sorbent should be used.

Commonly used exhaustive extraction techniques include liquid-liquid extraction (LLE) and solid phase extraction (SPE) [5, 6]. LLE is a batch extraction technique in which the sample is directly added into a large amount of organic solvent, where the analytes are distributed between the sample matrix and the organic solvent. Due to the high affinity of the organic solvent, most of the analytes are extracted into the organic solvent phase. After extraction, the organic solvent is separated from the sample phase and injected into the analytical instrument for separation and quantification. However, in most cases, due to the use of large amounts of organic solvent, the concentration of the final extracted solution is too low to be directly injected into the instrument. In these cases, an enrichment step, such as evaporation, is required. Although LLE, as a simple sample preparation technique, has been widely applied to a variety of samples, shortcomings such as emulsion formation, large sample volumes and the use of toxic organic solvents make LLE labor intensive, time consuming and environmentally unfriendly. Additionally, an effect due to insufficient clean-up is generally observed when using this technique, since the organic solvent can extract not only the analyte of interest alongside interference components from a sample.

Solid phase extraction was developed to eliminate the use of large amounts of organic solvent in LLE [7]. In this method, a solid extraction phase replaces the organic solvent. The liquid/gas sample passes through the sorbent bed, and the analytes presented in the sample are exhaustively retained on the solid sorbent. Then, unwanted analytes are selectively removed from the solid sorbent by a washing solvent. Finally, the analytes of interest are desorbed by an eluting solution, and the resulting eluent may then be concentrated by evaporation. In comparison to LLE, SPE uses less organic solvent, and includes a clean-up step. However, SPE is a time consuming and multi-step technique which is labor intensive and may cause analyte loss. For trace matrices, a large sample volume is usually required to meet the limit of detection (LOD), since only a few microliters of the final eluent can be injected into the instrument.

Other exhaustive techniques, such as supercritical fluid extraction (SFE), pressured fluid extraction (PFE), purge & trap (P&T) and microwave-assisted extraction (MAE), either require expensive equipment, skillful operation techniques, or are inadequate for on-site sampling and automation.

Alternatively, non-exhaustive approaches utilize a small amount of sorbent as the extraction phase to pick up a small portion of analyte from the sample matrix. Microextraction is a typical non-exhaustive extraction approach. The sample preparation of non-exhaustive extraction addresses the need for a reduction in solvent use and size of extraction device, while also facilitating rapid and convenient sample preparation. In addition, non-exhaustive microextraction causes minimal perturbation to the sample system. In comparison to exhaustive techniques, better characterization and more accurate information about the investigation system or process can be obtained when these microextraction based strategies are applied in monitoring chemical

changes, partitions equilibria and speciation in the investigation system. Furthermore, the miniaturization of the extraction device enables the automation of the technique [8].

Headspace [9], liquid phase microextraction (LPME) [10, 11] and solid phase microextraction (SPME) [12] are frequently reported microextraction techniques. Headspace includes static and dynamic sampling. In particular, the static headspace sampling utilizes a large gas-tight syringe to withdraw a specific volume of headspace vapor from the sample matrix. This technique involves of a simple operation procedure, and easy automation, but lacks the sensitivity necessary for trace analysis, since it does not have an enrichment step during the sampling process. Dynamic headspace employs a syringe with a sorbent trap, and allows vapor gas to be withdrawn in a number of sampling cycles. Thus, the analytes of interest from the headspace vapor are pre-concentrated in the sorbent. When the volume of the trapped sorbent is large, and most of the analytes from the sample matrix are purged and trapped by the sorbent, this technique is an exhaustive extraction technique called purge & trap.

Liquid phase microextraction was developed in the 1990s as an alternative to the miniaturized sample preparation approach [10, 11]. In LPME, a microliter volume of the organic solvent is used to extract analytes from the aqueous/gas samples. Also, this approach overcomes the disadvantages of LLE [13]. Single drop microextraction (SDME) was the first version of developed LPME. In SDME, the organic solvent is suspended on the tip of a syringe and exposed in the sample matrix for extraction. Then, the organic solvent drop is withdrawn into the syringe and directly injected into the instrument after sampling. The disadvantages of this method are the difficulty in manually operating the organic solvent drop and the formation of air bubbles [13]. As a solution to improve the stability and reliability of LPME, Pedersen-Bjergaard and Rasmussen introduced hollow fiber based LPME in 1999 [14]. In hollow fiber liquid-phase

microextraction (HF-LPME), the organic solvent is placed inside a piece of hollow fiber and exposed in the sample matrix during sampling. HF-LPME allows extraction and preconcentration of analytes from complex samples in a simple and inexpensive way, while preventing the loss of organic solvent.

Dispersive liquid–liquid microextraction (DLLME) as another form of LLME was introduced by Assadi and co-workers in 2006 [15]. It is based on the use of a few microliters of extractant, such as high density chlorobenzene, chloroform or carbon disulfide and a disperser solvent with high miscibility in both extractant and aqueous phases, such as methanol, acetonitrile or acetone. When the mixture of extractant and disperser solvent is rapidly injected into the sample, high turbulence is produced. This turbulent regimen gives rise to the formation of small droplets, which are dispersed throughout the aqueous sample. Once a cloudy solution formed, the contact surface area between the extracting solvent and the aqueous sample becomes very large, and the equilibrium state is achieved quickly. The cloudy solution is centrifuged once it reaches the equilibrium state; the high density extracting solvent is deposited in the bottom of a conical tube, and can be separated by a syringe for injection. The advantages of DLLME include simplicity of operation, rapidity, low cost, high recovery, and high enrichment factor. However, DLLME consumes a relatively large amount of dispersive solvent, and is difficult to automate, making it an unsuitable technique for sampling complex matrices.

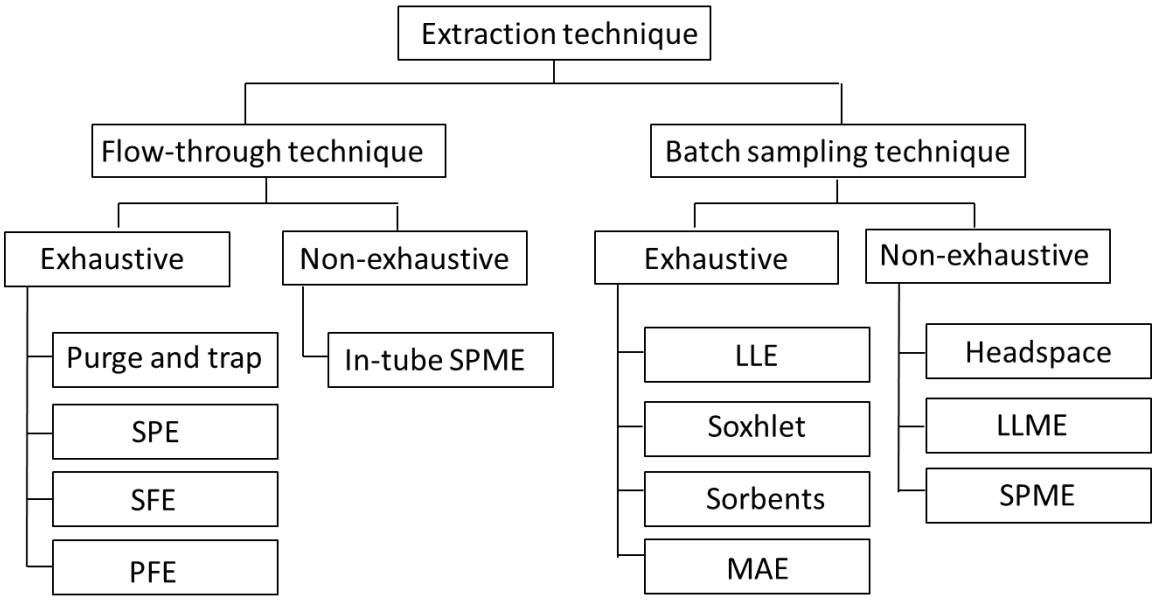

Figure 1.1 Classification of extraction techniques.

1.3 Solid phase microextraction (SPME)

1.3.1 The configuration of commercial SPME

Solid phase microextraction is a microextraction technique that has been rapidly developed in several formats and widely used to date. The originally developed and most commonly used model is the syringe-like fiber geometry [16] in which the extraction phase is coated on a fiber support, such as a fused silica fiber or metal wire (Figure 1.2). The supported fiber is attached to a tube which can be retracted into a protective needle used to pierce the septa. The syringe-like SPME fiber can be mounted on a commercial holder for easy handling. During sampling, the needle pierces through the vial cap septum, and the whole device sits on top of the vial that contains the sample (Figure 1.2). Next, the fiber coating is exposed to the sample or the headspace of the sample for a period of time during extraction. After sampling, the fiber can be directly injected into an analytical instrument such as gas chromatograph (GC) for analysis.

Since the whole device is similar to a syringe, SPME can be easily coupled with different autosamplers, thus become automated.

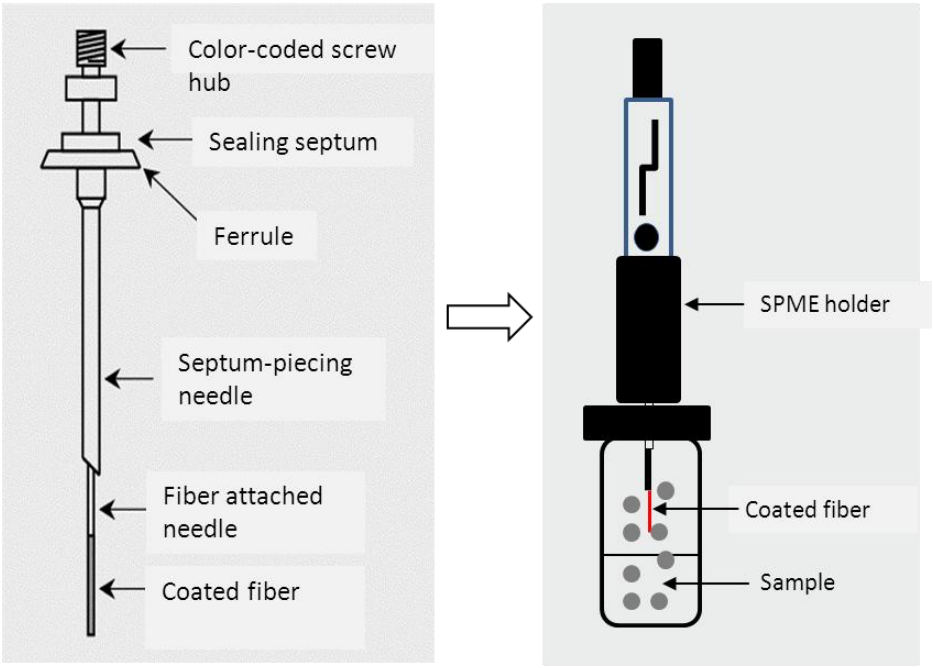

Figure 1.2 The configuration of the commercial SPME fiber

SPME can operate in direct immersion (DI), headspace (HS) and hollow membrane (HM) protection modes [4]. In DI-SPME, the fiber is immersed in the sample matrix and the analytes are transported directly from the sample matrix to the extraction phase. It is worth to note that agitation is normally used to accelerate the extraction rate. For gas samples, a mechanical pump is usually used to generate a high flow rate of sampled air. For aqueous matrices, rapid movement of fiber or vial is applied. In solid samples, sonication is commonly used to accelerate the diffusion of the analytes. The major disadvantage of DI-SPME is fiber contamination from complex sample matrices.

Headspace sampling was introduced to address the challenges associated with DI-SPME sampling; this was done by inserting the fiber into the headspace of the matrix [17]. Headspace

sampling prevents the fiber from coming into direct contact with a dirty sample matrix, which lengthens the lifetime of the fiber. In addition, headspace gas sampling fastens the sampling rate for volatile compounds due to a high diffusion coefficient in the gas phase. However, only relatively volatile analytes that are released in the headspace are extracted. Temperatures are usually used to increase the Henry's law constant so as to increase the concentration in the headspace.

Protective hollow membrane SPME sampling was introduced for samples containing both non-volatile target analytes and high molecular weight interfering compounds, such as humid acids or proteins. This technique is used when direct or headspace SPME is challenging. The major limitation of the HM-SPME is its low diffusion rate, since the analytes need to diffuse through the hollow membrane in order to reach the fiber.

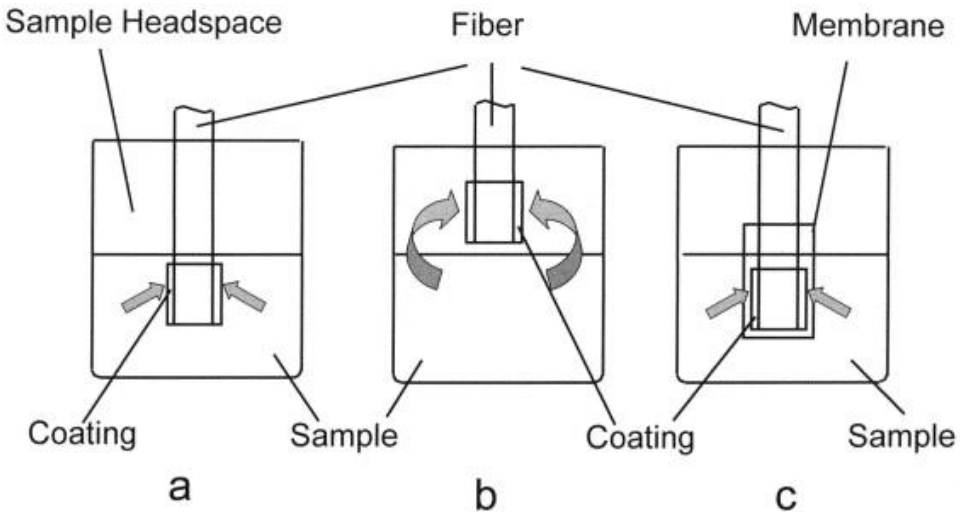

Figure 1.3 The SPME operation modes: (a) DI-SPME; (b) HS-SPME; and (c) HM-SPME [16]. Figure reprinted from reference with permission of publisher.

1.3.2 The principles of SPME

As mentioned above, SPME is a non-exhaustive extraction method. The coating is exposed in the sample matrix for a pre-determined period of time; extraction amount versus extraction

time can be expressed as seen on Figure 1.4. The extraction process is considered complete when the analyte concentration reaches equilibrium between the sample matrix and the coating. For liquid coating direct immersion extraction, the equilibrium extraction amount can be expressed by Equation 1.1. From this equation, we can see that the equilibrium extraction amount (n) is proportional to the distribution coefficient (K_{es}) and the volume of the extraction phase (V_e). In addition, when the volume of the sample matrix (V_s) is large enough, such as when conducting in-field sampling, the equilibrium equation can be simplified into $n = K_{es}V_eC_s$.

$$n = \frac{K_{es}V_eC_sV_s}{K_{es}V_e+V_s}\text{ , }when\ V_s \gg K_{es}V_e\text{ , }n = K_{es}V_eC_s \qquad \text{Equation 1.1}$$

Initial extraction rate and equilibrium extraction time (t_e) are usually used to describe the kinetic of an extraction process. The initial extraction rate of SPME was first derived by Koziel *et al*. [18], who utilized a heat transfer model to describe the mass transfer occurring in the fiber coating. The final formulated mathematical equation (Equation 1.2) shows that when the thickness of the boundary layer is much smaller than the outside radius of the fiber, the initial rate of an extraction process can be expressed by Equation 1.2. As shown, the initial extraction rate ($\frac{dn}{dt}$) is linearly proportional to the surface area of the extraction phase (A) and the diffusion coefficient (D), and inversely proportional to the thickness of the boundary layer (δ). The use of a larger surface area for the extraction phase and more effective agitation methods can enhance the initial extraction rate.

$$\left(\frac{dn}{dt}\right) = (\frac{DA}{\delta})C_st \qquad \text{Equation 1.2}$$

The equilibrium extraction time can be expressed by Equation 1.3. This equation was derived from a theoretical model [19, 20], where boundary layer exists between the coating the

sample matrix. Equilibrium extraction time is expressed as $t_{95\%}$ when the extraction amount reaches 95% of the theoretical equilibrium extraction amount.

$$t_{95\%} = 3 \times \frac{\delta K_{es}(b-a)}{D} \qquad \text{Equation 1.3}$$

Where δ and $b-a$ are the thickness of the boundary layer and the extraction phase respectively. D is the diffusion coefficient of the analyte in the boundary layer and K_{es} is the distribution coefficient. This equation indicates that a thinner extraction phase and effective agitation can shorten the equilibrium time.

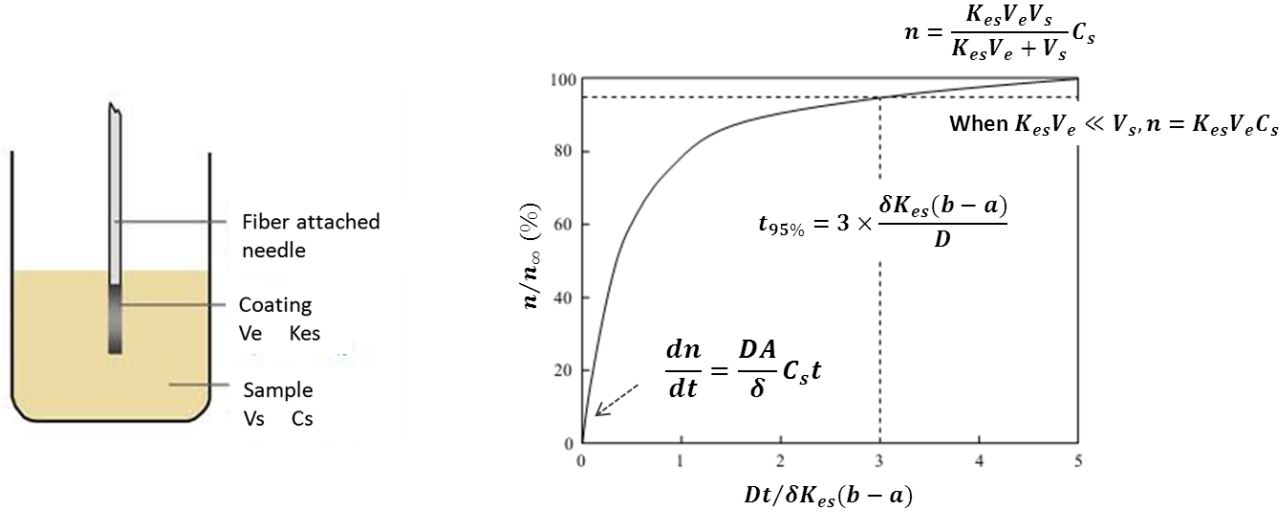

Figure 1.4 Universal extraction time profile for agitated sample of infinite volume, when the boundary layer controls the extraction rate.

1.3.3 The application of SPME

Solid phase microextraction has been widely applied in a variety of sample matrices, including gas [21-24], aqueous [25-28] and solid [29-31], and has proven to be a simple, fast and solvent-free technique.

1.3.3.1 SPME for gas sampling

Solid phase microextraction has been used for spot sampling and time-weighted average (TWA) sampling of air since 1995 (Table 1.1). When using spot sampling, in most cases, the fiber is directly exposed to the air for a short period of time, and then injected into the instrument for analysis. In contrast, for TWA sampling, the fiber is retracted back into the needle for a specific distance during sampling (Figure 1.5) [24]. Analytes presented in the sample matrix diffuse through the needle and are ab/adsorbed by the sorbent. The sampling can last for hours, and even for days; the quantification results represent the average concentration during the sampling period.

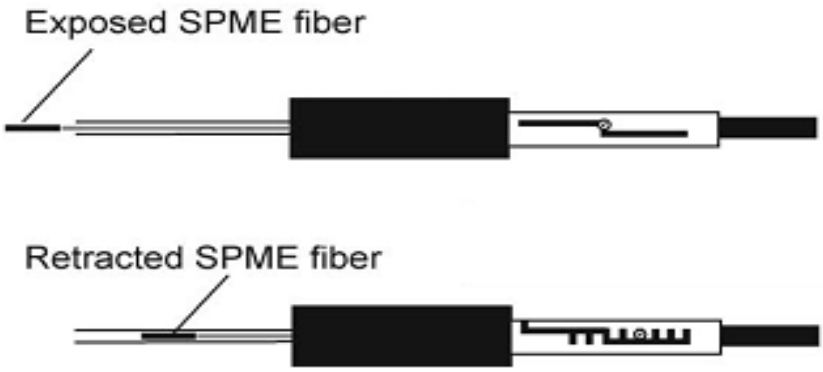

Figure 1.5 Schematic of sampling with exposed (for spot sampling) and retracted (for TWA sampling) SPME fibers [24]. Figure reprinted from reference with permission of publisher.

Polydimethylsiloxane (PDMS) and polydimethylsiloxane/divinylbenzene (PDMS/DVB) coatings are commonly used for air sampling (Table 1.1). The advantages of using a PDMS coating include easy quantification and fast equilibrium. As a liquid coating, PDMS extraction follows the principle of absorption described in the previous section; the equilibrium calibration method can be used for quantification. As well, volatile compounds such as benzene, toluene, ethylbenzene and xylene (BTEX) quickly reach equilibrium in PDMS coating. However, when using solid coatings such as PDMS/DVB, since the extraction mechanism is adsorption,

saturation or displacement could happen when sampling time is too long, or when other high affinity components are present in the sample matrix. Consequently, a pre-equilibrium calibration method is generally applied for solid coating sampling. In addition to the traditional external calibration method [32], Koziel *et al*. [18] and Chen *et al*. [33] proposed two new diffusion based calibration methods for solid coating air-sampling quantification. The major advantage of a solid coating is its affinity towards large range of volatile compounds when compared to PDMS coating. Figure 1.6 compares the extraction time profile of a 65 µm PDMS/DVB coating with a 100 µm PDMS coating in toluene sampling; here, it can be seen that the extraction amount of PDMS/DVB is much higher than the extraction amount of PDMS [32]. Additionally, Figure 1.6 demonstrates how the equilibrium time for a solid coating is longer than the equilibrium time for a liquid coating. Long equilibrium time provides capability of TWA sampling.

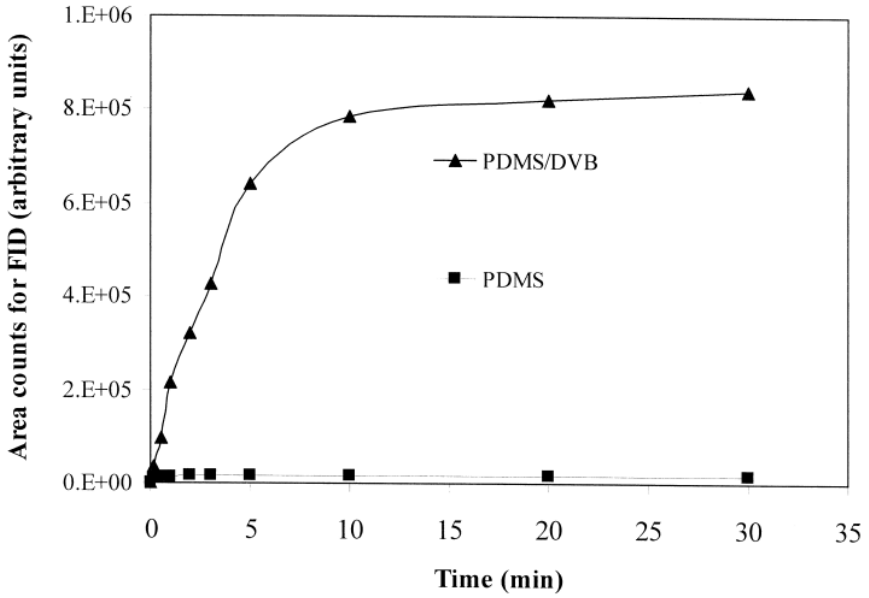

Figure 1.6 Comparison of the extraction time profiles of toluene at 1 ppb with the use of 65 µm PDMS/DVB and 100 µm PDMS fibers [32]. Figure reprinted from reference with permission of publisher.

The LOD of SPME air sampling depends on the selected fiber coating as well as sampling time. Taking BTEX as an example, literature reports LOD ranges from 0.06 ppbv to 5.5 µg/L for PDMS [34] [35], and 1-9 ppb for PDMS/DVB [36] [32] with pre-equilibrium extraction. Compared to traditional air sampling techniques, which can reach a LOD of parts-per-trillion, SPME requires further development to improve the capacity of the extraction phase.

Table 1.1 Some applications of SPME for air sampling

Analytes	**Fibers**	**Sampling mode**	**LOD**	**Calibration method**	**Compare with other methods**	**Ref.**
BTEX	PDMS	Spot sampling	0.06-2 ppbv	Equilibrium	EPA[2] method	[34]
BTEX Alkanes	PDMS	Spot sampling	0.02-5.5 µg/L	Equilibrium	Charcoal tube active sampling	[35]
BTEX	PDMS/DVB	Spot sampling	1 ppb	External calibration	NIOSH [3] method	[36]
Dodecane	PDMS	TWA sampling	720 ppt	Diffusion base	Fiber exposed	[36]
BTEX and Hexane	PDMS/DVB	Spot sampling	1-9 ppb	External calibration	NIOSH method	[32]
BTEX	PDMS/DVB PDMS/CAR	Spot sampling	ND	Diffusion base interface model	ND	[18]
BTEX	PDMS/CAR	Spot/TWA sampling	ND	Diffusion base cross flow model	NIOSH method	[33]
Pesticides	PDMS	Spot/TWA sampling	ND	Diffusion base	EPA method	[37]

ND=no data; EPA=Environmental Protection Agency; NIOSH=National Institute for Occupational Safety and Health.

Other parameters that may affect air sampling, such as humidity and sampling flow rate, were also discussed in the literature. Humidity effects on air sampling using PDMS coating and PDMS/DVB coating were reported; results showed that for PDMS coating, the effect of humidity was dependent on temperature. Lower temperatures resulted in a higher humidity effect. At room temperature, the extraction amount was reduced by less than 10%, while relative

humidity increased to 75% [34]. According to this study, high humidity interferes with the analyte mass uptake rate due to the absorption of water on the fiber surface, thus changing the characteristics of the fiber. However, in a paper later published by Perry *et al.* [35], this phenomenon was proven to be caused by the artifact of injection, and could be fully corrected by simply turning off the septum purge gas. This observed effect is due to the absorbed or capillary condensed water that evaporated inside the hot injector, where the vapor flushes back the purging gas, and takes away a percentage of the absorbed analytes through the septum purge gas. The humidity effect on solid coatings was investigated in a paper published by Koziel *et al*. [18]. In this study, extraction time profiles for BTEX gas at different humidity were obtained. Results indicated that during extraction, water molecules competed with other molecules, and occupied a portion of the active sites on the coating surface. Therefore, fewer active surface sites were available for the analyte molecules; this is particular true for samplings that are conducted over long periods of time.

As for air flow rate, during sampling, it influences the thickness of the boundary layer, affecting the sampling rate and the equilibrium time. In the other words, air flow rate only influences pre-equilibrium sampling, but not the equilibrium extraction amount. The relationship between the thickness of the boundary layer and the air sampling rate will be discussed further in Section 1.3.5.

Storage time is another important factor for SPME air sampling, since most samplings are conducted in-field and cannot be analyzed immediately after sampling. Storage methods and storage time for PDMS fiber extracted with volatile organic compounds (VOCs) [34] and pesticides [37] were evaluated. Results showed that samplings of volatile compounds such as BTEX, when stored in dry ice (-70 ℃), can last for up to 2 days without significant loss. On the

other hand, sampling of semi-volatile compounds such as pesticides can be stored at 2 ℃ for 3 days with no significant loss occurring.

1.3.3.2 SPME for solid sampling

SPME used for solid samples such as soil and sediment analysis has shown significant advantage over conventional liquid solvent extraction techniques, which tend to be time consuming, and require a large amount of organic solvent. Direct immersion as well as headspace sampling mode has both been reported. For direct sampling [38], the fiber is directly inserted into the soil sediment for a pre-determined period of time, and then removed from the sample. Before injecting into the analytical instrument for separation and quantification, a washing step is usually required for the fiber. A disadvantage of direct immersion sampling is long equilibrium extraction times due to low diffusion coefficients of analytes in the solid sample. As well, another distinct disadvantage is the possibility of fiber bio-fouling occurring during sampling, which may permanently damage the coating. Other mediums such as water [39], and micellar solutions [40] were also applied in the extraction of analytes from a solid matrix before using an SPME fiber for sampling.

As a result, headspace sampling is regularly used for soil and sediment sampling to improve extraction efficiency and reduce contamination of the fiber. For headspace sampling, the analytes need to be released into the headspace first. Other techniques such as sonication [41, 42], and microwave [43] are commonly used to assist the releasing process. However, for sonication and microwave assisting methods, external devices which are considered to be a potential hazard to the health of operators need to be utilized. Consequently, heating has become the most popular assisting method used for the release of analytes from a solid sample. Yet, as absorption is an exothermal process, increasing sample temperature also decreases the distribution coefficient

between the coating and the sample matrix, which results in a decrease in the sampling amount. Temperature profiles, such as the one demonstrated on Figure 1.7a, are usually observed for commercial SPME fibers. Typically, the amount of analyte being extracted is initially increased because more analytes are released into the headspace. However, this amount starts decreasing as the temperature further increases; this is because of the decrease of the distribution coefficient. One way to solve this issue is to cool down the coating temperature while increasing the temperature of the sample matrix; this technique is called cold fiber SPME [44], which will be described in detail in the Section 1.3.4.1, Chapter 1, and Chapter 2. Figure 1.7b shows preliminary results of sampling naphthalene-spiked silica gel using the cold fiber SPME. As can be seen, it is clear that increasing the sample matrix temperature while maintaining the fiber at a relatively low temperature improves the extraction efficiency without decreasing the extraction amount.

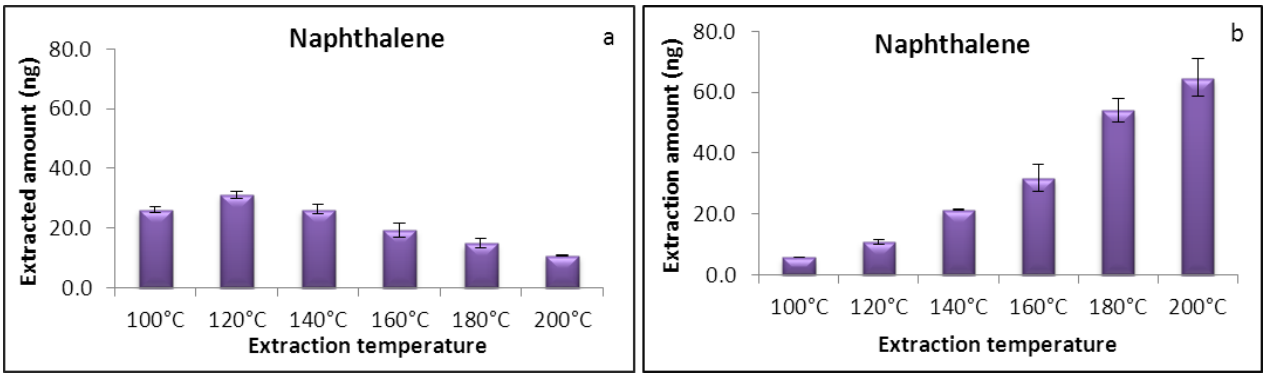

Figure 1.7 The temperature profiles of headspace sampling naphthalene-spiked silica gel using (a) DVB/CAR/PDMS fiber, (b) cold fiber with coating temperature of 40 ℃. The sample matrix was prepared by spiking 100 ng naphthalene into 2 g silica gel.

1.3.3.3 SPME for aqueous sampling

SPME for aqueous samples analysis have been well developed, and are the most widely used. SPME fibers can be used with DI, HS and HM sampling modes, and are easily coupled

with an autosampler. However, one challenge for SPME aqueous sampling is its relative insufficient sensitivity: this is due to the low capacity of the coating for specific groups of compounds. For instance, in previous research testing nitrosamines in drinking water, our group has found that the detection limit of the commercial fiber for N-nitrodimethylamine is 90 ng/L, while the regulation level from Health Canada is 40 ng/L for this compound [45].

1.3.4 Strategies on improvement of SPME sensitivity

Although SPME has been applied in a variety of sample preparation areas, its relatively low sensitivity is still a challenge for further development. The main causes of low sensitivity are small volumes of the extraction phase and/or the low distribution coefficient between the sample matrix and fiber. According to the fundamentals described in Section 1.3.2, strategies to improve the extraction amount (n) include using the extraction phase with higher distribution coefficients (K_{es}) and/or larger volumes (V_e).

1.3.4.1 Increase of the distribution coefficient (K_{es})

The distribution coefficient is a thermodynamic parameter which is defined as C_e^∞ / C_s^∞ (where C_e^∞ and C_s^∞ are the equilibrium concentrations of analyte in the coating and sample matrix, respectively). It reveals the affinity of a compound to a sorbent, and mainly depends on the physical properties of the coating. Different coating materials show varied distribution coefficients for diverse compounds, according to the polarity and volatility of these compounds. For example, in liquid coating, PDMS usually displays high K_{es} values for non-polar compounds, while polyacrylate (PA) and carbowax coatings have a high affinity for polar compounds.

In addition to liquid polymer coatings, solid sorbent impregnated coatings are also commercially available. These solid sorbents are porous polymers, porous carbon or silica. In the

extraction process, the analytes migrate into the pores of the adsorbent during the extraction process and interact with the sorbent via $\pi - \pi$ bonding, hydrogen bonding or Van der Waals force. The extraction capability of these solid coatings is largely determined by the total surface area, the amount of pores and the average diameter of the pores on the particles. Furthermore, the strength of the adsorbent is determined by the size of the analytes that it can retain, and is irreversibly proportional to the analyte size. A pore can retain an analyte that is about half of the size of the pore diameter. So a pore with a diameter of 12 Å can retain an analyte with an average molecular diameter of 6 Å. If a sorbent with a different pore-size ratio is used, it can retain a larger size range of analytes. Therefore, both degree of porosity and average size of the pores are important in determining the extraction capability of an adsorbent.

Two commonly used adsorbent coatings for SPME are porous divinylbenzene (DVB) and Carboxen 1006. The physical characteristics of these two adsorbents are shown in Table 1.2. DVB has a high degree of mesoporosity (20-500 Å), but it also has micropores (2-20 Å), as indicated in the table. DVB has more uniform, larger pores when compared to Carboxen 1006. Hence, DVB is primarily used for extraction of semi-volatile and large volatile analytes, while Carboxen 1006 is more applicable in the sampling of small, volatile compounds.

Table 1.2 Physical properties of adsorbents used in SPME fibers

Material	Surface area (m^2/g)	Porosity (mL/g)				Average micropore diameter (Å)
		Macropore > 500Å	Mesopore 20 - 500 Å	Micropore 2-20 Å	Total	
DVB	750	0.58	0.85	0.11	1.54	16
Carboxen 1006	950	0.23	0.26	0.29	0.78	12

The affinity of certain commercial types of fibers towards a specific group of compounds can be found in Figure 1.8. In addition to commercial fibers, other home-made SPME coatings have been reported in the literature, such as molecularly-imprinted polymers (MIP) [46-49], immunoaffinity coatings [50, 51] and restricted access materials (RAM) [52], all of which showed specific affinity toward a group of compounds. Recently, research in biocompatible coating has become a more attractive area of research, since SPME has been proven to be a potential *in vivo* sampling tool [29].

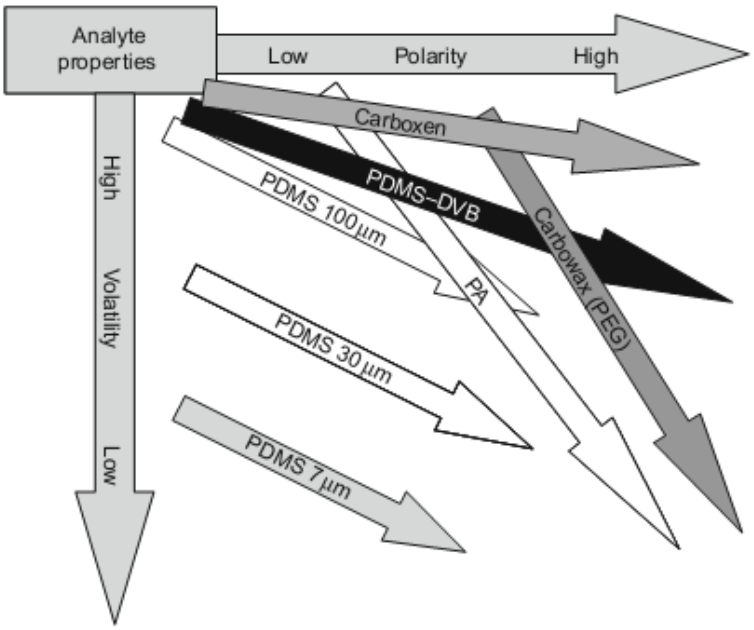

Figure 1.8 Coating selection guide

Other extraction conditions such as temperature, pressure, and sample matrix characteristics also affect K_{es} values. Generally speaking, since absorption is an exothermal process, lowering the fiber temperature usually results in a higher distribution coefficient. However, simply decreasing the sample matrix temperature slows down the mass transfer rate in the sample matrix, and results in low sampling rate. One way to solve this issue is to cool down the extraction phase while simultaneously heating up the sample matrix. This technique is called cold fiber SPME;

using this set-up, the sensitivity of SPME is enhanced, while the extraction rate is accelerated. The developed cold fiber device has been used for solid, aqueous and gas sample analysis.

Solid samples, such as sand or clay, can strongly retain analytes, and thus require high temperatures to release these compounds. When using traditional SPME fibers, a decrease in the extraction amount is usually observed when the sample matrix temperature is increased. To test its effectiveness, cold fiber SPME was used for quantitative sampling of BTEX in sand and clay [44]. The results show that in optimized conditions, BTEX recovery can be reached at levels higher than 80%. In another study, Carasek and Pawliszyn [53] compared the extraction efficiency of the cold fiber device with several commercial fibers in the screening of volatile compounds found in tropical fruits. In terms of extraction efficiency, results indicated that the cold fiber was the most appropriate fiber for extracting a large range of volatile compounds from five different fruit pulps.

Cold fiber results for aqueous headspace sampling of benzene were also reported. However, a recovery of only around 42% was achieved in the optimized condition. This modest percentage has been attributed to restrictions in temperature for both sample and fiber; the sample temperature could not be set higher than 100 ℃ due to the boiling point of the water, while the temperature of the fiber could not be set lower than 0 ℃ because of the solidification point of water.

Cold fiber used in on-site air sampling has not been reported as of yet due to restrictions associated with the CO_2 cylinder; the need for a cylinder makes cold fiber sampling an inconvenient method for on-site applications. However, cold fiber has previously been used for sampling spiked air in a 10 mL vial, and results were compared with non-cooling samplings of the same fiber [54]. As demonstrated on Figure 1.9, the majority of the analytes sampled reached

100% recovery when cold fiber was used. The development of cold fiber SPME using a thermoelectric cooler was also carried out for on-site applications [55]. For this study, a piece of a three-stage peltier cooler was used to cool down the coating. The limitation of this device lies in the geometry of the cooler (flat shape), which cannot effectively cool down the fiber configuration coating; this results in insufficient cooling temperatures. The lowest available temperature of a cold fiber device is dependent on sampling temperature as well as sampling time.

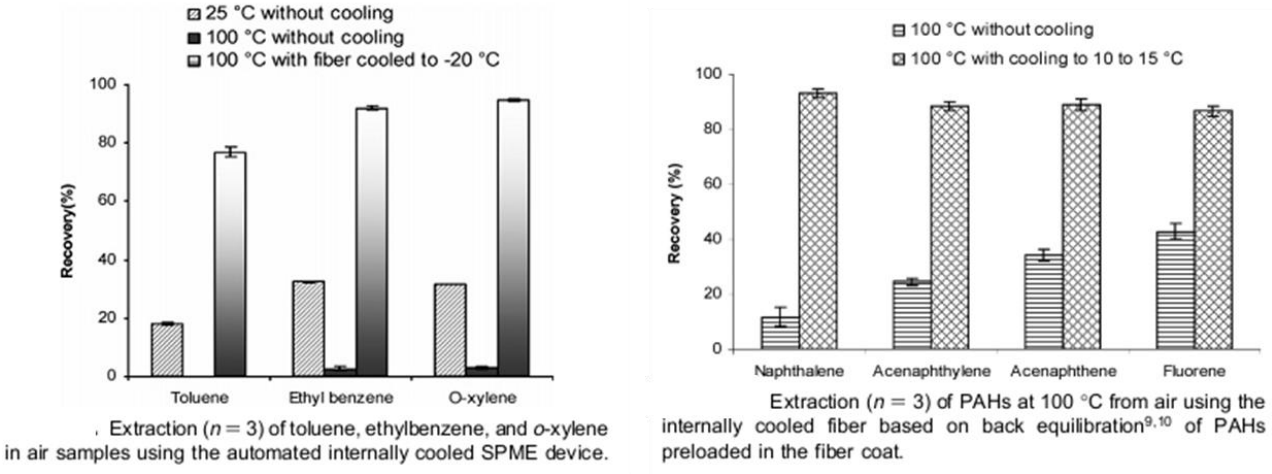

Figure 1.9 Comparison of cold fiber with and without cooling for vial seal air sampling [54]. Figure reprinted from reference with permission of publisher.

1.3.4.2 Increase of the volume of the extraction phase (V_e)

The volume of the extraction phase can be increased simply by using a thicker coating. However, according to Equation 1.3, a thicker coating would also result in a longer equilibrium time. Conversely, an alternate way to increase the volume of the extraction phase and enhance the extraction rate would be to employ a high surface area-to-volume ratio on the extraction phase. A high volume extraction phase would increase the equilibrium extraction amount (Equation 1.1), while a high surface area would improve the initial extraction rate (Equation 1.2).

Thin film microextraction (TFME) has been applied to a variety of sample matrices, including gas, liquid and solid samples (Table 1.3). In gas sampling, the TFME method has been applied in the analysis of chemical signatures associated with illicit drugs, as well as in the analysis of explosives. This was done by coupling TFME with ion mobility spectrometry (IMS) [56, 57]. Results have shown that this planar SPME provides significant improvement in sensitivity over the conventional fiber SPME and traditional IMS introducing methods. In a publication by Eom *et al*. [58], TFME was used to sample indoor air infested with *Cimex lectularius L*. Results indicated that TFME provided discriminative extraction coverage towards highly volatile analytes when compared to fiber and needle trap SPME. Furthermore, TFME has been used for monitoring breath after eating garlic and smoking (Figure 1.11A) [59]. Dietary markers were detected and semi-quantified using this technique.

Thin film microextraction has been widely used in the sampling of polyaromatic hydrocarbon (PAHs) [28, 60-63], pesticides [64-66], phenols [67] and nitrosamines [68] in water sample. Thin film for this application has been used as either an active [62, 69, 70] or passive sampler [60, 61]. For active on-site sampling, a new agitation method was utilized to enhance the thin film agitation during sampling, by attaching the thin film to an electronic drill (Figure 1.11B). The sampling efficiency of this active sampler was compared to stir bar sorptive extraction (SBSE), which is an alternative sample preparation technique that aims at improving the sensitivity of SPME. In SBSE, also called Twister, the extraction phase is coated on a magnet stir bar with a volume which is approximately 50 - 250 times larger than a typical SPME fiber. Due to the large volume of the extraction phase, SBSE was considered to be more sensitive than the SPME fiber in the determination of trace level pollutants in water [71]. However, the main drawback of this technique is the thick coating of the SBSE, which results in long equilibrium

times for this method; this limitation is clearly proven in Qin's research work [62]. For TFME, five model compounds (acenaphthene, fluorene, anthracene, fluoranthene and pyrene) reached equilibrium within 2 h, while the SBSE still progressively increased after 3 h extraction. The extraction rate of the TFME was also much higher than the SBSE sampling. Figure 1.10 shows the extraction time profile for both TFME and SBSE sampling of fluoranthene from water.

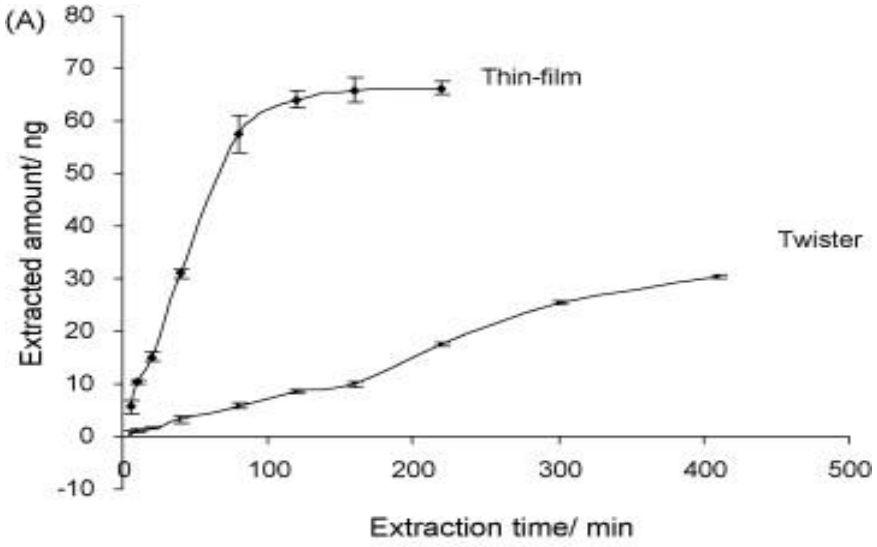

Figure 1.10 The time profiles of fluoranthene by thin film and Twister sampling [62]. Figure reprinted from reference with permission of publisher.

For in-field passive sampling, TFME was used to determine the TWA concentrations of PAHs in Hamilton Harbor (Lake of Ontario, ON, Canada) [60, 61]. A piece of PDMS thin film was mounted on a stainless steel wire (Figure 1.11C) and placed inside a copper cage; this was done to prevent bio-fouling of the membrane. The cage was placed in the sampling spot for passive sampling. Kinetic calibration with a pre-loaded internal standard on the membrane was employed for this on-site application. When compared to the fiber-retracted and PDMS-rod passive samplers, thin film sampler was shown to possess higher sensitivity as well as a greater mass uptake rate.

TFME as passive sampler has also been applied in the simulation of biological samples to investigate bioaccumulation of organic chemicals. In their research, Wilcockson and Gobas [72] utilized an ethylene vinyl acetate thin film to determine the fugacity of low-volatility substances found in fish tissue. In later studies, Gobas and his coauthors [73, 74] further evaluated the flexibility of using this film to measure the bioconcentration of organic chemicals present in sediment. These results were then compared to bioconcentrations obtained from the amphipod *Corophium colo* (clams). Excellent correlations were found between the thin film and biological tissue concentrations, demonstrating that TFME can be a useful tool in the characterization of the differences in bioavailability of organic chemicals present in sediment. Similar results were also obtained in Qin's research [63], which utilized the PDMS thin film to mimic the *Lumbriculus variegatus* (black worm) in order to determine the bioconcentration of PAHs pollutants in water.

Thin film microextraction for solid sample preparation is another important application to be considered due to the geometry of the membrane. In previous research, PDMS thin film was used for *in vivo* sampling of the sebum [75], with the purpose of quantifying volatile compounds releasing from human skin [76, 77] (Figure 1.11D). During sampling, the membrane was directly/headspace placed on top of the sampling area. Compounds emanating from the skin were absorbed by the membrane which can later be desorbed by high temperatures or using organic solvent. Chiefly, the major advantages of thin film in this application are its high extraction efficiency, as well as the convenience of operation of the thin film geometry in comparison to the fiber SPME. More detail of this application will be discussed in Chapter 3.

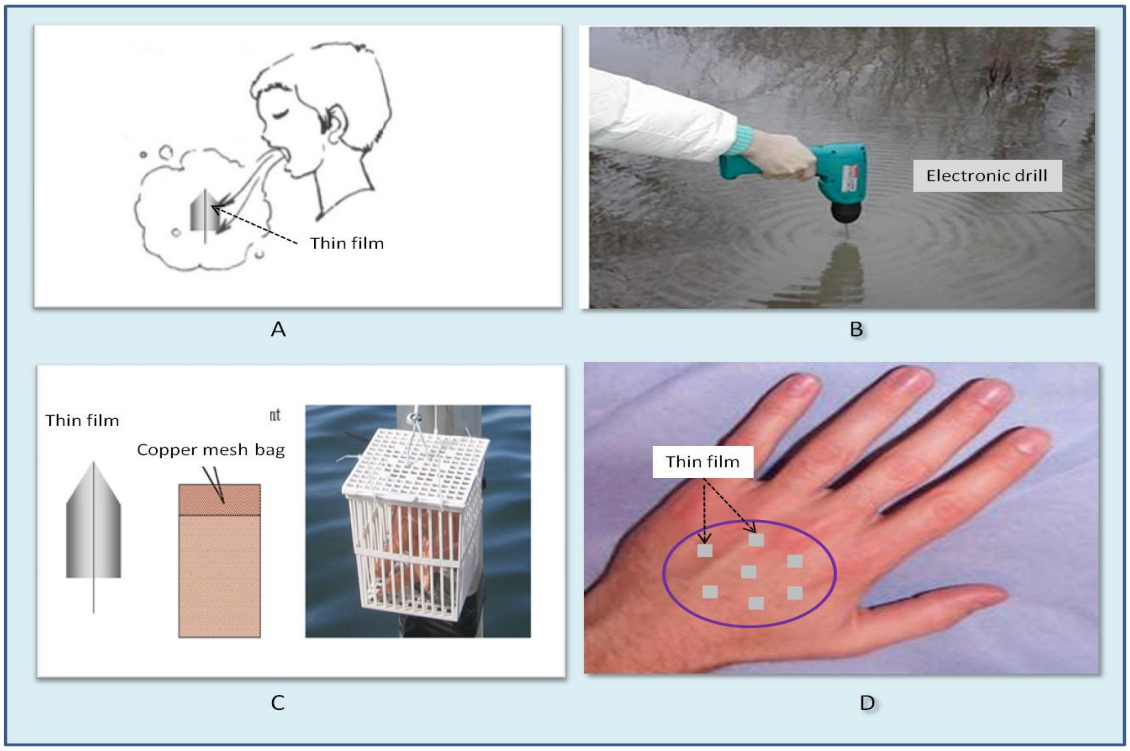

Figure 1.11 Various application of TFME. (A) Breath analysis [59]; (B) Active water sampling [69]; (C) Thin film passive sampler [60]; (D) Skin sampling.

Table 1.3 Summary of the literature on TFME [78]

Sample matrix and analytes	**Desorption and instrument**	**Film material**	**Ref.**
VOCs in water	Coupled to IR	Parafilm, PDMS	[79, 80]
Aromatics in gasoline, jet Fuel, diesel fuel in water	Coupled to UV	PDMS (OV-1)	[81]
Herbicides in water	Solvent desorbed by chloroform and analyzed by GC/MS	MIP material	[66]
PAHs in water	Thermal desorbed in GC/MS	PDMS	[60-63, 70]
PAHs and Phenol in water	Solvent desorbed by acetonitrile and analyzed by GC/MS	PDMS/β-cyclodextrin	[67]
Pesticides in water	Coupled to corona beam ionization MS	PDMS	[65]
Pesticide from water	Solvent desorbed by chloroform followed by GC injection	Polypyrrole-polyamide nanofiber	[82]
Chlorobenzenes from water	Solvent desorbed by acetone followed by GC injection	Polyaniline-nylon-6 nanofibers	[83]
Organochlorine pesticides	Solvent desorbed by acetonitrile and analyzed by GC/ECD	PDMS with smooth and rough surface	[64]

Poorly volatile hydrophobic compounds in fish tissue	Solvent desorbed by DCM or thermal desorbed in self-assemble thermal desorption unit coupled to GC/MS	Ethylene vinyl acetate	[72]
Sebum from human skin	Thermal desorbed in GC/MS	PDMS tape	[75]
Volatile fraction from biological solid matrices	Thermal desorbed in GC/MS	PDMS tape	[84]
Hydrophobic organic chemicals in sediment	Solvent desorbed by hexane and analyzed by GC/MS	Ethylene vinyl acetate	[73, 74]
Acetaldehyde and acetone from human skin	Sorbent desorbed by acetonitrile and analyzed by HPLC	Derivatives loaded film	[85]
VOCs from human skin	Thermal desorbed in GC/MS	PDMS	[76, 77]
PBCs contained fish tissue	Solvent desorbed by acetone and analyzed by GC	PDMS	[86]
Methyl jasmonate in leaf tissue	Solvent desorbed by methanol	PDMS	[87]
Explosives or illicit drugs	Coupled to IMS	PDMS , sol-gel PDMS or diethoxydiphenylsilane-base	[56, 57, 88, 89]
Air infested by *Cimex lectularius L*	Thermal desorbed in GC/MS	PDMS	[58]

1.3.4.3 Increase of both K_{es} and V_e simultaneously

Since method sensitivity can be increased by increasing the distribution coefficient or the volume of the extraction phase, simultaneously increasing both K_{es} and V_e values may further improve the extraction efficiency. Thus, two separate tasks need to be taken into consideration in the production of this new method: developing an effective cooling membrane device (see Chapter 4), while also preparing a particle loading membrane that has a high K_{es} towards the compounds of interest (see Chapter 5).

1.3.5 The calibration methods of SPME

As mentioned above, SPME is a non-exhaustive extraction technique. Therefore, calibration methods are developed in order to obtain the relationship between the extraction amount and the initial sample concentration. Several calibration methods have been developed for SPME sample

preparation [90]. Traditional analytical calibration methods such as external calibration, standard addition, and internal calibration are commonly used for SPME quantification, and both equilibrium and pre-equilibrium extraction can be employed for these calibration methods. Other methods for SPME calibration can be classified into two categories: equilibrium based and pre-equilibrium based methods.

External calibration involves the preparation of several standard solutions using matrix matched blank samples [91-94]. The standard solutions and unknown samples are subsequently analyzed using the same extraction conditions in order to establish the relationship between the extracted amount and the analyte concentration in the sample. The concentration of the target analytes is then determined from the obtained calibration curve. This is the simplest calibration method for simple sample matrices. However, it may not be an appropriate method when the sample matrix or the extraction conditions are difficult to reproduce.

Standard addition method is accomplished by preparing a series of known concentrations of the target analytes using the unknown sample solution. The signals obtained from all the sampling are then plotted against the spiking concentration. The concentration of the original sample is determined by the extrapolation of the calibration curve to zero. Compared to external calibration, this approach is able to compensate for matrix effects, and therefore can be used for quantification of complex sample matrices [95-98].

Internal standard approach involves adding a known concentration of internal standard that is not present in the sample matrix, and can mimic the behavior of the analytes during extraction and analysis [99-102]. Calibration then is done by comparing the ratio of the analytes signals to the internal standard with a known concentration. This method shows significant advantages in terms of minimizing matrix effects and loss of target analytes during the sample preparation or

transportation process. However, it is difficult to determine suitable compounds to use as internal standards. Isotopically-labeled internal standards are preferable, but they are usually not easy to find and are generally expensive. Additionally, isotopically-labeled compounds require expensive instrument use such as MS for analysis.

Equilibrium calibration method is based on the relationship between the equilibrium extraction amount (n) and the sample matrix concentration (C_s) [35, 103-105]. This has been previously described in Equation 1.1. When the distribution coefficient (K_{es}) and the sample volume (V_s), are known, the concentration of the sample matrix can be calculated by determining the equilibrium extraction amount (n). This calibration method is simple and can be used for on-site sampling calibration when the sample matrix volume is difficult to determine. However, the limitation of this technique lies in the difficulty in obtaining K_{es} values for all compounds. For semi-volatile compounds, it may take from several hours to days to reach the equilibrium extraction. It is important to note that SPME has been proven to be a useful and convenient tool for determining the distribution coefficient of analytes on liquid coating. For PDMS coating, some of the K_{es} can be found in the literature or be approximated by using the K_{ow} value of the compound of choice [106-111].

Pre-equilibrium calibration methods overcome the limitation of long equilibrium extraction times by ceasing the sampling before reaching the equilibrium. Diffusion-based calibration methods and on-fiber standard calibration methods (kinetic calibration) are all based on pre-equilibrium sampling.

Diffusion-based calibration utilizes the initial linear stage of an extraction process, where the extraction amount is lower than 10% of the equilibrium extraction amount. Different modes

can be used to interpret the relationship between the extraction amount and the sample matrix concentration.

The first model is based on the Fick's first diffusion law. This model assumes that analytes can access the fiber coating only by means of diffusion through the boundary layer between the sample matrix and fiber coating, and the amount of analytes accumulated during the sampling time can be predicted by Fick's first diffusion law. If the sorbent is "zero sink" for the target analytes, the concentration of the target analytes in the sample can be calculated by Equation 1.4

$$n = \frac{DA}{\delta} C_s t \qquad \text{Equation 1.4}$$

Where D is the diffusion coefficient; A is the sampling medium surface area and δ is the thickness of the boundary layer; t is the sampling time. This model is suitable for the fiber retracted TWA sampling (Figure 1.5), in which the distance from the fiber opening to the surface of the sorbent is defined as the diffusion boundary layer [112-114]. This equation is actually the same as Equation 1.2, which is derived from the following interface model, as proposed by Koziel *et al*. [18]. This model is derived using the analogy of heat transfer in a concentric tubes with inside and outside diameter of b and δ, respectively. By replacing the temperatures with concentrations, heat flux with mass flux, and heat transfer coefficients with mass diffusion coefficients, the heat transfer solution can be translated into a mass transfer solution. As a result, the extracted mass can be estimated using the following equation:

$$n = \frac{2\pi DL}{\ln((b+\delta)/b)} C_s t \qquad \text{Equation 1.5}$$

Where D is the analyte molecular diffusion coefficient sample matrix; L is the length of the coating; b is the outside radius of the fiber coating; δ is the thickness of the boundary layer.

When the thickness of the boundary layer is much smaller than the outside radius of the fiber coating ($\delta \ll b$), Equation 1.4 can be simplified to Equation 1.4, when $\ln((b+\delta)/b) \approx b/\delta$, $2\pi bL = A$.

Chen *et al*. [33] have later employed a new physical model also translated from heat transfer to a circular cylinder in cross-flow, which has been used to describe the rapid SPME extraction of VOCs in aqueous samples (Equation 1.6).

$$n = \bar{h}\mathrm{A}C_s t = \frac{ER_e^m P_r^{1/3} DA}{b} C_s t \qquad \text{Equation 1.6}$$

Where D is the analyte molecular diffusion coefficient in the sample matrix; $\bar{h}$ is the average mass-transfer coefficient; A is the surface area; Re is the Reynolds number ($R_e = 2ub/v$); u is the linear air velocity; v is the kinetic viscosity for air; b is the outside radius of the fiber coating; P_r is the Prantl number ($P_r = v/\mathrm{D}$); E and m are constants depending on the Reynolds number, and available in the literature.

In the above diffusion based calibration equation, the terms, $\frac{DA}{\delta}$, $\frac{2\pi DL}{\ln((b+\delta)/b)}$ and $\frac{ER_e^m P_r^{1/3} DA}{b}$ can be defined as sampling rates, and can be determined either by experimental data, or calculation data if the experimental conditions are well controlled and known.

By conducting an experiment, the sampling rate can be obtained from the slope of the initial linear range of an extraction time profile in which the sample concentration is known. When using calculations, for a defined geometry extraction phase, the sampling rate is influenced by experimental conditions such as temperature and air flow.

Temperature influences the analyte diffusion coefficient while air flow rate defines the thickness of the boundary layer. The diffusion coefficient can be found from the literature and

corrected according to the sampling temperature using empirical equations [18, 33]. Similarly, the thickness of the boundary layer can be determined from the empirical Equation 1.7 when the air flow is perpendicular to the fiber axis [20].

$$\delta = 9.52(b/R_e^{0.62}P_r^{0.38}) \quad \text{Equation 1.7}$$

Diffusion based calibration has been extensively applied in a variety of applications [26]. However, the major limitation for this calibration method is the strict sampling conditions needed to ensure the consistency of variables such as air flow rate. In some applications, such as for on-site sampling, the sampling conditions may be difficult to control, but are important variables in the quantification of the compounds under study. Also, sampling time should be short enough to ensure the "zero sink" condition; shorter times however, usually result in insufficient sensitivity. Therefore, for high sensitivity sampling, a high capacity extraction phase such as thin film or cold fiber is generally recommended when using a diffusion based calibration method.

The on-fiber standard calibration method has been introduced to address the limitations of diffusion calibration when the condition of agitation is difficult to control. In this calibration process, the fiber is preloaded with a deuterated standard prior to exposing it to the sample matrix. During sampling, the analytes present in the sample matrix are extracted onto the fiber while the preloaded deuterated compounds are desorbed into the matrix. After sampling, the extracted compounds and remaining preloaded compounds are quantified by the analytical instrument. According to the symmetric relationship between the desorption and extraction processes, when the volume of the sample matrix is large enough to use the simplified Equation 1.1, the concentration of the analytes can be determined by Equation 1.8 [115, 116],

$$C_s = \frac{q_0 n}{K_{es} V_e (q_0 - Q)}$$ Equation 1.8

where q_0 is the amount of preloaded deuterated standard on the extraction phase; Q is the amount of the deuterated standard remaining on the extraction phase after exposure; n is the analyte extracted amount and C_s is the sample concentration.

On-fiber standard calibration has been widely used in *in vivo* [95, 117-119] and *in situ* [60, 61, 120, 121] sampling, and has proven to be an accurate method. There are three main limitations to this technique. First, we must consider the use of deuterated standards, which are expensive and may be difficult to obtain. Next, we must take into consideration the requirement of symmetry conditions for desorption and absorption processes, which may not be observed in solid coating. And last, the difficulty in obtaining K_{es} values for all the analytes.

1.4 The objectives of the thesis

The main objective of this thesis is to investigate strategies for improving the sensitivity of SPME based on the effect of coating temperature, geometry and sorbent addition. To achieve this, four sampling methods were developed and applied in solid, liquid and trace gas analysis.

In the first approach, a cold fiber which improves the sensitivity of SPME by cooling down the coating during sampling was studied. For the first time, the cold fiber was coupled with a GERSTEL® autosampler and a septumless head injector to achieve full automation for high throughput analysis. The automated cold fiber was evaluated with a large range of compounds representing different volatilities and polarities.

Next, high surface area geometry (thin film) was applied in skin volatile emissions sampling. A simple, non-invasive sampling set-up was developed for headspace, non-contaminated sampling of volatile compounds emitted from the skin. Evaluation experiments were conducted

to investigate the performance of this sampling set-up, which was later applied for sampling the dietary biomarker emitting from the skin after eating garlic and alcohol.

The third approach, combining the advantages of cold surface area effect and high surface area geometry, was investigated. Here, a cooling membrane sampling device was developed and evaluated in terms of reproducibility, temperature effect, membrane size effect, flow rate effect, humidity effect, and analytical figure of merits. The proposed cooling membrane sampling device was applied in real air sampling and results were compared with the same membrane without the cooling step.

Last, the sorbent effect was implemented to further improve the capacity of the TFME by preparation of a solid sorbent impregnated PDMS membrane. Bar coating, a simple and easy operation membrane preparation method, was utilized to prepare this particle loading membrane. The prepared membrane was thoroughly evaluated and applied in indoor and outdoor air semi-quantitative and quantitative sampling.

Chapter 2 **Fully Automated Cold Fiber Device for High Throughput Sample Preparation**

2.1 Introduction

2.1.1 Miniaturization of the cold fiber device

The first cold fiber device was developed by Zhang in 1995 [44]. In this version of cold fiber, the cooling process was done by simply inserting a CO_2 delivering capillary into another larger diameter capillary, with its tip encased by a piece of PDMS tube as the extraction phase. The cooling efficiency was simply controlled by using different diameters of the CO_2 delivering capillary: larger diameters resulted in lower coating temperatures. Later in 2006, Chen *et al.* miniaturized the original cold fiber device and coupled it to a Combi PAL® autosampler for automation [54]. The configuration of this automated cold fiber device is shown in Figure 2.1; as can be seen, it was built on a 100 µL syringe that had its plunger replaced by a 22 gauge stainless steel tubing. A 33 gauge stainless steel tubing used to deliver liquid CO_2 was inserted inside the 22 gauge tube, together with a pair of thermocouples used to monitor the temperature of the extraction phase. A piece of PDMS tube was encased on the tip of the plunger and used as the extraction phase. The outside needle was an 18 gauge tube, which was used to protect the extraction phase during handling. Further details on construction of this cold fiber device can be found elsewhere [54].

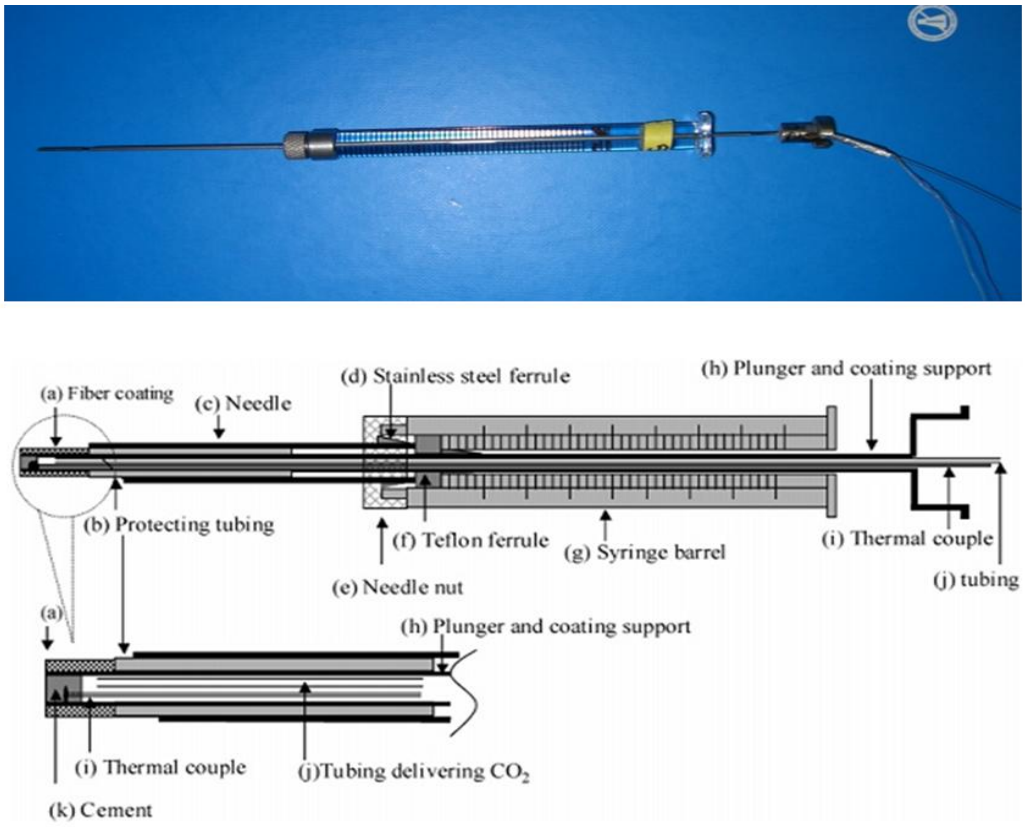

Figure 2.1 The configuration of cold fiber [54]. Figure reprinted from reference with permission of publisher.

The miniaturized cold fiber device is very similar to a traditional SPME fiber and can be coupled with an autosampler (shown in Figure 2.2). The temperature of the cold fiber coating is regulated by the flow of liquid CO_2, which is controlled by a solenoid valve. The temperature of the coating is detected by the thermocouples. When the temperature becomes lower than the value set on the temperature controller, the controller switches on the solenoid valve, and more liquid CO_2 flows to the tip of the plunger. Conversely, when the temperature rises above the set value, the controller switches off the solenoid valve. The variations in temperature are related to the temperature of the sample and the temperature of the coating setting ranging from ± 3-5℃. In order to couple the cold fiber with a CombiPAL autosampler, the temperature controller needs to be connected to the autosampler through the signal cable.

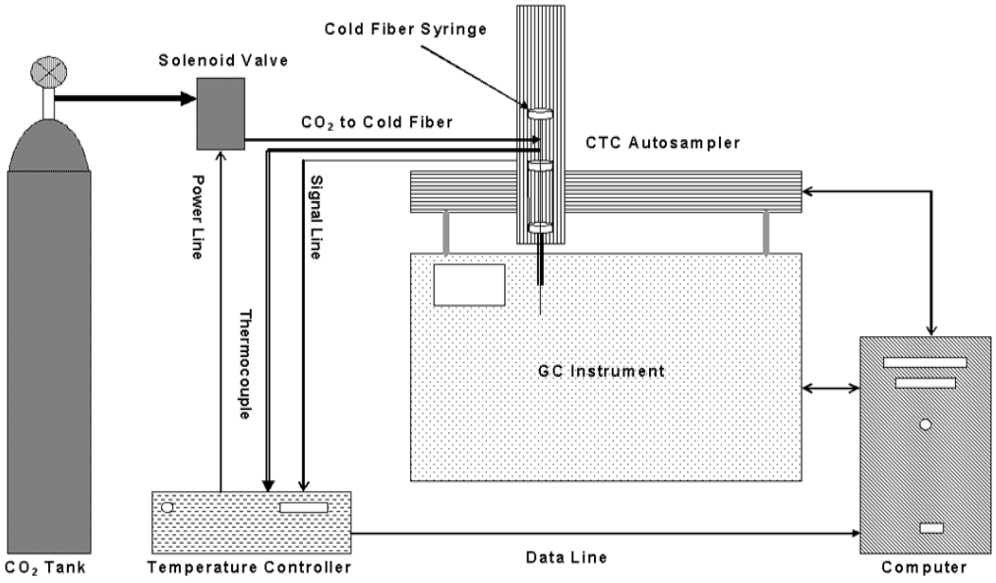

Figure 2.2 The configuration of the automated cold fiber device [30]. Figure reprinted from reference with permission of publisher.

2.1.2 Principle of cold fiber SPME

In 1995, Zhang [44] introduced the first cold fiber device, which was used for headspace sampling BTEX from aqueous and solid samples. As well, the author derived the equation for the determination of the cold fiber distribution coefficient (Equation 2.1).

$$K_T = K_0 \frac{T_s}{T_e} \exp\left[\frac{C_p}{R}\left(\frac{\Delta T}{T_e} + ln\frac{T_e}{T_s}\right)\right] \qquad \text{Equation 2.1}$$

where K_T is the cold fiber distribution coefficient; K_0 is distribution coefficient when the extraction phase and sample matrix temperature are both at T_e, which is extraction phase temperature; T_s is the sample matrix temperature. ΔT=T_s - T_e; C_p and R are the constant pressure heat capacity of the analyte and the gas constant, respectively. From the equation, we can see that the cold fiber distribution coefficient is proportional to the K_0, which is higher when the

fiber temperature is lower. Also, it is proportional to the temperature gap (ΔT) between the sample matrix and the extraction phase. The accuracy of the equation has been demonstrated by experimental results, which can be found in Zhang's paper.

2.1.3 Limitations of the previous automated cold fiber

There are a variety of advantages associated with the automated cold fiber device when compared to relying on manual operation. The automation of the device improves the sample analysis throughput and minimizes experimental variation during operation. Additionally, automated injection increases the injection number for each septa. Since the outer needle of the cold fiber (18 gauge) is much larger than the traditional SPME fiber (23 gauge), septa coring is commonly observed after a few injections when using the septa injector. However, when the autosampler is used, a longer lifespan for each septa (15 injections) has been reported when compared to manual injection (5 injection) [54].

After the development of the automated cold fiber device, Ghiasvand *et al*. [30, 122], Haddadi, *et al*. [55, 123] and Caresek *et al*. [53, 124] used this new automated device for several applications. However, despite the obvious advantages of the cold fiber method, the approach still lacked absolute automation and was confronted with various challenges that required human intervention. This situation often led to overall lower sample analysis efficiency. As part of the fundamental reasons for automated sample preparation systems, in addition to robustness and reliability, it is essential to eliminate human intervention in order to improve overall sample analysis. However, the previous semi-automated cold fiber device fell short of this distinctive principle due to the large needle size and shape often led to septa coring inside the GC injector, which required regular replacements in the middle of analysis. Thus, successful analysis of larger number of samples required human presence and intervention. As well, a standard cold fiber

device configuration and setup coupled to the CTC CombiPal® autosampler posed serious challenges in effectively maintaining a stable coating temperature during sample analysis.

2.1.4 The objective of this project

In this study, a fully automated cold fiber device was developed by modifying the existing semi-automated unit, and coupling it to a GERSTEL® MPS 2 autosampler and a septumless head (SLH) injector. This significant modification improved the headspace analysis of volatiles and semi-volatiles from aqueous and solid matrices. The main objective of this project was the provision of a new, fully automated cold fiber device that is capable of analyzing a larger number of samples with little to no human intervention.

2.2 Experimental

2.2.1 Reagents and supplies

HPLC grade methanol was obtained from Caledon laboratories Ltd. (Georgetown, ON, Canada). BTEX and 14 other compounds of varying polarities and volatilities (Table 2.1), used to evaluate the automated cold fiber device, were purchased from Sigma-Aldrich (Bellefonte, PA, USA). 8 µL of pure BTEX compounds were spiked into 80 g of inland 45 pump oil (Agilent Technologies, Mississauga, ON, Canada), mixed well, and left to achieve equilibrium for at least one day before being used. A stock standard was prepared by dissolving known amounts of all the compounds in methanol. Using the stock solution, two working standard solutions were also prepared in methanol; the final concentrations for each standard can be found on Table 2.1. All standard solutions were then stored at 4 ℃. Polycyclic aromatic hydrocarbons including naphthalene, acenaphthylene, acenaphthene, fluorene, anthracene, fluoranthene and pyrene were also purchased from Sigma-Aldrich and prepared in methanol with a concentration of 100 µg/mL.

Ultrapure water used for preparation of the sample matrix was obtained from Barnstead/Thermolyne NANOpure water system (Dubuque, IA, USA). Silica gel was obtained from SiliCycle Inc. (Quebec City, QC, Canada) with an average pore diameter of 60 Å.

Table 2.1 Data for 14 analyzed compounds and their standard solutions

Compounds	Stock solution concentration (mg/mL)	Working solution #1 concentration (µg/mL)	Working solution #2 concentration (µg/mL)	Retention time from Agilent GC (min)
2-Hexanone	2.44	144	215	6.162
Ethyl butanoate	2.55	150	225	6.552
2-Heptanone	2.47	145	218	10.242
Heptanal	2.46	145	218	10.715
1-Heptanol	2.02	119	179	13.879
Octanal	2.40	141	71	15.086
2-Nonanone	2.43	143	71	18.672
Ethyl heptanoate	2.39	141	70	18.930
Nonanal	2.37	140	70	19.213
Nonanol	2.71	160	80	21.831
2-Tridecanone	3.59	211	106	32.747
Heptadecane	2.86	168	84	38.614
2-Heptadecanone	2.38	140	70	43.857
Ethyl hexadecanoate	2.49	147	73	46.061

Stainless steel tubings with different inner and outer diameters were purchased from Vita Needle (Needham, MA, USA). A Hamilton gas-tight syringe (1710 series, 100 µL) was obtained from Sigma-Aldrich. A temperature controller and thermocouples were obtained from Omega Engineering (Stamford, CT, USA). Solenoid valve was from ASCO Valve Canada (Brantford, Canada). The solenoid valve and temperature controller were modified by the electronic shop at University of Waterloo. After modification, the temperature controller can automatically control the on/off switch of the solenoid valve according to the temperature settings.

Clear vials (10 mL and 20 mL) with screw caps and polytetrafluoroethylene (PTFE) coated silicone septa were provided by Sigma-Aldrich. Two commercial SPME fibers, PDMS, 100 µm and DVB/CAR/PDMS, 50/30 µm were also provided by Sigma-Aldrich. Both fibers were conditioned according to the manufacturer's recommendation prior to their use. A 170 µm PDMS liquid polymer tubing used as cold fiber coating was obtained from Dow Corning (Midland, MI, USA). The coating was conditioned at 250 ºC with a nitrogen gas flow for an hour prior to usage.

2.2.2 Instrumentation

The GERSTEL® MultiPurpose Sampler (MPS 2) (GERSTEL, Mülheim an der Ruhr, GE) and the Agilent 6890 GC coupled with a 5973 MSD quadrupole mass spectrometer (Agilent Technologies, Mississauga, ON, Canada) were used in this study. All extractions and injections involving the modified cold fiber device were made possible by coupling it to the GERSTEL autosampler with a SLH (Figure 2.3). Without injection taking place, the plunger (part 7) with the inner O-ring (part 6) is pushed towards the needle path by the spring (part 8), and the GC system is air seal. During injection, the plunger and O-ring are pushed away by the needle. The Teflon needle guide provides effective sealing, preventing air leakage. Theoretically, the Teflon needle guide should be able to be used permanently; however, in practice, the sharp needle tip can damage the Teflon needle guide after a number of injections, causing air leakage during injection.

Chromatographic separations were performed using a SLB™-5MB (30 m × 0.25 mm × 0.25 µm) fused silica column from Sigma Aldrich with helium (Praxair Canada, Mississauga, ON, Canada) as the carrier gas at a flow rate of 1 mL/min. For BTEX analysis, the oven temperature was held at 40 ℃ for 2 min and then ramped to 80 ℃ at a rate of 10 ℃/min, then held for 1 min.

The injector temperature was set at 250 ℃. For the analysis of the 14 compounds, the oven temperature was initially held at 40 ℃ for 5 min and gradually increased to 204 ℃ at a rate of 5 ℃/min, and then set to 250 ℃ at a rate of 10 ℃/min. The injector temperature was set at 250 ℃. For PAHs analysis, the oven temperature was kept at 50 ℃ for 1 min and then increased to 270 ºC at a higher rate of 20 ℃/min, then held for 13 min. Injector temperature was held at 270 ℃ throughout the chromatographic run time.

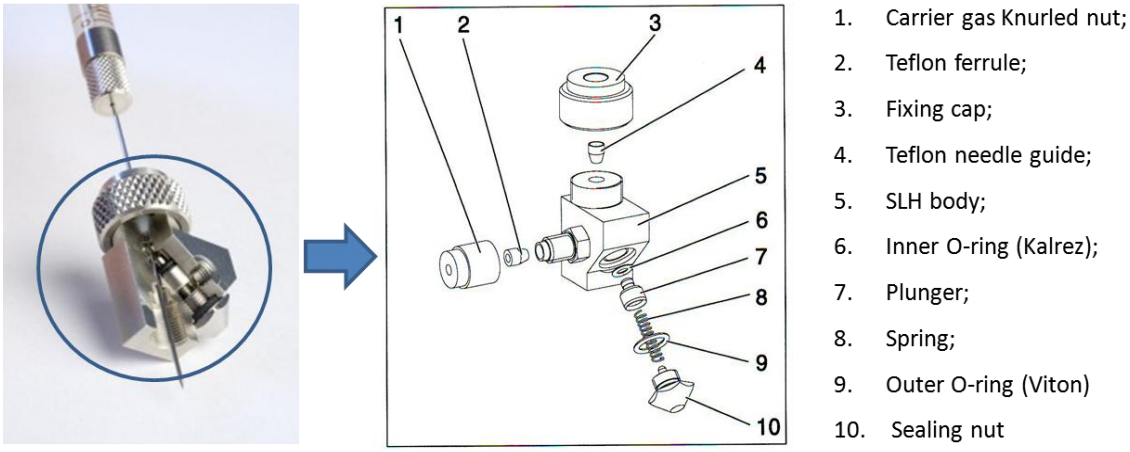

Figure 2.3 The configuration of GERSTEL SLH injector. (Picture from Gersetel® website)

With the MS operating in electron ionization mode, the transfer line, MS Quad and MS source were set at 270 ℃, 150 ℃ and 230 ℃, respectively during the analysis of the 14 compounds. However, with the PAHs, the transfer line, MS Quad and MS source temperature were set at 280 ℃, 150 ℃ and 230 ℃, respectively. While a full scan mode (40 - 300 m/z) was used for the 14 compounds, a SIM mode was chosen for the PAHs. The qualifier ions for the respective PAHs were 138, 152, 154, 166, 178, 202 and 252 for naphthalene, acenaphthylene, acenaphthene, fluorene, anthracene, fluoranthene and pyrene.

2.2.3 Experimental procedure

The experimental design involved an initial evaluation of the new fully automated cold fiber device using 14 compounds with varying volatilities and polarities in aqueous medium, followed by an extraction of spiked samples of PAHs in silica gel (solid matrix). The evaluation procedure was carried out by optimization and determination of extraction time and temperature, as well as desorption temperature. Aqueous samples used for the optimization process were prepared by spiking 1 µL working solution into 3 mL of ultrapure water in a 10 mL vial, then capped immediately and sealed with parafilm to prevent analyte loss. The vial was placed on a mechanical shaker (Fisher Vortex Genie 2TM) for a minimum of 1 min. Each vial was used for one extraction. The set of fibers used for the experiments were commercially available PDMS (100 µm), DVB/CAR/PDMS (50 µm/30 µm) and PDMS tube (170 µm). Prior to the extractions, aqueous samples for commercial fibers analysis were incubated in the autosampler agitator for 10 min at 250 resolution per minute (rpm). Subsequently, extractions were performed in the agitator with a constant agitation speed (250 rpm). The fibers were thermally desorbed in the GC injector for 5 min and 7 min for PDMS and DVB/CAR/PDMS coating respectively. A longer desorption time for the DVB/CAR/PDMS was chosen to prevent any form of carryover, which is often characteristic of this fiber type. Similar experiments were performed using the cold fiber device but without agitation during extraction and incubation. This was done because the cold fiber external needle was not flexible enough for agitation.

Samples used for PAHs analyses were prepared by spiking 1 µL stock solution (100 µg/mL) into 0.5 g silica gel placed in 10 mL vials. The vials were sealed with a screw cap immediately and shaken for 60 min at 900 rpm. The spiked samples were later kept in the refrigerator for about 4 months prior to the analyses. This was done to ensure that the PAHs were completely and evenly distributed in the silica gel. Again, the extraction time and temperature as well as

desorption temperature were optimized. All extractions were carried out by 10 min incubation followed by 20 min extraction with the cold fiber device and 30 min with DVB/CAR/PDMS fiber. Both fibers were desorbed at 270 ℃ for 7 min.

2.3 Results and discussion

A major setback in analyses involving the use of the cold fiber device coupled to an autosampler was the lack of complete automation. Previous versions of the device had always required human intervention in order to perform successful serial extractions of multiple samples with subsequent injections. Proper cautionary measures were needed so as to prevent any possible damage to the cold fiber needle itself and the CO_2 delivering tubing, which is in charge of maintaining the stability of the cold fiber coating temperature. As well, because the larger size of the cold fiber needle led to septa coring, any further analyses required the replacement of the injector septa intermittently, so as to prevent leakages and rubber deposition in the GC liner. Thus, the combination of these challenges limited the total number of samples that can be analyzed at a time. In order to improve the overall performance of the device, several modifications had to be made to ensure complete automation of the cold fiber device coupled to the GERSTEL® MPS 2 autosampler.

2.3.1 Modification of the automated cold fiber device

Detailed information on the design and structure of the cold fiber device has been published elsewhere [30, 54]. First, in order to prevent any possible damage of the liquid CO_2 delivery tube, the metal tubing was integrated into the GERSTEL® autosampler arm by introducing a long narrow opening on the side. This design ensured that movement of the autosampler arm would not cause any kinks in the tubing, which would impede the effective flow of the liquid CO_2. This further ensured that variations in the temperature of the cold fiber coating during extractions

were significantly minimized, and thus provided better reproducibility. In addition, to automatically control the cold fiber coating temperature, a new version of Maestro® software (1.3.7.27) was used to regulate the temperature controller. Furthermore, to integrate the cold fiber device with the GERSTEL® MPS 2 autosampler, the rubber septum of the injector was replaced by a special made SLH injector (Figure 2.4). Compared to the conventional SLH, the injector made for the cold fiber injection has a bigger hole for fixing cap and needle paths, in addition to a shorter tip for the plunger. In order to prevent the bevel needle tip from damaging the SLH Teflon needle guide, the cold fiber needle tip was modified to a blunt tip. In addition, the plunger tip of the cold fiber device was sealed by applying high electrical currents to fuse the metal, rather than the high temperature cement [30], which was not robust enough for long term use.

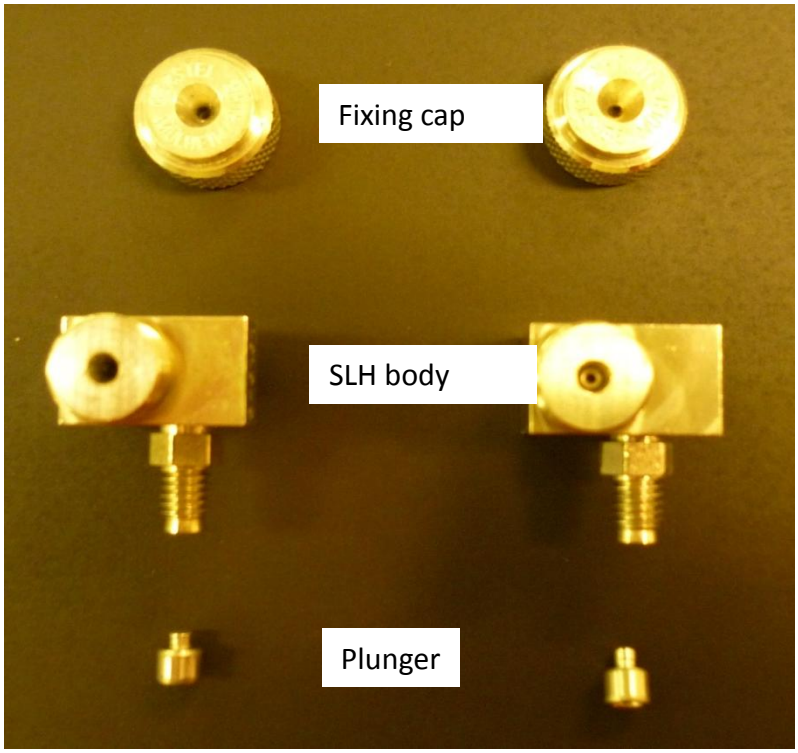

Figure 2.4 Comparison of cold fiber SLH and conventional SLH.

2.3.2 Evaluation of the new automated cold fiber device

Since this was the first time SLH was used for cold fiber injection, it was very critical to ascertain its overall performance by determining the total number of GC injections that can be made without any leakages. As mentioned in Section 2.2.2, in practice, Teflon needle guides may be damaged after many injections due to the mechanical friction between the needle tip and the Teflon needle guide. The evaluation experiment was done by headspace sampling BTEX spiked pump oil (3 g of the spiked pump oil in 20 mL vial). The extraction time and desorption time were 5 min and 2 min respectively, and the sampling temperature was 30 ℃. Each vial was sampled 10 times. All injections were done with one Teflon needle guide. Figure 2.5 shows that the SLH used in this study could be used for up to 240 injections without any leaking issues or fiber damage, compared to the septum injector which required replacement for every 15 injections [54]. Another feature of the new cold fiber setup was that the entire extraction, desorption processes and temperature were completely automated and controlled by the Maestro software.

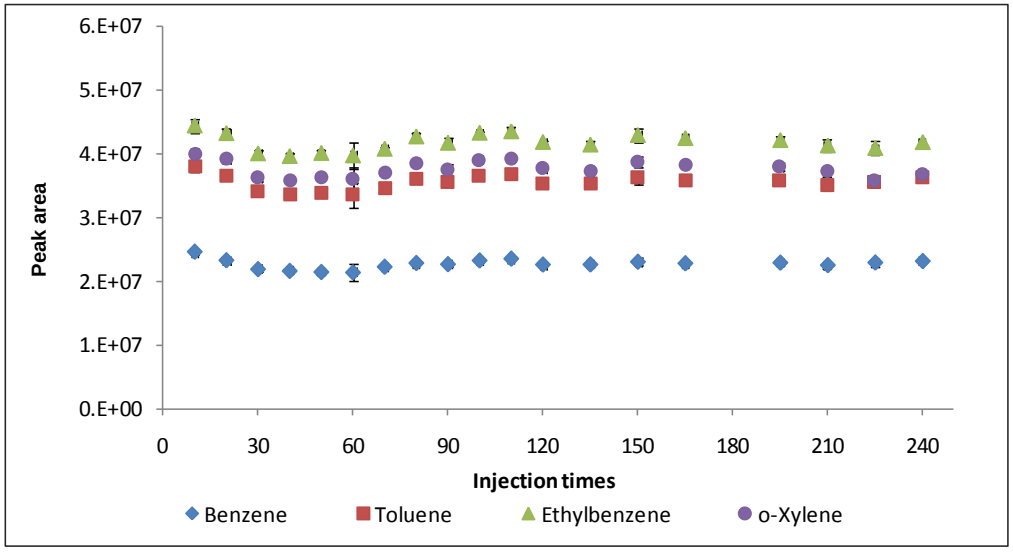

Figure 2.5 The stability of SLH for cold fiber injection

To determine the reproducibility of the system for different volatility compounds in aqueous samples, a 15 min headspace extraction of the aqueous standard samples was carried out using all 3 types of fibers (cold fiber, commercial PDMS and DVB/CAR/PDMS) while maintaining the sample temperature at 80 ℃. In the case of the cold fiber extractions, two types of experiments were performed: extractions while maintaining the coating temperature at 30 ℃ and extractions without cooling. Subsequently, each fiber was thermally desorbed in the GC injector, and the retention time as well as the peak area of each compound was determined. As indicated in Table 2.2, all the fibers recorded a similar percentage of relative standard deviation (RSD%) pattern for all the compounds extracted. Generally, volatile compounds had lower RSD% compared to semi-volatiles, which ranged from 12.5% to 32.6% for all extraction phases. The relatively high RSD% recorded for most of the semi-volatiles could be attributed to the fact that the15 min extraction was inadequate for the semi-volatiles to reach equilibrium. This is because the mass transfer of the semi-volatiles from the aqueous sample to the headspace was relatively slow, and thus required a much longer time for the analytes to migrate to the headspace. To confirm this observation, similar extractions of the compounds were performed from an empty vial spiked with these analytes. In this case, the analytes already occupied the empty vial, and thus, the extraction rate limiting step would be the relative difference in their ability to diffuse into the fiber. Generally, as shown on Table 2.2, the RSDs% for all analytes were low (≤ 13.5%), and in particular, for semi-volatiles, which were below 9%.

Table 2.2 Comparison of the peak area repeatability and retention time deviation using different fibers

	Cold fiber		DVB/CAR/PDMS		CF no cooling		Commercial PDMS		CF empty vial [a]	
Compounds	PA [b] RSD% (n=10)	RT [b] variation (min)	PA RSD% (n=10)	RT variation (min)	PA RSD% (n=10)	RT variation (min)	PA RSD% (n=10)	RT variation (min)	PA RSD% (n=10)	RT variation (min)
2-Hexanone	11.8	0.490	6.2	0.023	14.4	0.042	16.4	0.025	6.9	0.029

Ethyl butanoate	8.4	0.387	4.8	0.024	9.1	0.035	7.4	0.009	12.0	0.016
Heptanone	7.6	0.281	5.9	0.020	9.8	0.021	10.7	0.007	11.5	0.011
Heptanal	9.6	0.271	5.0	0.019	7.6	0.014	6.1	0.006	10.4	0.008
1-Heptanol	6.8	0.103	9.4	0.016	12.6	0.010	ND	0.000	9.9	0.022
Octanal	11.5	0.121	7.0	0.011	8.6	0.009	8.7	0.006	13.5	0.011
2-Nonanone	9.0	0.055	8.1	0.010	9.6	0.004	7.1	0.002	9.7	0.011
Ethyl heptanoate	8.6	0.051	6.1	0.008	7.0	0.004	6.5	0.003	9.4	0.009
Nonanal	14.1	0.052	6.9	0.008	8.3	0.003	6.1	0.004	10.0	0.014
Nonanol	11.2	0.021	11.4	0.006	14.4	0.002	6.5	0.003	9.2	0.006
2-Tridecanone	6.1	0.005	2.9	0.003	7.4	0.002	4.9	0.002	8.6	0.004
Heptadecane	27.9	0.006	19.7	0.001	29.2	0.001	12.5	0.004	7.6	0.004
2-Heptadecanone	18.3	0.007	22.5	0.001	14.6	0.003	13.3	0.003	8.8	0.003
Ethyl hexadecanoate	32.6	0.004	31.8	0.001	23.8	0.002	24.8	0.003	8.9	0.003

[a] Empty vial means the standard was spiked directly to the empty vial without aqueous medium.

[b] PA and RT represent peak area and retention time respectively.

Aqueous solution: 1 µL working solution #2 was spiked into 3 mL ultrapure water.

In addition to the peak areas of the compounds, it was essential to verify whether there were any considerable variations in the retention times of the analytes. This is because during headspace sampling of aqueous samples, the presence of moisture could affect effective extraction and/or desorption of the cooled fiber due to possible condensation of water molecules. The presence of the condensed water inside the injector leads to significant increase in pressure as a result of evaporation. The variation in retention time was estimated based on the time difference between the shortest and longest retention times of a particular analyte for 10 independent GC injections. As shown in Table 2.2, the cold fiber recorded the greatest (0.49 min for 2-hexanone) retention time shift compared to the other fibers, as expected. Relatively small retention shifts obtained for extractions performed from the empty vial and also with the same cold fiber device but without cooling also confirmed this observation. First, the extractions carried out from the spiked empty vial had no water molecules. Secondly, at elevated sample

temperatures without cooling of the coating temperature, there was no temperature gap between the fiber and the headspace, which led to condensation of the gas phase water molecules.

2.3.3 Analyzing factors that affect cold fiber extractions

The extraction efficiency of the cold fiber method primarily depends on the temperature difference between the sample matrix and the coating. When sample matrix temperatures are elevated, the mass transfer of the bulk analyte from the sample into the headspace is significantly increased. However, this lowers the distribution coefficient of the analytes between the coating and the headspace. Thus, simultaneously heating the sample and cooling the fiber is required in order to improve the overall extraction efficiency. To fully understand this phenomenon, the effect of the sample matrix and coating temperatures were investigated. This was carried out by analyzing 2-heptanone extraction time profiles at various temperature combinations between the sample matrix and fiber. The coating temperatures were set at 5 ℃, 15 ℃ and 30 ℃ ,while the sample temperatures were 30 ℃, 60 ℃ and 80 ℃ respectively. Various coating temperatures for different sample matrix temperatures were chosen since the extent to which the coating could be cooled was dependent on the sample matrix temperature. However, due to the relatively high heat enthalpy of water, at high aqueous sample temperatures, it is impractical to achieve very low fiber temperatures. Thus, the above temperature combinations were chosen based on the minimum coating temperature that could be obtained at a specific sample matrix temperature.

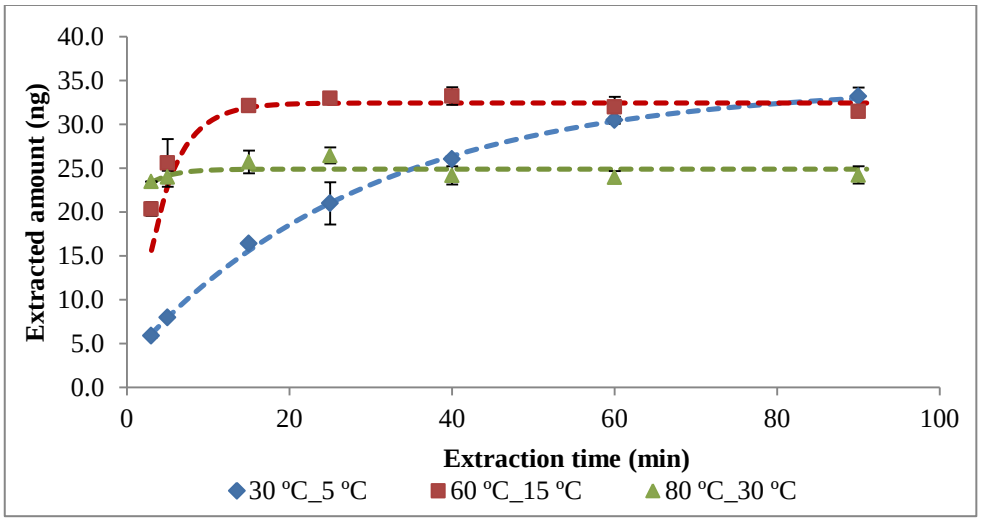

Figure 2.6 The cold fiber extraction time profiles of 2-heptanone with three different combinations of sampling temperatures. Aqueous solution: 1 µL working solution #1 was spiked into 3 mL ultrapure water. 2-heptanone total spiked amount was 145.3 ng.

As seen from Figure 2.6, an increase in the sample matrix temperature generally results in a decrease in the equilibrium time; this is due to an increase of the diffusion coefficient. For example, the equilibrium time for 2-heptanone was about 15 min at 80 ºC sample matrix temperature (with coating temperature at 30 ℃). However, when the sample temperature was reduced to 30 ℃ (with coating temperature at 5 ℃), the analyte could not reach equilibrium even after a 90 min extraction. As well, the amount of analyte extracted at equilibrium was mainly affected by the fiber coating temperature, as it primarily determined the distribution coefficient. At lower coating temperatures, relatively higher amounts of the analyte would be extracted at equilibrium. As shown in Figure 2.6, the equilibrium extracted amount increased from 26 ng to 33 ng when the coating temperature decreased from 30 ℃ to 15 ℃. Still, a fiber temperature ≤ 0 ºC could not be used for analysis of the aqueous sample, due to the formation of ice on the surface of the coating: the ice formation prevented the plunger from retracting into the needle, and thus resulted in damage to the plunger tip. As well, it must be noted that cooling the coating

to such low temperatures would lead to a decrease in the diffusion of the analytes in the coating, thus lowering the mass uptake and extending the equilibrium time.

In addition to the extraction time profiles, extraction temperature profiles were also obtained (Figure 2.7) to ascertain the effect of temperature differences between the sample matrix and the cold fiber coating. To obtain these profiles, 40 min aqueous extractions of the 14 compounds were performed using the cold fiber device and commercial fibers at varying sample matrix temperatures. Figure 2.7A displays a temperature profile that has not been obtained by traditional SPME fibers. The cold fiber extracted amount for all compounds, including volatiles and semi-volatiles, increased as the sample matrix temperature increased. This result verified that the temperature gap between the coating and the sample matrix enhanced the distribution coefficient, which was predicted by the theoretical calculation (Equation 2.1). For traditional SPME methods, since the fiber cannot be cooled down when the sample matrix is heated, a typical extraction temperature profile is similar to Figure 2.7B. Generally, for volatile compounds that reached equilibrium, the extracted amount decreased as the sample temperature increased due to the decrease of the distribution coefficient. In the case of the semi-volatile compounds that were extracted via pre-equilibrium extraction, the extracted amount initially increased as a result of the high Henry constant, and then decreased because the distribution coefficient decreased. In conclusion, the cold fiber temperature profile demonstrated that this device had advantages for high temperature sampling. However, although a general increase in sample matrix temperature resulted in higher extraction efficiency, extreme caution must be taken so as to not heat aqueous samples to temperatures close to the boiling point of water under atmospheric conditions. A high temperature will build up excessive pressure inside the closed vial as a result of the water vapor expansion. Care must therefore be taken during optimization to

select appropriate sample and fiber temperatures required to improve extraction efficiency. Last, it is important to note that this optimization process becomes more challenging when a mixture of volatiles and semi-volatiles is present in the sample.

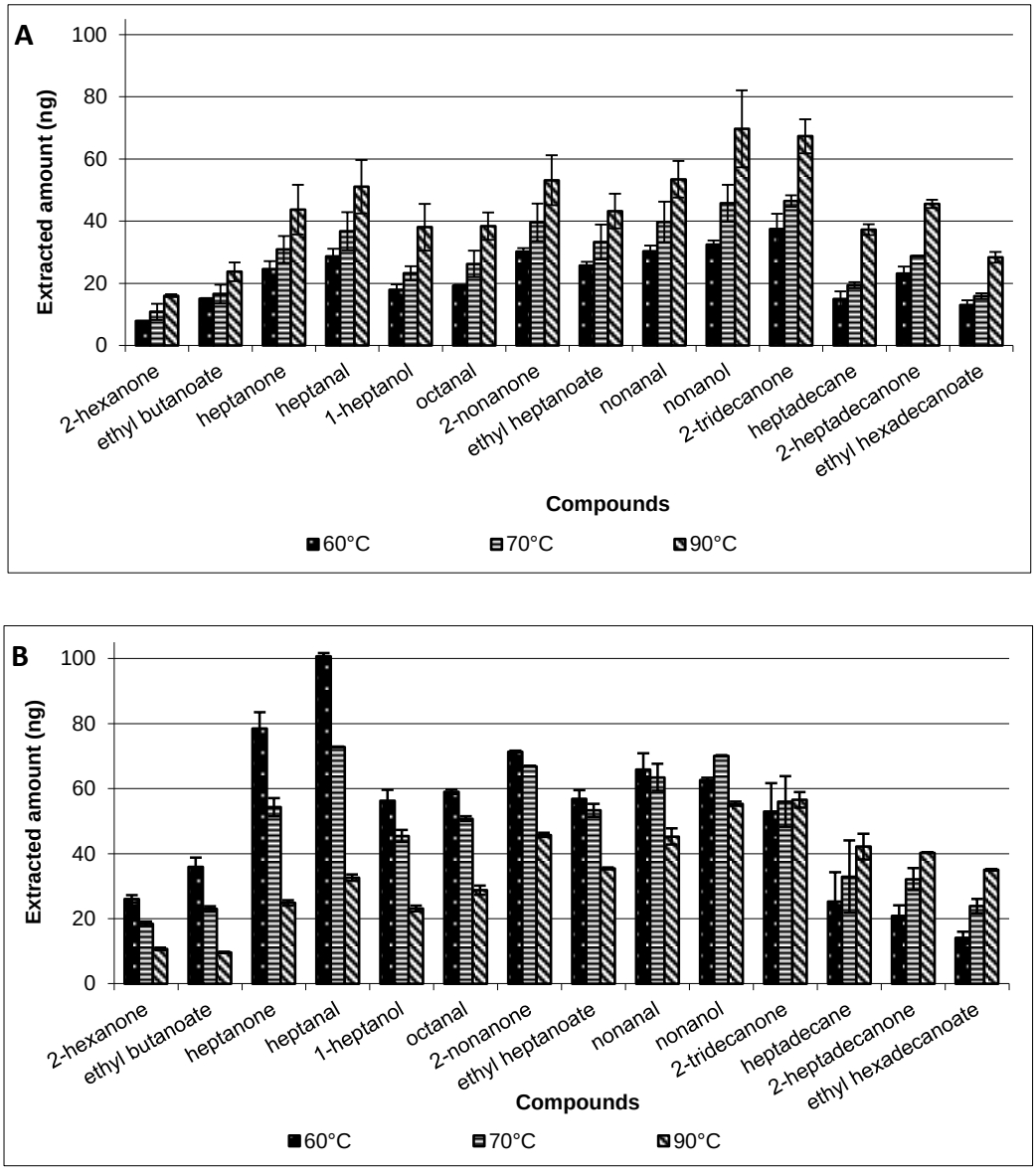

Figure 2.7 Extraction temperature profile of (A) cold fiber and (B) DVB/CAR/PDMS fiber for aqueous sampling. Cold fiber coating temperature, 35 ℃. Aqueous solution: 1 µL working solution #2 was spiked into 3 mL ultrapure water.

2.3.4 Comparison of extraction efficiency of cold fiber device with commercial PDMS fiber

The extraction efficiencies of the cold fiber device and the commercial PDMS fiber were compared by sampling the aqueous standard sample containing the 14 compounds, using optimized sampling conditions. In the case of the cold fiber device, two types of extraction protocols were used: headspace extractions while maintaining a low coating temperature, and extractions without cooling the coating. Forty minutes extraction was conducted for the PDMS commercial fiber as well as the cold fiber without cooling, with sample matrix temperature set at 70 ℃. In the case of cold fiber extractions with cooling, the fiber was maintained at 35 ℃, while the sample temperature was 90 ℃. Results obtained for the cold fiber extraction efficiency significantly exceeded those for the commercial PDMS (Figure 2.8). The most prominently extracted were volatile compounds, where the amounts extracted by the cold fiber device were about 4 to 7 times higher than that extracted with the commercial PDMS. The relatively small differences in the extracted amount of semi-volatile compounds (2-tridecanone, heptadecane, 2-heptadecanone and ethyl hexadecanoate) by both the cold fiber and the commercial PDMS could be attributed to the slower mass transfer properties of the semi-volatiles from the aqueous medium to the headspace. The situation can be improved with longer extraction times. However, care must be taken not to cause loss of volatile compounds as a result of prolonged extractions at elevated temperatures. Also, it is possible that at lower coating temperatures, the condensation of the water molecules at the surface of the coating may have decreased the mass transfer of the semi-volatiles, which are more hydrophobic than the volatile compounds. As a proof of concept, the extraction efficiency of the cold fiber device with cooling of the coating temperature was significantly higher than all extractions performed without cooling of the fiber. This is observed because of the simultaneous elevated sample temperatures and lower coating temperatures,

which lead the distribution coefficient of each of the analytes to increase, thus leading to an overall improvement in the extracted amount.

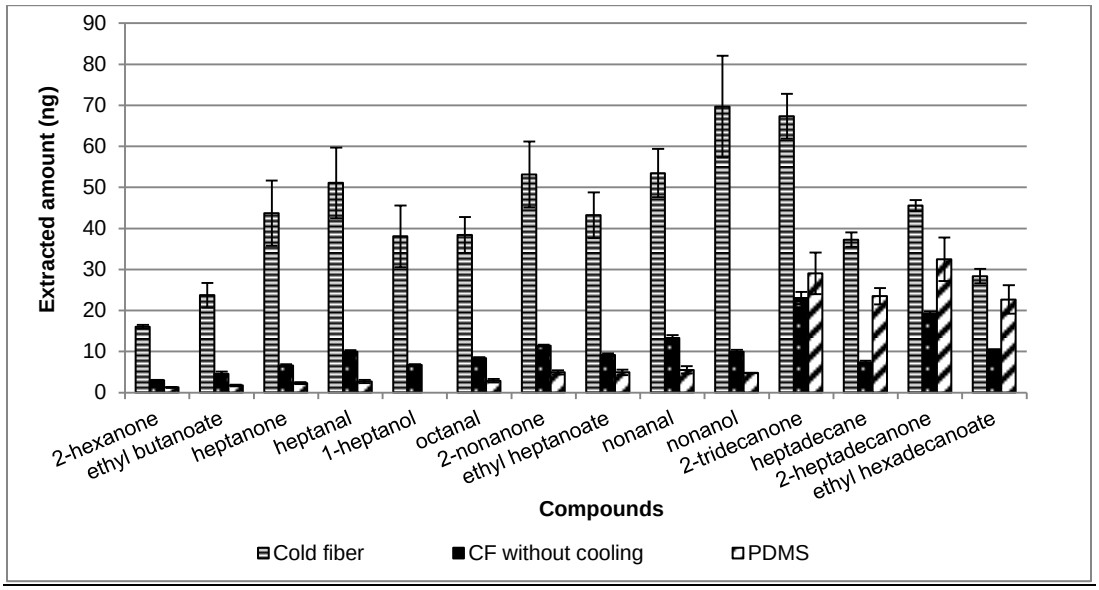

Figure 2.8 Comparison of extraction amount of cold fiber, cold fiber without cooling and commercial PDMS fiber for 14 compounds under the optimized conditions for each fiber. These extractions were performed with a solution spiked with 1 µL working solution #2 into 3 mL ultrapure water.

2.3.5 Extraction of analytes from solid matrices using the automated cold fiber device

Headspace extractions of analytes from solid matrices, such as soil samples, require the use of elevated temperatures. For solid samples, the analytes are usually trapped/adsorbed into the core of the solid micro-phase. Thus, higher temperatures, in certain cases over 100 ℃, are employed so that the analytes can overcome the energy barrier, and release from the core of the solid samples and into the headspace. However, at such elevated temperatures, the distribution coefficient of the analyte in the extraction phase (commercial fiber) would be significantly reduced, therefore lowering the extraction efficiency of the method. The cold fiber approach provides an effective alternative for analysis of solid samples at high temperatures by maintaining the coating at a low temperature, thus improving the distribution coefficient. In

order to ascertain this, a cold fiber device and a commercial DVB/CAR/PDMS were used for headspace extractions for PAHs from a silica gel matrix. The DVB/CAR/PDMS was chosen because it showed better extraction efficiency towards a large range of volatility compounds when compared to other commercially available fibers. The extraction temperature profiles of 7 PAHs were subsequently obtained for both fibers. As can be observed from the results found in Figure 2.9A, an increase in temperature led to an increase in the extracted amount of PAHs. Cold fiber recorded 2-6 times higher extraction efficiency for all the compounds when compared to DVB/CAR/PDMS coating, with the temperature profile of DVB/CAR/PDMS performing as expected from traditional SPME theory. For naphthalene, acenaphthylene, acenaphthene and fluorene, the amounts extracted by DVB/CAR/PDMS increased and then subsequently decreased when the sample extraction temperature was higher than 160 ºC, due to the decrease of the distribution coefficients. For less volatile compounds such as fluoranthene and pyrene, the extraction efficiency increased as the temperature increased. This revealed that high temperatures helped release more compounds from the silica gel.

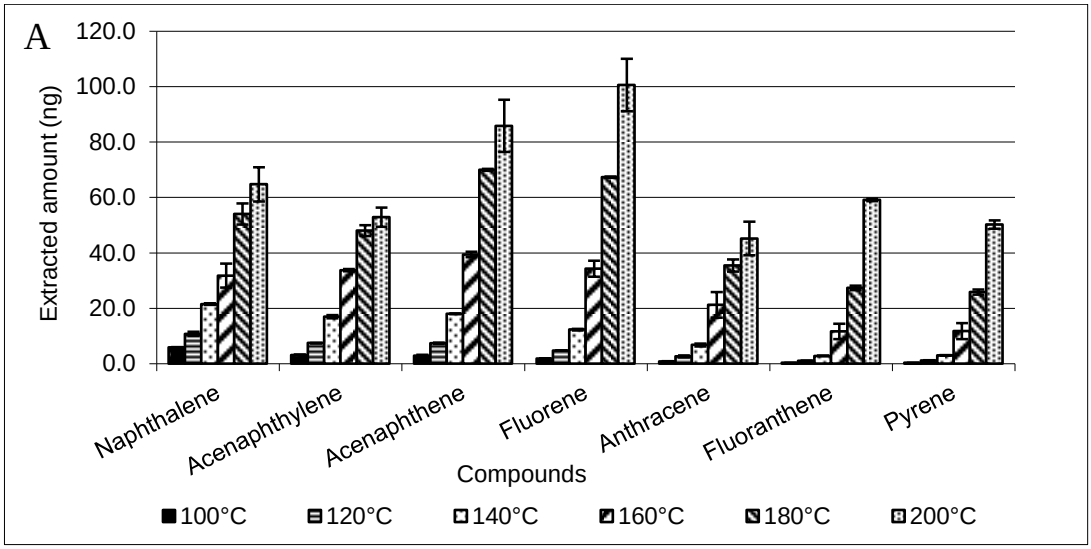

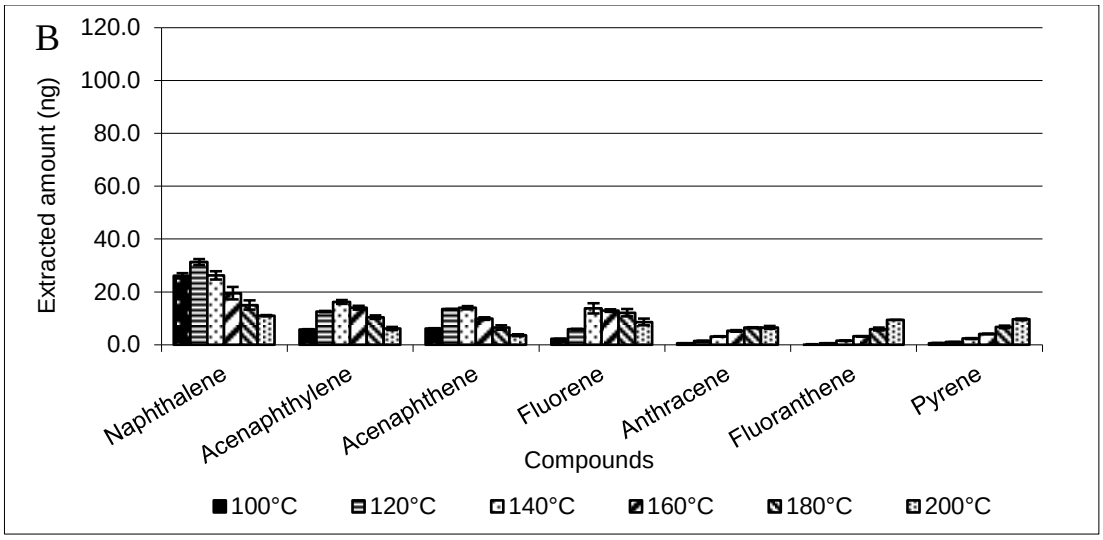

Figure 2.9: Extraction temperature profile of 7 PAHs in silica gel samples using (A) cold fiber device and (B) DVB/CAR/PDMS fiber. Extraction time for cold fiber, 20 min; for DVB/CAR/PDMS, 30 min. Cold fiber coating temperature: 40 ℃

2.3.6 Analytical figures of merit

The linear dynamic range and LOD of cold fiber and commercial fibers were investigated and compared. The calibration curve was done by extracting from seven different concentrations solutions ranging from 0.5 ng/mL to 200 ng/mL. The LOD was calculated based on the calibration curve. Results showed that the linear dynamic range for the proposed automated cold fiber device ranged from 0.5 ng/mL to 100 ng/mL, with a linear regression coefficient ≥ 0.9963 for all compounds. The LOD for all analytes ranged from 1.0 ng/mL to 9.4 ng/mL (Table 3). In comparison with the commercial DVB/CAR/PDMS, the automated cold fiber device recorded wider linear dynamic range and lower LOD for semi-volatile compounds such as nonanol, 2-tridecanone, heptadecane and 2-heptadecanone. Although the commercial PDMS also showed a large linear range, the LOD were relatively higher than that of the automated cold fiber device.

Table 2.3 Comparison of cold fiber aqueous sampling calibration curve linear range and LOD with commercial PDMS and DVB/CAR/PDMS fiber

	Cold fiber			PDMS			DVB/CAR/PDMS		
	Linear range (ng/mL)	R^2	LOD (ng/mL)	Linear range (ng/mL)	R^2	LOD (ng/mL)	Linear range (ng/mL)	R^2	LOD (ng/mL)
2-Hexanone	4.8-95.7	0.9976	7.3	47.8-191.4	0.9955	23.9	9.6-47.8	0.9999	0.8
Ethyl butanoate	5.0-100.0	0.9990	4.7	25.0-200.0	0.9975	15.8	0.5-10.0	0.9999	0.2
2-Heptanone	0.5-96.9	0.9995	2.9	4.8-193.7	0.9953	18.9	0.5-9.7	0.9999	0.3
Heptanal	0.5-96.5	0.9999	1.4	4.8-192.9	0.9972	14.0	0.5-24.1	0.9831	6.1
1-Heptanol	0.8-94.1	0.9996	2.2	19.8-158.7	0.9940	23.3	39.7-158.7	0.9880	39.3
Octanal	0.5- 94.1	0.9992	4.1	4.7-188.2	0.9945	20.8	0.5-23.5	0.9975	2.3
2-Nonanone	0.5-95.3	0.9996	2.7	1.0-190.6	0.9972	14.0	0.5-47.6	0.9982	3.3
Ethyl heptanoate	0.5-93.9	0.9999	1.1	0.9-187.8	0.9959	16.7	0.5-47.0	0.9986	3.0
Nonanal	0.5-93.5	0.9995	3.1	9.3-186.0	0.9940	22.8	0.9-46.5	0.9995	2.0
Nonanol	0.5-106.4	0.9998	1.8	10.6-212.7	0.9904	28.8	10.6-212.7	0.9973	15.3
2-Tridecanone	0.7-140.7	0.9999	1.3	1.4-281.4	0.9969	14.5	1.4-140.7	0.9981	6.5
Heptadecane	0.6-112.2	0.9998	1.0	11.2-112.2	0.9956	10.3	1.1-56.1	0.9662	16.2
2-Heptadecanone	4.7-46.7	0.9985	9.4	9.3-186.7	0.9977	12.4	9.3-93.3	0.9987	12.8
Ethyl hexadecanoate	4.9-48.9	0.9963	5.8	9.8-195.5	0.9963	17.7	1.0-48.9	0.9948	6.2

The extraction conditions for cold fiber: extraction time, 15 min, extraction sample temperature, 80 ℃ and fiber temperature 30℃.
The extraction conditions for the PDMS and DVB/CAR/PDMS: extraction time, 25 min, extraction temperature, 60 ℃ for both sample matrix and fiber temperature.

2.4 Summary

A fully automated cold fiber device coupled to the GERSTEL® MPS 2 autosampler has been developed and thoroughly evaluated. For the first time, the use of a septumless injector device was made possible, allowing for the analysis of a larger number of samples without the need for human intervention, and thus improving throughput and overall cost. Evaluation of the device revealed a very robust and reliable automated device, which was successfully applied in the analysis of both volatiles and semi-volatiles with varying polarities from different sample matrices (aqueous and solid samples). Further improvement of the device setup is possible by completely integrating the temperature controller into the autosampler device. Additionally, the cold fiber device configuration limits the types of coating that can be used. Still, the device

creates a platform for high throughput headspace GC analysis of various compounds from different matrices.

Chapter 3 **Development of a Non-invasive and Convenient Method for Skin Volatile Compounds Sampling**

3.1 Introduction

3.1.1 Significance of skin volatile compounds sampling

Volatile organic compounds emitted from human skin carry useful signalling information pertaining to a variety of biological functions. For example, unsaturated acids, 2-methyl C6-C10 acids, and 4-ethyl C5-C11 acids, along with (E)-3-methyl-2-hexenoic acid, are said to be major odour-causing compounds [125]; 2-nonenal detected from the skin is an age-specific component [126], and acetone is related to diabetes and ketogenic conditions [127, 128]. VOCs have also been studied as potential mosquito attractants [129, 130], indicators of seasonal changes [131] and moderators of fragrances [132]. This important information, found on the volatile profiles of our skin, has broad applications and can be used to find specific biomarkers to diagnose, manage and assess a variety of disorders [133-135]. Therefore, development of an effective and non-invasive skin volatile collection method is of paramount interest. As well, the low concentration of VOCs on biological surfaces requires the development of a preconcentration step to enrich the target components for quantitative and/or qualitative analysis [136].

3.1.2 Traditional methods for skin volatiles sampling and their limitation

Reported methods for the collection of human skin volatiles involve the use of organic solvents [137, 138], cotton pads [139, 140], glass beads [129, 130, 141], solid phase microextraction (SPME) fiber [131, 134, 137, 140] and the stir bar [142, 143] as the extraction phase.

For organic solvent sampling [137, 138], a glass cylinder with a suitable diameter that covers the sampling area is used to hold the organic solvent on the skin surface. After extraction, the extracted organic solvent is withdrawn from the cylinder using a syringe and directly injected into the analytical instrument for separation and quantification. The major issue for this sampling method is the invasive property of the organic solvent that may cause the irritation on the skin. Relative low sensitivity is another issue limiting the application of this method: the organic solvent dilutes the concentration of the emission analytes to a certain extent.

Cotton pad and glass bead sampling are two materials used to overcome the limitations of the organic solvent. Cotton pads can directly collect sweat from skin and desorb it in the organic solvent for solvent injection [139], or be placed inside a container and be sampled by another sampling tool such as SPME [139, 140]. Glass bead sampling requires a glass cylinder to hold the glass bead during sampling, and can be desorbed directly into a high temperature GC injector [129, 130, 141]. The limitation of these two extraction phases is their low capacity toward the sampling compounds, resulting in low sensitivity.

SPME fiber and stir bar sampling have been reported as simple, sensitive and non-invasive approaches in skin VOCs sampling. Particularly, SPME fiber can be used for *in vivo* or *in vitro* skin sampling. Generally, for *in vivo* sampling, the SPME device is fixed on top of the skin surface by using a facilitating device such as a vial without a bottom. The vial is pressed on top of the surface while the fiber is placed on top of the vial cap during sampling [137]. For *in vitro* sampling, a skin biopsy [134] or another medium that collects skin sweat should be collected and placed inside the sampling vial for SPME sampling [140, 144]. The major advantage of SPME fiber is its convenient thermal desorption into GC for analysis.

The stir bar sample preparation technique was introduced to improve the sensitivity of the SPME fiber by increasing the volume of the extraction phase. To utilize the stir bar for skin volatiles sampling, Soini *et al*. developed a roller device to handle the stir bar during sampling [142]. The authors demonstrated its use for qualitative detection of VOCs from human fingerprints. For quantification purposes, the stir bar can be spiked with suitable internal standards. The main disadvantages of using the stir bar are the difficulties associated with handling the device during direct sampling due to its cylinder geometry, and the possible introduction of air contamination during sampling. Furthermore, headspace sampling is difficult to achieve by stir bar.

3.1.3 Advantages of TFME for skin volatiles sampling

The TFME (sorptive tape extraction) method has significant advantages when compared to traditional methods. First of all, the high volume extraction phase results in high sampling sensitivity. This is important when volatile compounds found in skin are present mainly at trace levels. Second, the flat geometry of the thin film provides great flexibility for skin *in vivo* sampling. Both headspace and direct contact sampling are easy to conduct, and both methods avoid air contamination. Finally, thin film sampling can be directly coupled with the GC instrument for analysis after sampling.

This sampling technique has been used to study skin conditions after the application of cosmetics [75]. Results were compared with the lipid index obtained using a sebumeter, and a good linear correlation between these two techniques was found. In terms of profiling human skin volatiles, a “skin-patch method” utilizing PDMS membrane to identify the biomarkers of chronic wounds was described [77, 145].

Direct contact sampling and headspace sampling were both implemented for thin film surface sampling. In direct contact mode, the membrane was placed on top of the skin surface without a barrier between the thin film and the skin. Components generally present on skin surface include volatile compounds, lipids and dust, and could be absorbed by the thin film. These lipids together with dust could contaminate the GC injector, column and MS, which would require periodical clean up [142]. In addition, the high intensity of the contamination peaks may mask the potential trace biomarker. Headspace sampling prevents this contamination from happening by introducing a medium/barrier between the extraction phase and the skin. To achieve this, Bicchi *et al*. [146] developed a headspace sampling holder shown in Figure 3.1a to sample VOCs released from agricultural products, plant materials, and bird feathers. As well, Sekine *et al*. [85] developed a headspace sampler to determine the emission fluxes of potential biomarkers from human skin by placing a piece of membrane inside a Petri dish (Figure 3.1b). During sampling, the Petri dish was placed on top of the skin surface. The compounds emanating from the skin diffused through the headspace of the dish and were absorbed by the membrane.

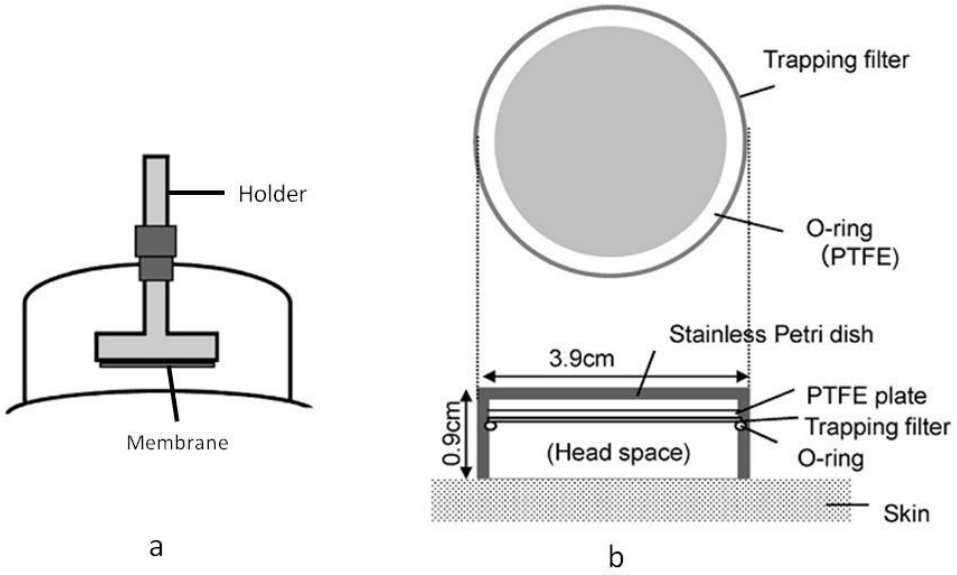

Figure 3.1 The reported headspace sampling holder for skin volatile compounds sampling [146] [85]. Figure reprinted from reference with permission of publisher.

3.1.4 The motivation and objective of the current work

In this project, a simple and reproducible headspace sampling method was introduced. In order to reduce contamination of the thin film by skin lipids, a piece of stainless steel mesh was used to separate the thin film from coming into contact with the skin. To investigate what factors influenced the reproducibility of the method, an in vial sampling set-up was employed. Additionally, optimized storage conditions before and after sampling were investigated to minimize analyte loss and prevent contamination during transportation. Thus, the developed method was applied *in vivo* first to identify the dietary skin biomarkers after garlic and alcohol ingestion, and then in the study of the VOCs composition released from different locations of the human body.

3.2 Experimental

3.2.1 Reagents and supplies

Twelve target compounds listed in Table 3.1 were purchased from Sigma-Aldrich (Mississauga, ON, CA). These compounds were used for evaluation of the proposed method and instrument quality control. Most of these compounds were found in skin emissions reported in the literature, and are potential biomarkers for melanoma biopsy sampling [134]. Inland 45 pump oil was purchased from Agilent (Agilent Technologies, CA, USA) and the 60/80 mesh DVB particles were purchased from Ohio Valley (Marietta, OH, USA).

A piece of PDMS membrane with a thickness of 254 μm was obtained from Specialty Silicone product (Ballston Spa, NY, USA). The membrane was cut into a round shape with a diameter of 6 mm using a metal tubing pressing against the membrane. The membrane was preconditioned in a vacuum oven for 3 hours at 120 ℃, and then transferred to the GERSTEL®

thermal condition tube. The membrane was baked under nitrogen flow for 2 hours at 200 ℃ and 3 hours at 250 ℃. Before sampling, the membrane was again conditioned in a GERSTEL® twister desorption unit (TDU) for 1 hour at 250 ℃ to remove potential contaminants and to obtain a reasonable clean baseline that has no contamination, with the exception of some small siloxane peaks. These siloxane peaks are unavoidable due to the large amount of extraction phase.

The stainless steel mesh was purchased from Small Parts (Logansport, IN, USA) and the aluminum foil was from Morfoil (Montreal, QB, CA). Micropore surgery tape used to fix the aluminum foil on the skin was from 3M (London, ON, CA). Twenty millilitre clear vials with screw top and Teflon coated silicone septa were provided by Supelco (Bellefonte, PA, USA).

3.2.2 Instrumentation

The instrument used for separation and quantitation was an Agilent 6890 GC and a 5973 quadrupole MS (Agilent Technologies, CA, USA) coupled with a GERSTEL® cooled injection system (CIS) and twister desorption unit (TDU) (GERSTEL GmbH, Mullheim, GE).

The TDU is connected to the CIS, which serves both as a cryo-focusing trap and a temperature programmed GC inlet. After sampling, the membrane is inserted into the TDU tube by tweezers (Figure 3.2a), and placed in the TDU tray. The autosampler subsequently picks up the tube from the tray and injects into the TDU body, which was kept at a relative low temperature originally (Figure 3.2b). As the TDU temperature increased, the analytes desorbed from the membrane and cryo-focused on the CIS injector, which is set at a low temperature. After membrane desorption, the CIS is heated and the analytes are desorbed into the column.

Solvent vent carry gas flow mode is the most often used mode for TDU desorption. In this mode, the CIS injector split vent is open during the TDU desorption period, and a carrying gas with high flow rate passes through the membrane to improve the desorption efficiency. Because the CIS injector is cooled down during TDU desorption, even though the split mode is open, all the analytes can be trapped in the inlet without loss, if a proper trapping temperature is utilized. The cooling source for this CIS system is liquid nitrogen, which can cool the system down to −150 ℃. After TDU desorption, the CIS split or splitless mode can be chosen to introduce the analytes into the column. Split mode was used for large injection amounts while the splitless mode was more suitable for trace amounts of analyte injection.

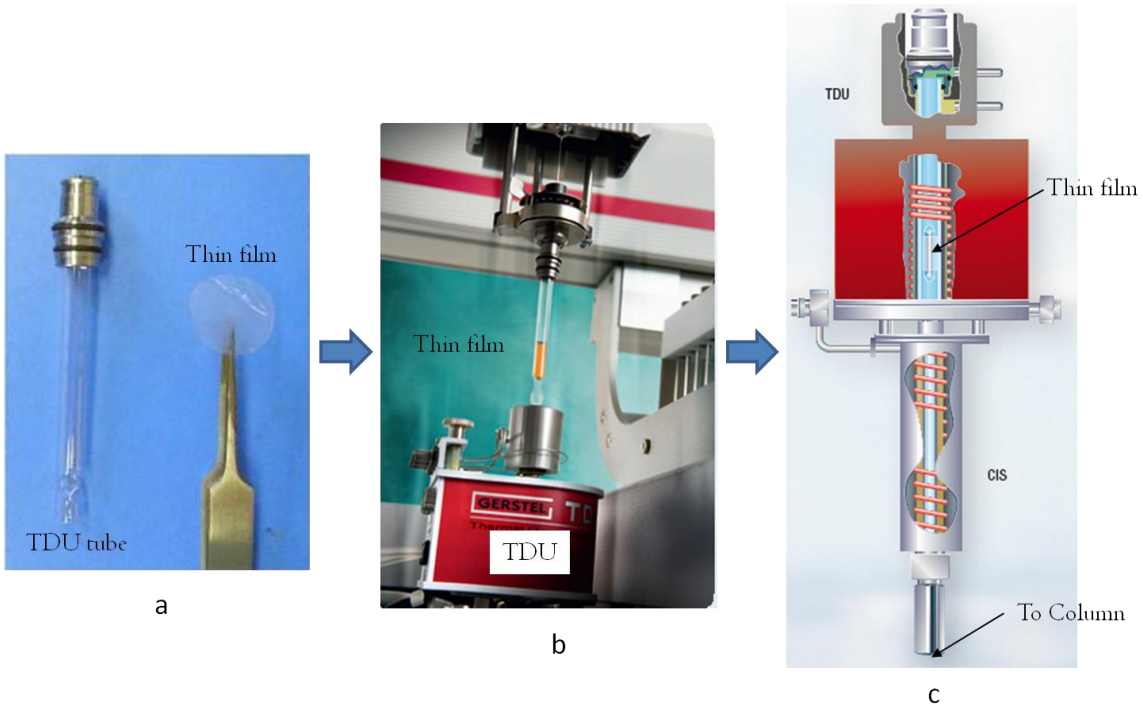

Figure 3.2 The diagram of thin film TDU injection. (Figure from GERSTEL® website)

The desorption temperature program was held at 25 ℃ for 1 min and then ramped to 250 ℃ with a rate of 700 ℃ /min, then held for 3 min. The TDU liner was retained in the injector after

desorption and set at 220 ℃ during the GC running. The CIS injector was initially maintained at -120 ℃ and ramped to 280 ℃ with a rate of 12 ℃/s. The CIS injection mode was splitless.

Chromatographic separation was performed using a 30 m × 0.25 mm I.D, 0.25 µm thickness SLB^{TM}-5 fused silica column (Sigma-Aldrich, Mississauga, ON, CA) and a 30 m × 0.32 mm I.D, 1.8 µm thickness Restek RK13870 for the volatile compounds column (Chromatographic Specialties Inc., Brockville, ON, CA). Helium was used as carrier gas at a flow rate of 1 mL/min and 1.5 mL/min for Supelco and Resteck column respectively. The column temperature was initially held at 40 ℃ for 2 min, increased to 250 ℃ with a rate of 5 ℃/min, then kept for 16 min.

The MSD transfer line temperature was set at 280 ℃ while the MS Quad and MS source temperature were set at 150 ℃ and 230 ℃, respectively. The MS system was operated on electron ionization (EI) mode, and mass fragments were collected in the m/z 30- 300 range.

The AMDIS (Version 2.71) (Automated Mass Spectral Deconvolution and Identification System) is a computer program that extracts spectra for individual components in a GC/MS data file, and identifies target compounds by matching these spectra against a reference library. It was developed at NIST (National Institute of Standards and Technology) with support from the United States Department of Defense, and is freely available. By using this software, the chromatograms can be deconvoluted and the overlapped peaks can be detected. In addition, a custom library can be used to search the target compounds.

3.2.3 In vivo set-up for thin film sampling of skin volatiles

The thin film sampling approach for skin volatiles is shown in Figure 3.3. First, a piece of stainless steel mesh was used to separate the membrane from the skin surface. Next, the PDMS membrane was placed between two pieces of stainless steel mesh. Here, the mesh should be thin

enough to be flexible and larger than the membrane in size. The bottom mesh was used to separate the membrane from coming into contact with the skin, while the top one fixed the membrane to prevent it from moving. The mesh was first sonicated for ½ hour in pure methanol, and then in acetone. After sonication, it was baked at 180 ℃ for ½ hour. A piece of 3x3 cm aluminum foil paper was placed on top of the stainless steel mesh. The aluminum foil paper was wiped by Kimwipe soaked in methanol, and baked at 180 ℃ for 1 hour before use. A PDMS membrane protected by meshes was placed on the chosen skin spot for sampling, and covered by an additional piece of aluminum foil, then finally affixed by surgery tape. Both pieces of aluminum foil were used in order to protect the membrane from environmental air contamination.

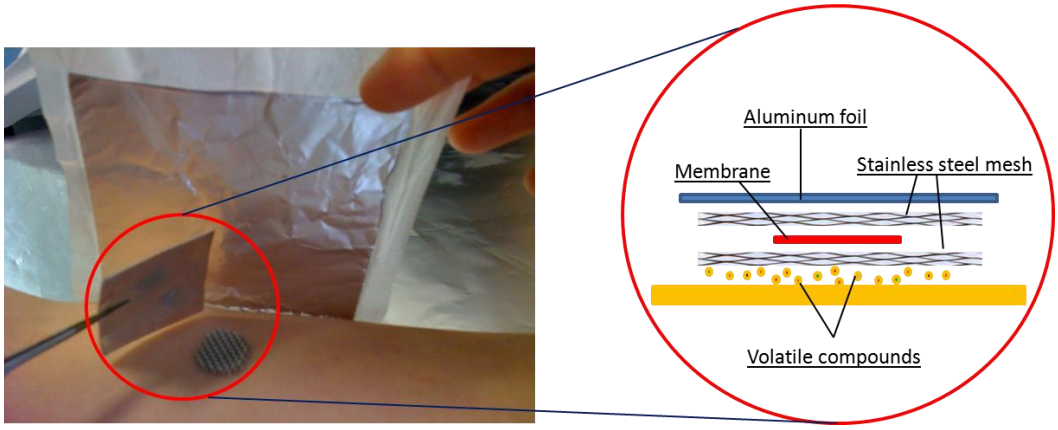

Figure 3.3 Schematic diagram of the membrane *in vivo* sampling device used for skin volatiles sampling

3.2.4 In vial sampling set-up for evaluation of thin film skin volatiles sampling

This experimental set-up was introduced to evaluate the performance of the proposed skin volatile sampling approach and the instrument response. Figure 3.4 shows the schematic diagram of the sampling set-up. In order to simulate skin emission, pump oil spiked with target compounds was used as the sample matrix. The use of pump oil to generate a standard gas has been previously reported by our group [147]. However, the concentration of highly volatile compounds in the headspace was too high due to a high Henry constant. To reduce the headspace

concentration of highly volatile compounds, DVB particles were added. For semi-volatile compounds, the headspace concentration was increased by spiking larger amounts of pure compounds. The amounts use for different compounds spiked into 10 g pump oil and 4.5 g DVB particle after optimization occurred are listed in Table 3.1. Each target compound was separately spiked into the pump oil and DVB particle mixture, and then the vial was closed and agitated for 24 hours at 40℃. Lower incubation temperatures required longer agitation times so as to ensure equilibrium of the system. During sampling, the vial was kept in 40 ℃ agitator.

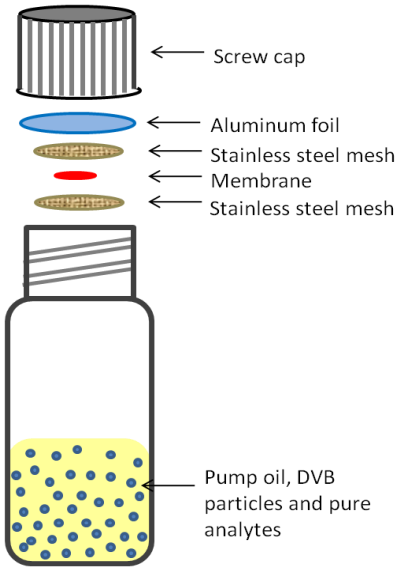

Figure 3.4 The in vial sampling set-up for evaluation of the proposed skin volatiles thin film sampling approach.

3.3 Results and discussion

3.3.1 Reproducibility of the sampling of skin volatile compounds

The reproducibility of the sampling approach is an important parameter for quantitative analysis. Both *in vial* and *in vivo* experiments were designed to fully investigate the factors that affect the reproducibility.

In vial sampling was conducted using the set-up protocol described in Section 3.2.4. The reproducibility of the intra- and inter- membrane sampling is shown in Table 3.1. The intra-membrane reproducibility, expressed as RSD%, was less than 9.8% (n=6) for all the compounds, indicating that our sampling design was reproducible. In addition, inter-membrane reproducibility revealed a RSD% lower than 8.2% for all the compounds. This result is important and significant for future clinical applications where the membranes are used only once. Good reproducibility of the inter-membrane sampling approach provides results that are comparable for different samples. In addition, small RSD% for inter-date sampling (fifth column in Table 3.1) proves that the *in vitro* sampling set-up is highly reproducible, and can be used as a standard gas generator for other purposes.

Table 3.1 The reproducibility of the skin sampling set-up.

Compounds	Spiked amount (mg)	Inter-membrane RSD% (n=7)	Intra-date/membrane RSD% (n=6)	Inter-date RSD% (n=7)
Hexanal	1	4.8	2.5	3.1
Ethylbenzene	0.5	5.1	4.3	2.3
p-Xylene	0.5	4.8	3.4	*2.2*
o-Xylene	0.5	4.5	3.1	2.0
Decane	0.5	3.7	2.2	2.7
Octanal	3	7.4	9.8	9.6
D-limonene	0.5	3.6	2.1	2.6
Undecane	1	3.5	4.0	3.4
Nonanal	3	8.2	8.1	8.5
Dodecane	1.5	4.0	5.5	4.5
Decanal	3	5.0	4.6	5.4
Tridecane	3	4.6	6.9	5.2

VOCs emanating from skin are influenced by both the environment and by the metabolism of the individual. The reproducibility of the proposed approach was evaluated for *in vivo* sampling as well. Two experimental designs were employed. The first design included sampling of four membranes in parallel for 60 min, and then analyzing the four membranes in turn. In between analyses, the other sampled membranes were stored in dry ice, as previously described in Section 3.3.4. In the second design, each membrane was sampled and analyzed immediately after sampling. Each sampling lasted for 60 min and four membranes were used. Reproducibility results of these two designs are shown in Table 3.2.

The 8 obtained chromatograms were analysed using the AMDIS software. The deconvoluted peaks were searched by the NIST02 MS library. Twenty three compounds detected in all chromatograms are listed in Table 3.2. The reproducibility of the *in vivo* sampling approach was lower than the reproducibility of the *in vial* sampling approach. This result was expected, since the concentration of skin volatile compounds is very low, which allows for higher RSD% between samples. In addition, for some semi-volatile compounds, a 60 min sampling time was not sufficient to reach partition equilibrium.

Comparison of the observed RSD% for the two *in vivo* sampling designs shows differences for most of the compounds. This result demonstrated that variation of the sampling efficiency was not only influenced by the sampling design, but also by the environmental conditions. For sequential sampling, the environmental conditions varied, and in particular temperature, which could significantly affect the extraction efficiency of volatile compounds. This result indicates that well-control the sampling environment is a critical step for the real sample analysis. On the other hand, some semi-volatile compounds could have accumulated on the skin surface after releasing from the skin. For semi-volatile compounds such as nonadecane, the extraction

amounts from the same spot decreased as the number of sampling times increased. This observation not only confirms the assumption that semi-volatile compounds accumulate on the skin after being released, but it also indicates that skin pre-treatment prior to sampling should be taken into account when interpreting the concentrations of these semi-volatile compounds.

Table 3.2 Comparison of the reproducibility of two *in vivo* sampling designs

Chemical Name	**CAS No.**	**Same sampling time RSD% (n=4)**	**Different sampling time RSD% (n=4)**
Hexanal	66-25-1	8.6	13.0
Nonane	111-84-2	1.8	27.5
Heptanal	111-71-7	9.6	23.9
5-Hepten-2-one, 6-methyl-	110-93-0	9.7	17.6
Decane	124-18-5	6.6	7.7
Octanal	124-13-0	9.8	9.9
Nonanal	124-19-6	13.0	13.2
Cyclooctane, methyl-	1502-38-1	14.4	13.3
Decanal	112-31-2	6.1	5.6
3',4',5,7-Tetramethoxyflavone	855-97-0	12.4	10.6
Undecanal	112-44-7	1.1	6.8
Dodecanal	112-54-9	7.9	12.8
5,9-Undecadien-2-one, 6,10-dimethyl-	689-67-8	9.8	21.1
1-Dodecanol	112-53-8	13.3	12.2
Propanoic acid, 2-methyl-, 1-(1,1-dimethylethyl)-2-methyl-1,3-propanediyl ester	74381-40-1	13.8	15.7
Isopropyl Myristate	110-27-0	17.0	26.1
4,8,12-Tetradecatrienal, 5,9,13-trimethyl-	66408-55-7	5.0	28.9
Galaxolide	1222-05-5	21.9	25.5
Nonadecane	629-92-5	8.0	17.7
Hexadecanoic acid, methyl ester	112-39-0	20.3	18.7
Phthalic acid, butyl 2-pentyl ester	ND	24.8	29.5
Eicosane	629-94-7	7.1	40.3
Isopropyl Palmitate	142-91-6	13.3	63.8

3.3.2 Comparison between headspace and direct contact sampling

The main feature of the developed skin sampling approach is its simple set-up for headspace sampling. By simply using a piece of stainless steel mesh, headspace sampling was

achieved in this experiment. The stainless steel mesh protects the membrane from coming into direct contact with the skin surface, thus avoiding contamination of the membrane from skin surface. The comparison between headspace and direct sampling was done by sampling with and without the bottom stainless steel mesh at the same time in a close skin area. The chromatograms found in Figure 3.5 show that for volatile compounds such as octanal (1), nonanal (2), decanal (3), similar peak intensity was observed in both headspace and direct contact sampling. However, for less volatility compounds, such as 1-tetradecanol (4) and 1-octadecanol (5), higher peak intensity was obtained in direct contact sampling. Some of the heavy compounds, such as squalene, one of the main sebum components [148], were only appeared in the direct contact sampling. These high intensity peaks may cover the potential biomarker peaks and influence the quantification results. Beside the compounds in the chromatogram shown in Figure 3.5, direct contact sampling also introduced lipids and dust, which were left on the injector and head of the column. These, in turn, can influence carry over and peak shape of the chromatograms, and requiring periodical baking and clean up of the instrument [142].

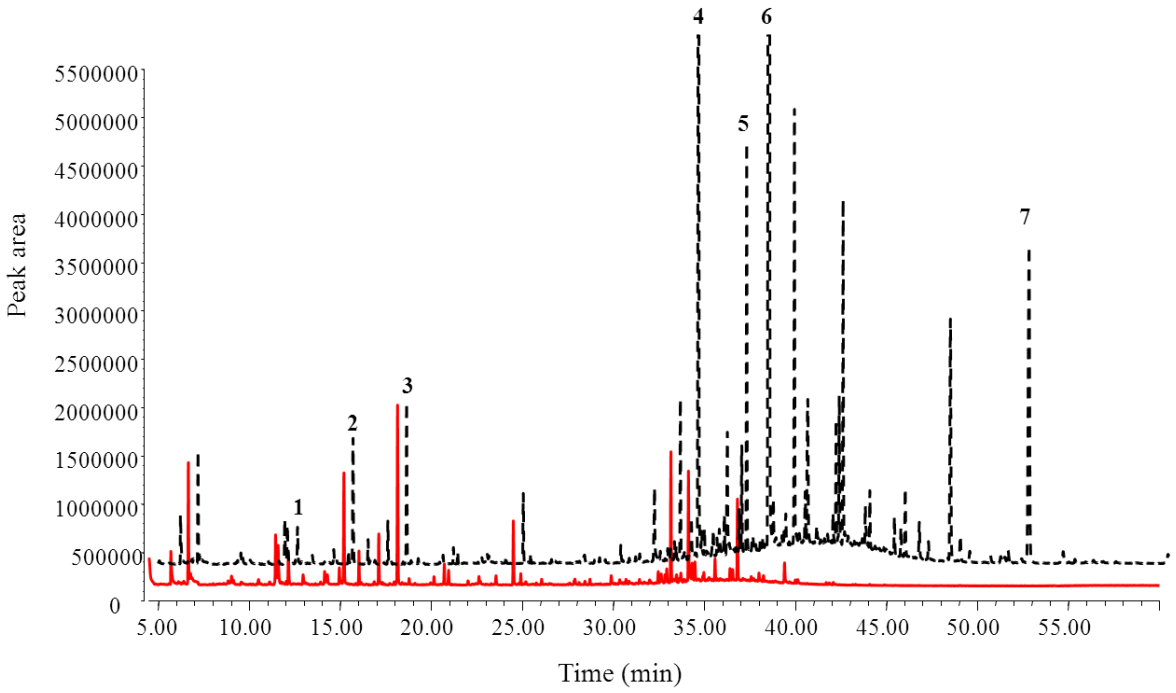

Figure 3.5 The comparison of the HS (solid line) and direct sampling (dash line) chromatogram from the same area of the skin. 1. octanal; 2. nonanal; 3. decanal; 4. 1-tetradecanol; 5. isopropyl palmitate; 6. 1-octadecanol; 7. squalene.

3.3.3 Effect of membrane size

Membrane size is a significant parameter that determines the sensitivity of the sampling. Theoretically, larger membranes should be used to obtain higher sampling sensitivity. However, the membrane size also depends on the size of the lesion area. If the lesion area is small, membranes with small diameter should be used to avoid high background being sampled from the normal skin area. Membrane sampling provides the flexibility of extraction size. In this experiment, three membranes with different membrane diameters of 6, 11 and 17 mm were assembled as described previously for *in vivo* sampling. Three membranes were sampled simultaneously for 1 hour and analysed by GC/MS individually after sampling. The resultant peak area was plotted against the membrane surface area. Results demonstrated the theoretical prediction that larger membrane sizes provide higher sampling amounts.

3.3.4 Storage method evaluation

Sample storage after volatile collection and before GC/MS analysis is very important in body odor sampling processes [149]. Furthermore, compound volatility, environment contamination and bacterial activity [145] can result in compound loss and biodegradation, and thus influence the analysis results. It is always better to analyze samples immediately after collection; however, in some experimental situations it is simply not possible, and sample storage and transportation cannot be avoided.

In this experiment, various storage conditions were investigated in order to prevent the loss of volatile compounds, and for convenient injection in the GC port. First, after sampling, storage of the membrane into the TDU tube is recommended. A house-made Teflon cap was used to minimize analyte loss and prevent dust from falling into the tube during transportation. After capping the tube, the liner was wrapped with aluminum foil and stored. Three different storing temperature conditions were tested: room temperature, ice (4 ℃) and dry ice (lower than -50 ℃). The *in vial* sampling set-up was first chosen to determine the best storing condition, and then the determined storing condition was further evaluated by *in vivo* sampling.

For *in vitro* sampling, 16 pieces of membrane with diameter of 6 mm were sampled for 5 min. Two membranes were analyzed immediately, four membranes were stored in room temperature, four membranes were placed in ice and 6 membranes were placed in dry ice for different periods of time. For *in vivo* sampling, 4 pieces of membrane with a diameter of 6 mm were sampled for 60 min at the same time. One of them was analyzed immediately after sampling, while the others were stored in dry ice for 23, 48 and 72 hours. The obtained chromatograms were compared.

For room temperature storage, 25 hours and 50 hours of storage were tested, and results are shown in Figure 3.6A. The loss of compounds was significant. After 25 and 50 hours, very few volatile compounds could be detected, and the intensities of their peaks were significantly reduced. Even membranes stored in ice (4°C) showed significant loss of volatile compounds (data not shown). For volatile compounds like hexanal, ethylbenzene, p-xylene and decane, the loss was more than 50%. In addition, air contamination was observed during ice storage (in the fridge).

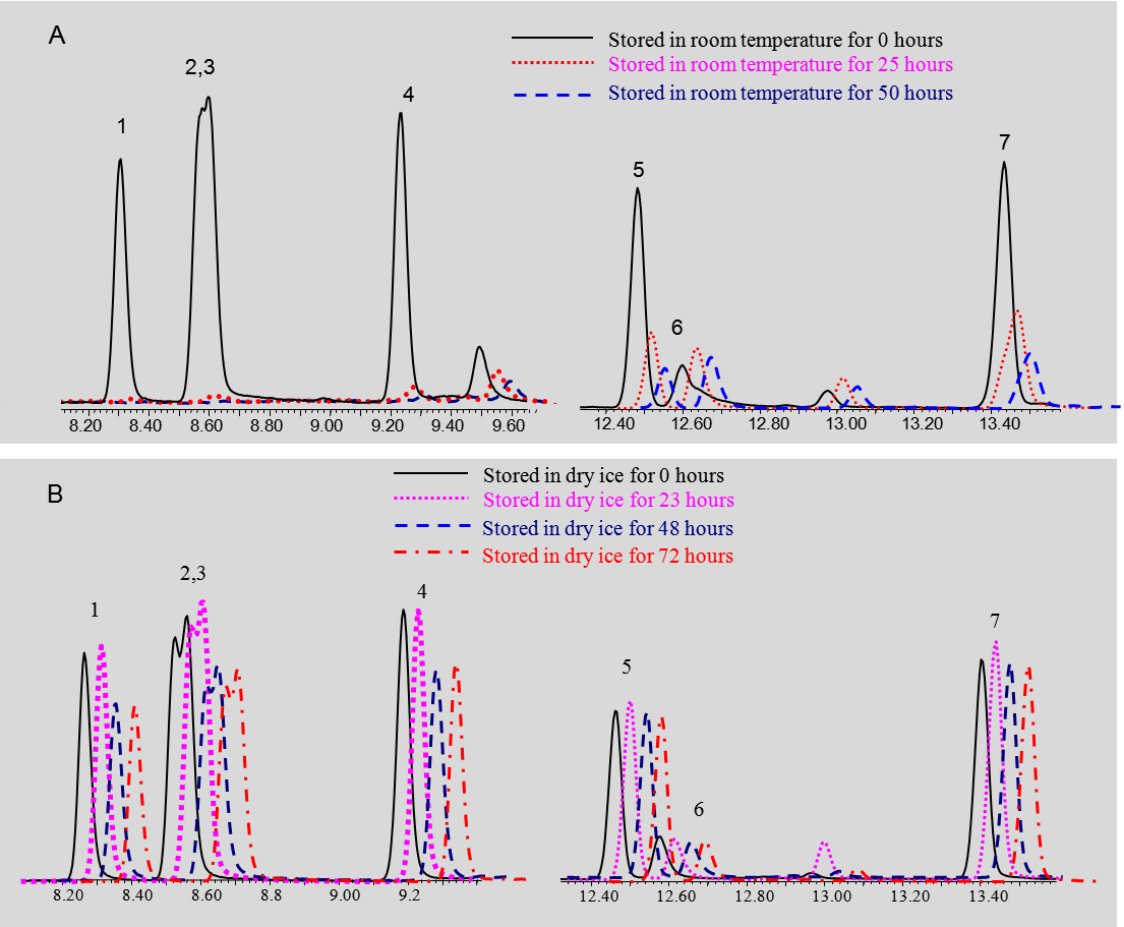

Figure 3.6 Comparison of different storage methods of the sampled membrane. 1. toluene; 2. ethylbenzene; 3. p-xylene; 4. o-xylene; 5. decane; 6. octanal; 7. D-limonene.

The temperature of dry ice is much lower than the temperature of ice, which may significantly decrease the volatility of the compounds during storage and prevent analyte loss.

Twenty three hours, 48 hours and 72 hours of storage time were evaluated. The comparison chromatograms were shown in Figure 3.6B. These results show that dry ice can effectively prevent the loss of most of volatile compounds for up to 72 hours. Although small amounts of highly volatile compounds such as toluene decrease after 48 hours of storage, we believe that storage on dry ice is the best way to preserve volatiles on the membrane. In addition, no contamination was observed. This may be due to the sublimation phenomenon of the dry ice. The CO_2 gas fills up the space of the storage container, and the environmental contaminants are not able to diffuse into the tube.

In vivo sampled membranes were also stored in the dry ice for different periods of time. Evaluation results showed that a similar number of components could be detected after different storage times (up to 72 hours), demonstrating that no bacterial activity or contamination during the storage occurred. In summary, our results show that membrane storage on dry ice is the best way to preserve volatile compounds.

We also tested various conditions for storing membranes before sampling (blank membrane). Final protocol for storing blank membrane should be as follows: place the membrane inside the Teflon capped TDU tube, place the capped TDU tube inside a 20 mL vial, seal the vial with the cap and seal the cap with parafilm. Using this protocol, the blank membrane can be stored anywhere for more than 14 days without environmental contamination occurring.

3.3.5 Dietary biomarker for garlic and alcohol intake

In this experiment, we used our *in vivo* skin sampling approach to detect biomarkers of garlic and alcohol intake. Garlic (*Allium sativum*) has been investigated extensively for its health benefits. The mechanism of garlic metabolism is still not fully understood. However, it is believed that the main bioactive components of garlic related to its beneficial health effects

include flavonols, soluble fibers, fructo-oligosaccharides and various organo-sulfur compounds. Among these compounds, organo-sulfur compounds and their metabolism are the main focus of research [150].

When raw garlic is crushed, the enzyme alliinase (stored in a separate compartment in garlic), combines with an alliin and produces allicin. When allicin is ingested, it decomposes in the acidic environment of the stomach, and releases a number of volatile compounds, including dimethyl disulfide, dially disulfide and diallyl sulfide. Part of the dimethyl disulfide is later metabolized into dimethyl disulphone [151], while dially disulfide is transformed into allyl mercaptan, allyl methyl sulphide, allyl methyl sulphoxide [152]. All these compounds have been detected after garlic ingestion in human urine [153], blood [154] and breath [155].

When an alcoholic drink is consumed, the alcohol is quickly absorbed into bloodstream by diffusion and transported to various tissues. A large amount of the alcohol is metabolized in the liver, while less than 10% of the consumed alcohol is excreted from the body by breath, sweat, and urine. The concentration of alcohol in breath, urine and sweat mirrors the concentration in the blood, and can be used to calculate a person's blood alcohol concentration (BAC). Alcohol breath tests are a common way to measure the BAC. However, this method is influenced by physiological and dynamic factors in the composition of the expired breath, as well as the operator's actions, cooperation or limitations. In contrast, the amount of alcohol released from the skin is under control of the autonomous nervous system. Thus, important information can be obtained by comparing breath, blood and skin alcohol levels. It is worthwhile to test if the amount of alcohol released from skin is a better representative of BAC than breath analysis, and less prone to other complicating factors.

The sampling was conducted using a piece of home-made DVB particle loaded membrane with a surface area of 5.7 cm^2 (details of the membrane are described in Chapter 5). The sampling time was 20 min and 10 min for garlic and alcohol, respectively. The sampling was conducted 30 min after garlic intake. We detected trace metabolic compounds: dimethyl disulphone, allyl methyl sulfide, and allyl mercaptan in the chromatogram obtained after eating garlic with a detection threshold of 80 (100 for perfect match). None of these compounds were present in the chromatograms sampled from skin before eating garlic. For alcohol biomarkers, the amount of skin ethanol being released was monitored before and after drinking 20 mL of Whisky. The relative releasing amount versus fasting time was expressed in Figure 3.7, and this result showed the maximum peak was around 50 min after drinking alcohol, which has good agreement with peak BAC (around 40 to 90 min from literature) [156].

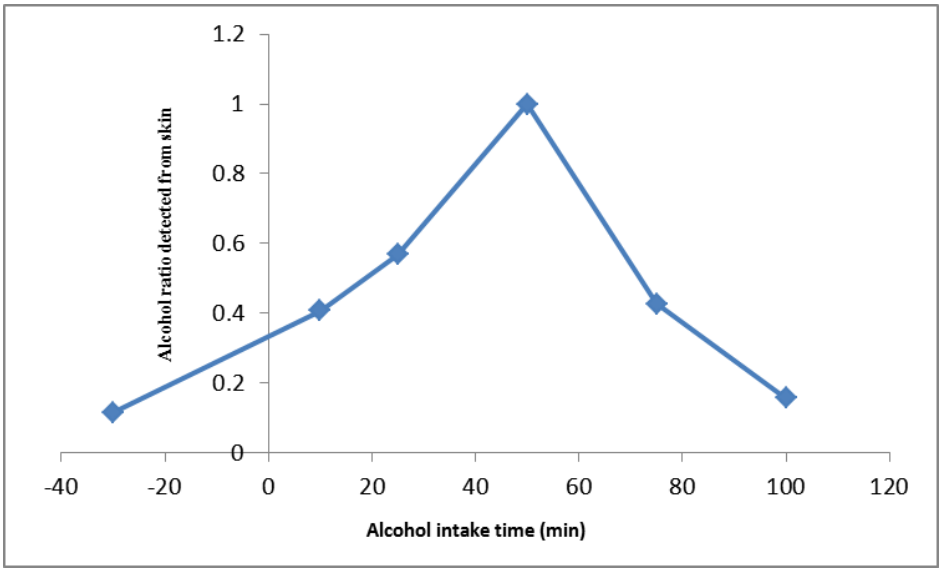

Figure 3.7 The trends of alcohol amount detected from skin before and after drinking.

The dietary biomarker monitoring first demonstrated the high sensitivity of the proposed thin film approach for skin volatile compounds sampling. Successful sampling of these biomarkers from the skin establishes the possible wide applications of this technique. Last, a

sensitive response between the emission amount and the detected signal cements the ground for quantification analysis.

3.3.6 Comparison of the skin emissions from different areas of the body

The upper back, forearm and back thigh were chosen for sampling location because they are easily accessible. In addition, these body regions differ with respect to density of sebaceous glands (upper back > the other two regions) [157]. The sampling was conducted by sampling from each location three times. Only compounds which were detected at least twice were analyzed. These detected compounds are listed in Table 3.3. Twenty seven compounds out of 99 were detected at all three locations. In total, 77 volatile compounds were detected from upper back and 51 and 55 from forearm and thigh, respectively. The upper back released the most volatile compounds. This phenomenon may be due to the high density of sebaceous glands in this area.

Table 3.3 Compounds detected from three locations of the same individual.

Compounds	**CAS**	**Arm**	**Leg**	**Back**
2-Propenoic acid, 2-methyl-, methyl ester	80-62-6	*		*
Methanesulfonyl chloride	124-63-0	*		*
Butane,2,2-dimethyl	75-83-2	*		*
2,2-Dimethylglutaric anhydride	2938-48-9		*	
1-Hexene, 3,4-dimethyl-	16745-94-1	*		*
Pyrrolidine	123-75-1	*		*
1-Heptene, 6-methyl-	5026-76-6		*	
1-Pentanol, 3,4-dimethyl-	6570-87-2	*		*
1,3,5-Cycloheptatriene	544-25-2		*	
Methyl vinyl ketone	78-94-4		*	
Hexanal	66-25-1	*	*	
o-Xylene	95-47-6		*	
Styrene	100-42-5	*	*	
Nonane	111-84-2	*		*
Heptanal	111-71-7	*	*	*

Bicyclo[3.1.0]hex-2-ene, 2-methyl-5-(1-methylethyl)-	2867-05-2		*	
Benzene,1-ethyl-3-methyl-	620-14-4		*	
Oxilic acid, cylcobutyl isohexyl ester		*		
5-Hepten-2-one, 6-methyl-	110-93-0	*	*	*
Furfurylmethylamphetamine	13445-60-8	*		
Isooctanol	26952-21-6	*	*	*
Benzene, 1,2,3-trimethyl-	526-73-8		*	*
Decane	124-18-5	*	*	*
Octanal	124-13-0	*	*	*
Benzene, (1-methylethyl)-	98-82-8		*	
Decane, 4-methyl-	2847-72-5	*		
Cyclopropane, (1,2-dimethylpropyl)-	6976-27-8			*
4-Methyl-1,5-Heptadiene	998-94-7			*
Cyclopropane, pentyl-	2511-91-3	*	*	*
1,4-Hexadiene, 3,3,5-trimethyl-	74753-00-7	*		
3,4-Hexanedione, 2,2,5-trimethyl-	20633-03-8	*		
Undecane	1120-21-4	*	*	*
Nonanal	124-19-6	*	*	*
1-Azabicyclo[3.1.0]hexane	285-76-7			*
2-oxepanone	502-44-3			*
1-Nonanol	143-08-8	*		*
Cyclohexanol, 5-methyl-2-(1-methylethyl)-, [1R-(1.alpha.,2.beta.,5.alpha.)]-	2216-51-5	*		
2-Octanone	111-13-7		*	
Dodecane	112-40-3	*	*	*
Decanal	112-31-2	*	*	*
Benzaldehyde, 4-methoxy-	123-11-5		*	
1-Decanol	112-30-1		*	
4-tert-Butylcyclohexyl acetate	32210-23-4	*		*
3',4',5,7-Tetramethoxyflavone	855-97-0	*	*	*
Tridecane	629-50-5		*	
Undecanal	112-44-7	*	*	*
3-Pentanone, 2,2,4,4-tetramethyl-	815-24-7		*	
2,2,4-Trimethyl-1,3-pentanediol diisobutyrate	6846-50-0	*	*	*
2-Undecanal	2463-77-6			*
2-Decen-1-ol, (E)-	18409-18-2	*		*
Propanoic acid, 2-methyl-, 3-hydroxy-2,4,4-trimethylpentyl ester	74367-34-3	*	*	

Dodecanal	112-54-9	*	*	*
5,9-Undecadien-2-one, 6,10-dimethyl-	689-67-8	*	*	*
2,2-Dimethylpropionic acid, decyl ester	215667-91-7			*
1-Dodecanol	112-53-8	*	*	*
Propanoic acid, 2,2-dimethyl-, heptyl ester	17660-61-6			*
Pentadecane	629-62-9		*	*
Tridecanal	10486-19-8	*	*	*
Lilial	80-54-6			*
Dodecanoic acid	143-07-7			*
Propanoic acid, 2-methyl-, 1-(1,1-dimethylethyl)-2-methyl-1,3-propanediyl ester	74381-40-1	*	*	*
Diethyl Phthalate	84-66-2	*	*	*
9H-Fluorene, 9-bromo-	1940-57-4		*	
Undecane, 4,7-dimethyl-	17301-32-5	*		*
Tetradecanal	124-25-4		*	*
Benzene, (1-butylheptyl)-	4537-15-9			*
Decane, 2,5,9-trimethyl-	62108-22-9		*	
Oxalic acid, butyl 2-ethylhexyl ester			*	
n-Hexyl salicylate	6259-76-3			*
Propanoic acid, 2-methyl-, nonyl ester	10522-34-6		*	*
Dodecane,2,6,10-trimethyl-	3891-98-3			*
Benzoic acid, 2-ethylhexyl ester	5444-75-7		*	
Pentadecanal	2765-11-9	*	*	*
Benzene, (1-pentylheptyl)-	2719-62-2			*
Octanal, 2-(phenylmethylene)-	101-86-0			*
Tetradecanoic acid	544-63-8			*
Octadecane	593-45-3		*	*
Hexadecane, 2,6,10,14-tetramethyl-	638-36-8		*	
Benzene,(1-methylundecyl)-	2719-61-1			*
Phenol, 2,4,6-trinitro-	88-89-1			*
isopropyl Myristate	110-27-0	*	*	*
Hexadecanal	629-80-1	*		*
4,8,12-Tetradecatrienal, 5,9,13-trimethyl-	66408-55-7	*		*
Galaxolide	1222-05-5	*	*	*
Ethanone, 1-(5,6,7,8-tetrahydro-3,5,5,6,8,8-hexamethyl-2-naphthalenyl)-	21145-77-7			*
1,2-Benzenedicarboxylic acid, bis(2-methylpropyl) ester	84-69-5		*	*
1,2,3,6-Tetrahydropyridine	694-05-3		*	

4-Benzyloxybenzoic acid	1486-51-7			*
1-Hexadecanol	36653-82-4	*		*
Homomenthyl salicylate	118-56-9		*	*
Nonadecane	629-92-5	*	*	*
Sulfurous acid, 2-ethylhexyl isohexyl ester				*
Hexadecanoic acid, methyl ester	112-39-0	*	*	*
Phthalic acid, butyl 2-pentyl ester		*	*	*
n-Hexadecanoic acid	57-10-3			*
Eicosane	112-95-8	*	*	*
Isopropyl Palmitate	142-91-6	*	*	*
Oxybenzone	131-57-7			*
2-Propenoic acid, 3-(4-methoxyphenyl)-, 2-ethylhexyl ester	5466-77-3	*		*

3.4 Summary

A non-invasive thin film headspace sampling method was developed to facilitate reproducible and quantitative sampling of human skin VOCs profiles. The headspace set-up minimized the contamination from the skin surface and ensured the reproducibility of *in vivo* sampling, which was also influenced by skin metabolism and sampling environment. The stability of the samples under reasonable storage conditions and extended time periods allows the analyses to be performed in different locations. Additionally, the described method was applied for dietary biomarkers monitoring after garlic and alcohol ingestion. The results demonstrated that the developed approach has high potential for clinical and forensic investigation fields.

Chapter 4 **Development of a Cooling Membrane Approach for High Sensitivity Gas Sampling**

4.1 Introduction

Air is a complex, heterogeneous sample matrix that is composed of gases (inorganic and organic), liquid (moisture) and solid particulate material. These compositions can be influenced by continuously evolving atmospheric and geographic conditions. The concentration of organic components is usually characterized as low level due to the low density of the air. Thus, air sampling and sample preparation is crucial in air analysis. For this procedure, it is important to obtain representative samples while avoiding variation in their composition during transportation. Also, enrichment is often required in order to reach the acceptable LOD in the instrument used.

Traditional air sampling techniques include whole-air collection and sorbent tube sampling [158]. Whole-air sampling uses containers such as Tedlar bags or canisters to collect air through either active (pump required) or passive (no pump required) methods. This technique is the simplest method for collecting air. However, lack of an enrichment step makes it unsuitable for trace level analyte sampling. Another limitation regarding air sampling is the adsorption of compounds, especially semi-volatile compounds on the wall of the container. This phenomenon causes the variation in the air composition, causing negative quantification errors during calibration. Moreover, the large volume of the container is inconvenient for transportation.

For air enrichment sampling, sorbent-based air sampling methods are usually utilized for active and passive sampling, in which a tube packed with solid sorbent is used as the extraction phase [159, 160]. In active sampling, a mechanical pump is used to force the air flow through the sampling medium, whereas in passive sampling, the analytes flow freely through the sampling

medium, following Fick's first law. After sampling, the adsorbed sorbent follows either solvent desorption or thermal desorption to release the analytes from the sorbent [160].

Solvent desorption utilizes an organic solvent-to-analytes ratio of 1000:1 or more to desorb analytes from the adsorbent [161]. Because of the large amount of organic solvent used, the final concentration of analytes in the solution is relatively low. In order to obtain an amount that is concentrated enough for the final eluent, more air samples should be taken during sampling. However, this usually results in longer extraction time, or breakthrough issue for the sorbent.

In order to fully illustrate the performance of sorbent-tube solvent desorption and thermal desorption, benzene sampling can be used as an example: for the standard method (OSHA-12) provided by American Occupational Safety & Health Administration (OSHA), the LOD for benzene present in air is 0.04 ppm (0.12 ng/mL) [162]. Using this traditional method, ten liters of the benzene standard gas was sampled using a charcoal tube at 200 mL/min. The sorbent tube was desorbed using 1 mL of CS_2, and later 1 μL of the final solution was injected into the GC/FID (Flame ionization detector). The desorption recovery was 100%. The whole sampling and sample preparation lasted 80 min, with 50 min for sorbent-tube sampling and 30 min for solvent desorption. When using whole-air injection, assuming the FID detection limit is the same as the above method, 10 mL of the 0.12 ng/mL air should be injected into the instrument to achieve the detection limit. This volume is too large to directly inject into the GC, even if a large volume injector is used. On the other hand, if using sorbent-tube thermal desorption, all the analytes can be transferred into the instrument without dilution. Theoretically, only 10 mL of air needs to be sampled to reach the detection limit, while sampling in the OSHA-12 standard method would need 10 L. Thus, the thermal desorption method can achieve higher injection amounts with a shorter sampling time.

Thermal desorption has a long history in air sampling [163, 164]. However, the limitations of this desorption technique are very well documented as well. First, the sorbent tube sampling is an exhaustive sampling technique, which means all components present in the air, including moisture and solid particles, are exhaustively trapped on the sorbent during sampling. These, in turn, would influence the following instrument analysis and should be removed. Therefore, water traps and particle filters are usually used to purify the sampled air before passing it through the sorbent tube. In addition to the cost associated with the water traps and particle filters, they may also cause loss of the sampling compounds during the purification process [159, 165]. As well, a significant time factor is involved in the transfer of all the trapped analytes from a large diameter tube to the small column. Indeed, a cryogenic secondary trap is generally needed to prevent the peak broadening observed on the chromatograms. However, these cryogenic traps need expensive liquid nitrogen/CO_2 as the cooling source, and consume relatively large amounts of coolant during analysis. Last, the sorbent tube thermal desorption method reveals high background in the chromatograms because of the co-extracted contamination effect found in air. This is especially true for complex air analysis. As a result, alternative air sampling and sample preparation techniques should be investigated.

As introduced in Chapter 1, SPME has been used for air spot sampling and TWA sampling. The accuracy of this technique was demonstrated by the EPA, NIOSH standard air sampling methods. However, the reported detection limit of SPME when compared to conventional methods is relatively low, and inadequate for analysis. Again, benzene sampling can be used in illustration: In air with a benzene concentration of 0.12 ng/mL (detection limit for OSHA-12 method), using a SPME PDMS fiber with a thickness of 100 μm ($V_{es} = 0.612\ \mu L,\ K_{es} \approx 308$), the equilibrium extraction amount (n) at room temperature can be calculated by Equation 1.1

and is around 0.022 ng, which is much lower than the detection limit of the GC/FID used in the OSHA-12 method (~1.2 ng). This data would indicate that the SPME/PDMS fiber cannot achieve the detection limit obtained from the sorbent-tube sampling. With that in mind, a SPME technique with higher sampling sensitivity should be developed for air sampling.

Cold fiber SPME and TFME, as demonstrated in the previous chapters, has been developed to address the limitations of SPME for sampling sensitivity. However, challenges are still present in the current development of these two techniques for air sampling application. For cold fiber SPME, the need for a large external device (CO_2 cylinder) restricts on-site air sampling. Although potential cold fiber devices with electric coolant sources were investigated, difficulties in controlling the temperature, as well as the small volume of the extraction phase limited the further improvement of the sensitivity for trace gas sampling [55]. As for thin film SPME, no particular sampling set-up was previously developed for thin film gas sampling. In the literature, thin film was shown being placed in the sample matrix by attaching it to a stainless steel wire. In this set-up, uncontrollable sampling flow rates and temperatures result in difficult calibration. Moreover, commercially available thin film is limited by PDMS, which is commonly known for its lack of extraction efficiency in regards to highly volatile and polar compounds. This limitation was illustrated in the paper published by Eom *et al*. [58], in which thin film was used to sample air infected with *Cimex lectularius L*. Comparative results were obtained for SPME fiber, needle trap and thin-film sampling; thin film was shown to provide discriminative extraction coverage toward highly volatile analytes when compared to DVB/CAR/PDMS fiber and needle trap SPME. Reasons for the phenomenon include the low extraction efficiency of the PDMS membrane towards the volatile compounds and the potential loss of compounds during transportation due to low extraction affinity.

In the presented research work, the advantages of both TFME and cold fiber SPME were combined to further improve the extraction efficiency. This was achieved by simultaneously increasing the volume of the extraction phase and the distribution coefficient. A home-made extraction unit was designed to accomplish the sampling process and the sampling conditions. Three fragrance compounds (limonene, cinnamaldehyde and 2-pentadecanone), representing for different volatilities, were chosen as the target compounds in the investigation of the developed cooling membrane device. Lastly, the developed sampling approach was applied for the indoor air sampling.

4.2 Experimental

4.2.1 Reagents and supplies.

Compounds, limonene, cinnamaldehyde, 2-pentadecanone and benzene were purchased from Sigma-Aldrich (Mississauga, ON, CA). The acetone used for preparation of the standard solution was from Caledon Laboratories Ltd. (Georgetown, ON, CA). Two types of Teflon tube with wall thickness of 279 µm and 483 µm were purchased from Weico Wire & Cable, INC. (Edgewood, NY, USA). A sheet of PDMS membrane with a thickness of 102 µm was obtained from Specialty Silicone Product (Ballston Spa, NY, USA). Membranes were cut in a round shape with different diameters and preconditioned in a GERSTEL® thermal conditioner under a nitrogen flow for 5 hours at 200 ^{o}C, and 5 hours at 250 ^{o}C prior to use. Ultra-pure helium and nitrogen were purchased from Praxair (Waterloo, ON, CA). A thermoelectric cooler was purchased from TE technology (Traverse city, Michigan, USA).

4.2.2 Instrumentation

The analytical instrument used for separation and quantitation was an Agilent 6890 GC and 5973 quadrupole MS (Agilent Technologies, Mississauga, ON, Canada) coupled with a GERSTEL® MPS 2 autosampler. A CIS 4 and twister desorption unit (TDU) was used for membrane analysis (GERSTEL, Mülheim an der Ruhr, GE). For more information regarding thin film desorption, please refer to Section 3.2.2, Chapter 3.

The GC oven, CIS, and TDU conditions are shown in Table 4.1. Chromatographic separation was performed by a 30 m × 0.25 mm I.D × 0.25 µm thickness SLB™-5 fused silica column from Supelco (Sigma-Aldrich, Mississauga, ON, CA). Helium was used as carrier gas. The temperatures for the MS detector transfer line, MS quadrupole and MS source were set at 270 ℃, 150 ℃ and 230 ℃, respectively. The MS system was operated in electron ionization mode and mass fragments were collected at m/z 35-300 range.

Table 4.1 The GC conditions for different experiment

Instrument parameters	**Fragrance compounds from SGG**	**Benzene from SGG**	**Real gas sampling**
GC CIS mode	Solvent vent/split solvent vent/splitless	Solvent vent/split	Solvent vent/splitless
CIS temperature	Initially -60 ℃, ramp to 280 ℃ at 12 ℃/s, kept for the whole GC run.	Initial -120 ℃, ramp to 250 ℃ at 12 ℃/min, hold for the whole GC run	Initial -120 ℃, ramp to 280 ℃ at 12 ℃/min, hold for the whole GC run
TDU desorption temperature	Initial 30 ℃ (1 min), ramp to 250 ℃ at 700 ℃/min (3 min), kept at 240 ℃ for the whole GC run.	Initial 30 ℃ (1 min), ramp to 220 ℃ at 700 ℃/min (1.5 min), kept at 220 ℃ for the whole GC run.	Initial 3 ℃ (1 min), ramp to 250 ℃ at 700 ℃/min (2.3 min), kept at 230 ℃ for the whole GC run.
GC column temperature	Initial 50 ℃ (3 min), ramp to 250 ℃ at 20 ℃/min, hold for 10 min	Initial 40 ℃ (4 min), ramp to 50 ℃ at 5 ℃/min and then increase to 160 ℃ at 20 ℃/min, hold for 0.5 min	Initial 40 ℃ (2 min), ramp to 200 ℃ at 5 ℃/min and then increase to 250 ℃ at 10 ℃/min, hold for 11 min.
Column flow rate	1.5 mL/min	1 mL/min	1 mL/min

SGG: standard gas generator

4.2.3 Standard gas generator

Evaluation experiments were done by sampling from the standard gas generator. In the literature, several types of standard gas generators have been introduced for SPME laboratory method development. The simplest one consists of spiking the standard solution into a gas container such as a Tedlar bag or glass bulb (Figure 4.1). By knowing the spiked amount and the volume of the container, the concentration of the standard gas inside the container can be determined. This standard gas generator is not suitable for semi-volatile compounds, which can be easily adsorbed on the container wall. Also, the volume of the sampling gas is limited by the container [166]. Multi-sampling requires multiple preparations of the standard gas. Furthermore, this generator can only be used for static sampling.

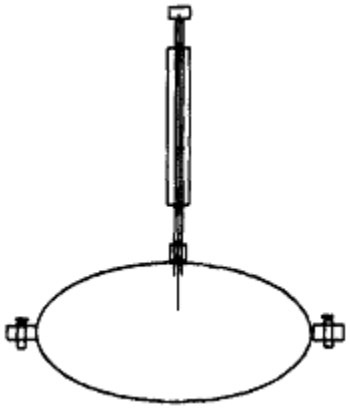

Figure 4.1 SPME sampling using a gas sampling bulb.

The second standard gas generator is a flow system in which a clean gas is continuously introduced into a container. The standard solution is injected into the container with a syringe pump at a constant flow (Figure 4.2). By controlling the flow rate of clean air and the injection rate of the standard solution, the concentration of the standard gas can be determined. The limitations of this standard gas generator are the high concentration of solvent needed to dissolve the standard compounds, and the need to periodically refill the standard solution into the syringe.

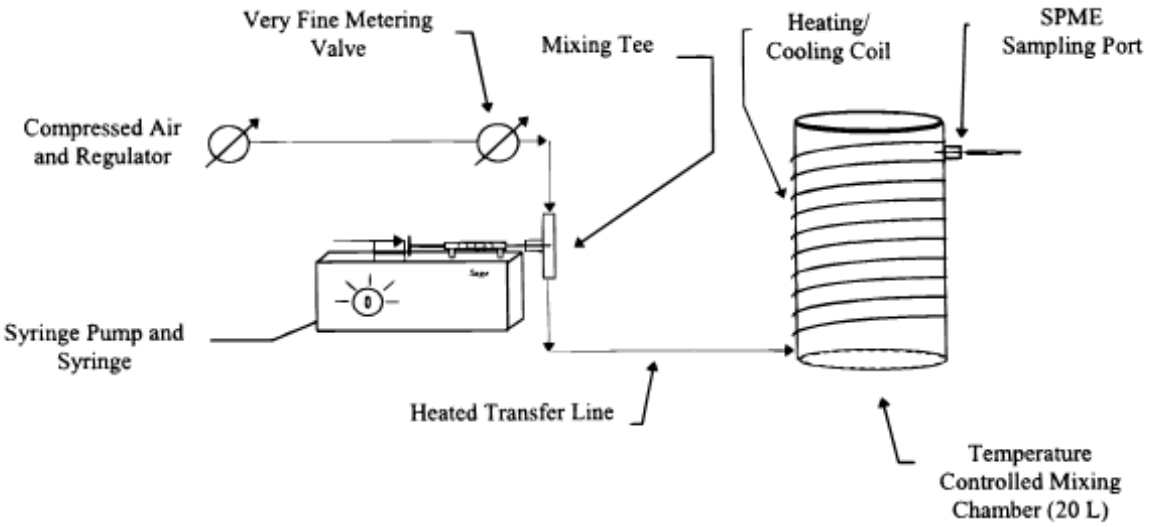

Figure 4.2 The syringe pump standard gas generator [35]. Figure reprinted from reference with permission of publisher.

The third standard gas generator is similar to the above mentioned, with the exception of the standard supplying source. In this version, a permeation tube is used to store the standards (Figure 4.3). The tubes can be made from Teflon or another material, and are incubated inside a chamber where the temperature and flow rate can be kept constant. A very small, but stable flow (nanograms-per-minute) of analyte vapour is emitted through the wall of the tube and carried out of the permeation chamber by a stream of gas.

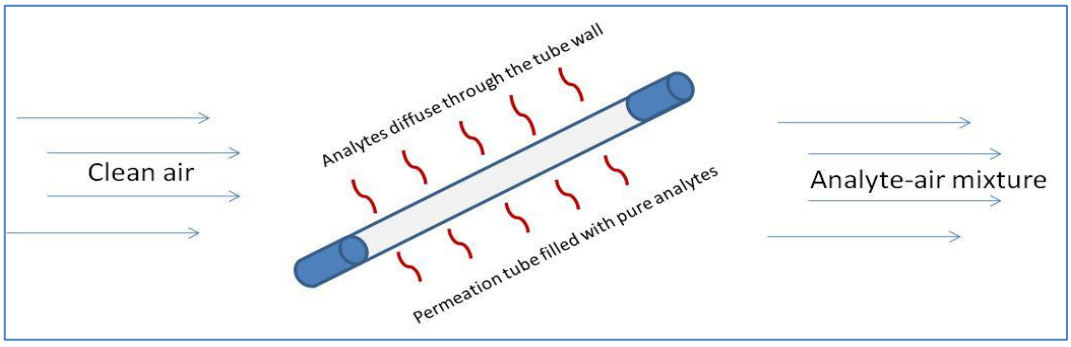

Figure 4.3 The configuration of the permeation tube.

The permeation tube based standard gas generator minimizes the effect of adsorption on the surface of the system, provides unlimited standard gas, and easily generates a range of diluted

gas concentrations, flow rate and humidity for analytical purposes. Furthermore, a large range of volatility compounds can be generated in one system.

In this experiment, home-made permeation tubes were prepared by encapsulating pure analytes inside the Teflon tubing, and were then capped with solid Teflon plugs and Swagelok caps. Two types of Teflon tubes with different thicknesses were used for different compounds with different volatilities. Further details on the preparation of the permeation tube can be found elsewhere [167]. Next, the prepared permeation tubes were placed inside the permeation chamber, which was swept by constant ultra-pure nitrogen flow. The flow rate was controlled by a Sidetrack^{TM} mass flow controller (Sierra Instruments, Monterey, CA). The permeation chamber was held inside an oven where the temperature was controlled by an electric heat control device designed and constructed by the Electronic Science Shop (University of Waterloo, CA).

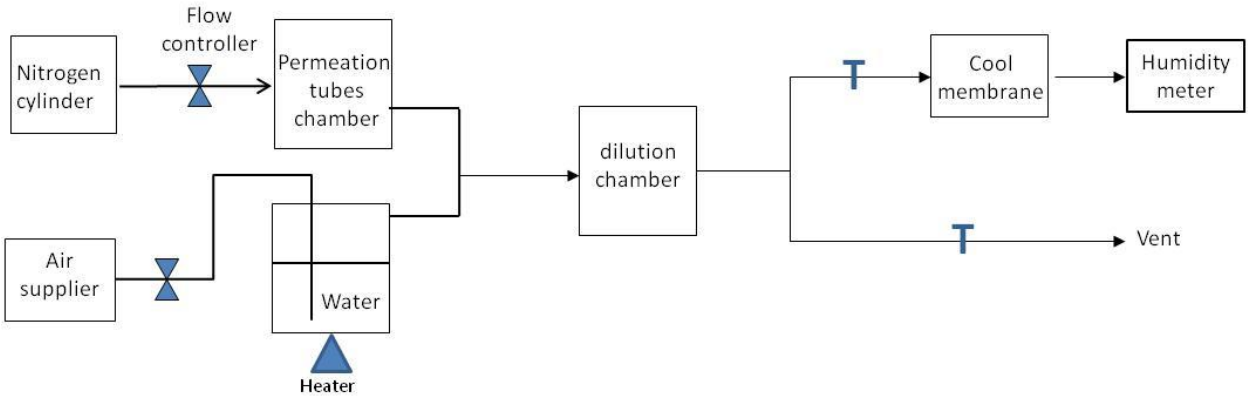

Figure 4.4 Configuration of the standard gas generator

In order to obtain a standard gas with different concentrations, a dilution gas line was connected to the downstream of the permeation chamber, and both gases were passed through the dilution chamber where the temperature was set to 40 ^{o}C (Figure 4.4). The gas from the dilution chamber was separated into two gases. Flow rates were regulated by two flow-limiting valves and determined by a soap bubble flow meter. Gases with different humidity indexes were

obtained by connecting the dilution gas to a water-impinge trap. The humidity was adjusted by manipulating either the water temperature or the flow rate of the dilution gas. The relative humidity of the sampling gas was measured by a relative humidity meter.

The concentration of the target compounds from the permeation chamber can be determined by different methods. The most common one is by determining the mass difference in the permeation tubes before and after placing in the permeation chamber for a period of time. The concentration of analyte is calculated by dividing the mass difference over the volume of the gas passing through the chamber during that period of time.

Another method is using the sorbent-tube sampling method. Sorbent tubes such as a needle trap or other commercial tubes are connected to the downstream of the permeation chamber. A pump is used to withdraw a specific volume of the gas through the tube. By quantifying the amount of trapped analytes on the sorbent tube, the concentration found in the permeation chamber can be calculated.

In this experiment, the concentration of the permeation chamber was determined using a GERSTEL® TDU Tenax@ TA packed tube. The tube was connected to the downstream of the permeation chamber, and a specific volume of standard gas was withdrawn through the sorbent with an air sampling pump. The sampled tube was then injected directly into the TDU-CIS-GC-MS for desorption, separation and quantification. The sampled amount was determined by a liquid injection calibration curve, and the concentration of standard gas from the permeation chamber was calculated by dividing the sampled amount by the sampled volume. In addition, the stability of the standard gas generator was monitored by daily quality control (QC) tests. The test was performed by sampling directly from the permeation chamber with a specific membrane for 30 min at room temperature, using the cooling membrane device described in the following

section. Any deviations in peak-area counts greater than 15% required an explanation for the source of error. Direct liquid injection was usually used in instrument QC testing. If the instrument signal performed normally, the conditions of the permeation chamber would then be checked to ensure a constant emission rate.

4.2.4 Construction of the cooling membrane device

For construction of the cooling membrane device, the required coolant source had to be portable, affordable, compact, environmentally safe and precise in temperature control. Although liquid nitrogen, dry ice and running water are commonly known cooling sources, they all require a heavy external container for storage and are inconvenient for transportation. In addition, the flat geometry of the membrane requires an extra box to place and simultaneously cool the membrane during sampling. The device that meets all of these criteria is a thermoelectric cooler (TEC), which had already been utilized for cold fiber SPME applications [55]. However, the flat shape of the particular model of cooler used prior could not effectively cool down the fiber geometry. Alternatively, the flat geometry of the membrane can be coupled with a TEC to achieve high cooling efficiency. Since commercial TECs are available in a variety of sizes and shapes, it was a matter of finding an exact model that met the requirements for this project.

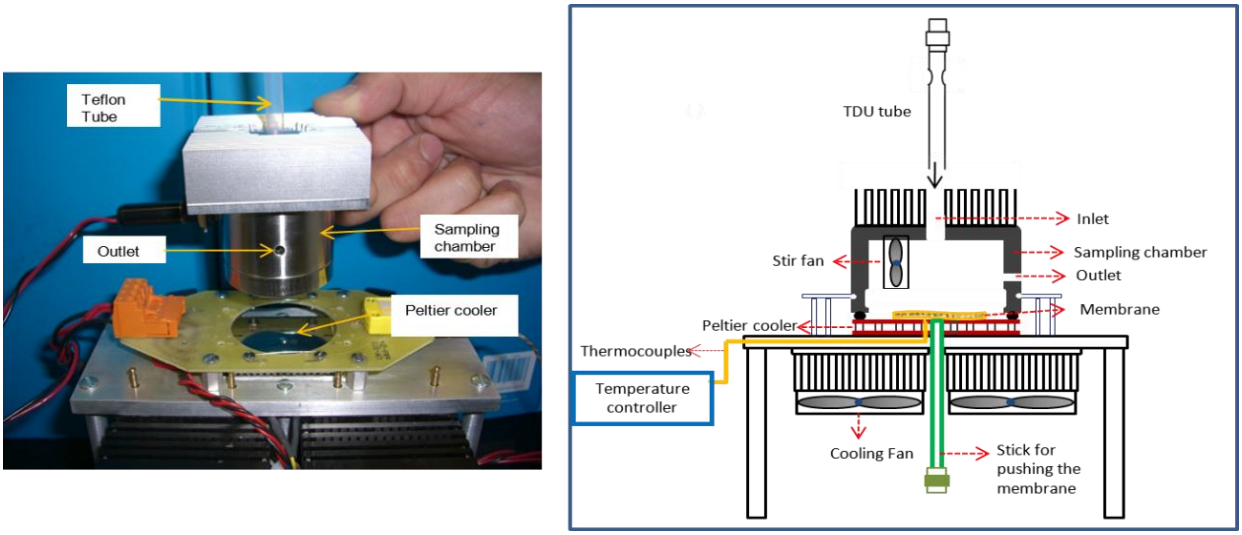

Figure 4.5 The configuration of the cooling membrane device.

Figure 4.5 shows the picture/diagram of the cooling membrane device constructed by the Electronic Science Shop. In this device, a rectangle TEC with a center hole was placed on top of a stainless steel desk that had its bottom attached to two heating sinks, which were used to release the heat generated by the cooler. The center hole provided a channel to place the thermocouples and a stainless steel rod, which was used to push the membrane into the TDU tubing after sampling. A piece of aluminum paper covered the top of the TEC to prevent the membrane from coming into direct contact with the TEC surface. A cylinder-like sampling chamber with an inlet on the top and an outlet on the side was placed on the TEC during sampling. A small fan inside the chamber was used to facilitate air convection inside the chamber when the sampling flow rate was low. During sampling, the gas from the standard gas generator or external pump was delivered into the inlet and purged towards the membrane. This design of the gas flow path maximized the flow rate towards the membrane and minimized the boundary layer. After sampling, a TDU tube replaced the tubing delivering gas in the inlet, and the membrane was pushed inside the TDU tube by a stainless steel rod mounted on the bottom of the TEC. This was designed to simplify the transportation of the sampled membrane into the

TDU tube while avoiding the loss of volatile analytes after sampling. The TDU tube with the sampled membrane was stored in dry ice immediately after sampling and before GC/MS analysis. The temperature of the membrane was regulated by thermocouples and a temperature controller. The temperature could be set on the controller and achieved variations smaller than 0.5 ℃. This cooling membrane gas sampling device was portable and convenient for in-field sampling. A power supplier for the on-site application was considered during construction, so the device could connect to a portable power supply.

4.3 Results and discussion

4.3.1 Evaluation of the cooling membrane device

The reproducibility of cooling membrane gas sampling device was evaluated by intra-membrane and inter-membrane sampling. Three fragrance compounds: limonene, cinnamaldehyde and 2-pentadecanone, were selected as model compounds to represent for different volatility compounds. All experiments were conducted with constant sampling conditions, including sampling temperature, sampling time and flow rate. For intra-membrane reproducibility, one membrane was used for 5 extractions, and the relative standard deviation (RSD%) of the extraction amount was then calculated. Inter-membrane reproducibility was tested by using three membranes of the same size. The RSD% of the extracted amounts was calculated and are shown in Table 4.2. For the volatile compound limonene, both intra- and inter-membrane RSD% were lower than 5%. This result verified the innovation of the membrane transportation design, which minimized analyte loss during transportation. Similarly, the semi-volatile compound cinnamaldehyde also observed a RSD% lower than 5% for both intra- and inter-membrane sampling. In contrast, 2-pentadecanone provided a relatively high RSD% for the reproducibility test. This may be result from the short extraction time in this experiment.

Table 4.2 The analytical figure of merits of the cooling membrane sampling.

Compounds	Intra-membr. RSD% (n=5)	Inter-membr. RSD% (n=3)	LOD (ng/L)
Limonene	4.6	4.2	9.2
Cinnamaldehyde	4.7	3.7	0.12
2-pentadecanone	8.2	12.8	0.10

In order to verify the performance of the home-made cooling membrane sampling agrees with the extraction thermodynamic theory, three extraction time profiles with different membrane temperatures, set at 23 ^{o}C, 13 ^{o}C and 5 ^{o}C , were conducting by sampling for benzene standard gas. Benzene was selected in this experiment because of the fast equilibrium time by PDMS membrane sampling compared to limonene, cinnamaldehyde and 2-pentadecanone, especially when the membrane sampling temperature is low. In addition, benzene is a well studied compound with thermodynamic parameters that are easily found in the literature.

Three extraction time profiles were performed to determine the equilibrium amount. According to Equation 1.1, the K_{es} value can be calculated if the equilibrium extraction amount and the volume of the extraction phase are known. From experimental results, the distribution coefficient for sampling at three different temperatures were calculated and shown in Table 4.3.

Table 4.3 Comparison of the calculated and experimental data

***Temp.*(K)**	ΔH^{v} (J·mol^{-1}) [a]	C_p (J·K^{-1}·mol^{-1}) [b]	n_e (ng)	$K_{es(exp.)}$	$K_{es(Cal.)}$
297	33860	82.7	168	305±14	309
286	34469	81.2	302	550±24	534
278.5	34884	80.2	446	813±5	809

Kes at 25 ^{o}C is 296; Ve is 35.3 µL; Ce is 15.6 ng/mL.

[a] Data from Weast, R. C., Ed. Handbook of Chemistry and Physics , 64th ed.; CRC Press, Inc .: 1984.

[b] Data from ref [44]

The K_{es} value can also be calculated from Equation 2.1 when the thermal dynamic parameters ΔH and C_p are available in the literature. Experimental and calculated results are

shown in Table 4.3: as can be seen, no significant differences were observed. This conclusion demonstrates that the cooling membrane device has good agreement with the cold fiber theory proposed by Zhang [44]. Therefore, the characteristics of the cooling membrane sampling can be predicted by the Equation 2.1. For example, lower membrane temperatures provide higher distribution coefficients, which improve membrane capacity. In addition, higher K_{es} values can be obtained by increasing the sampling gas temperature. This feature can be applied to specific applications where the matrix gas is found at a high temperature.

4.3.2 Extraction time profile for the cooling membrane sampling

Two extraction time profiles with membrane temperature of 21 ± 0.5 ℃ and 0 ± 0.5 ℃ were completed by sampling three fragrance compounds from the standard gas generator with a linear velocity towards the membrane of 1.3 cm/s. Figure 4.6A shows that for the volatile compound limonene, the equilibrium time is within 30 min, whereas for semi-volatile compounds cinnamaldehyde and 2-pentadecanone, equilibrium was not reached even after 150 min of sampling. Moreover, lower membrane temperature extractions (shown in Figure 4.6B) resulted in longer equilibrium times and higher equilibrium extraction amounts. According to the previously discussed theory (Section 1.3.2, Chapter 1), lower coating temperatures (T_e) result in higher distribution coefficients of sample matrix/extraction phase (K_{es}), which increase the equilibrium extraction amount (n) and equilibrium time ($t_{95\%}$). Results shown in Figure 4.6B reveal good agreement with the SPME extraction fundamental.

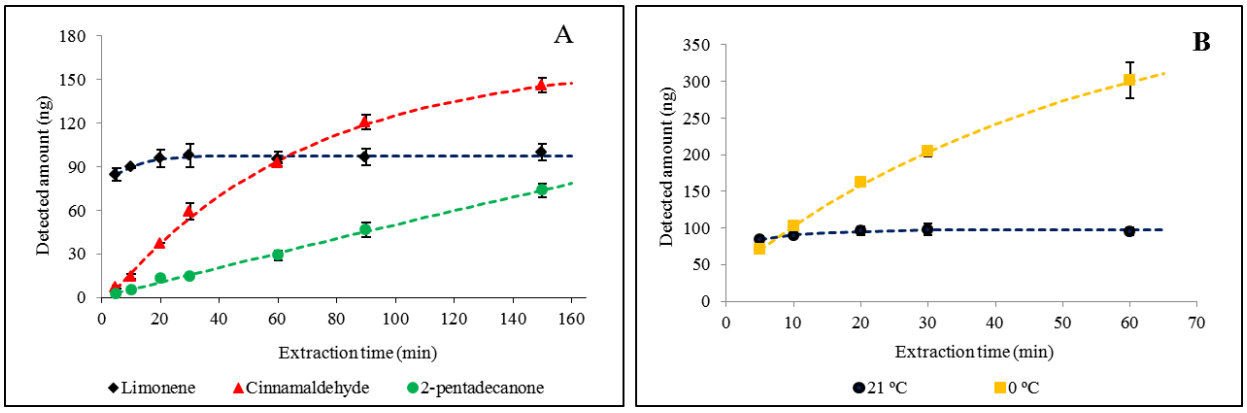

Figure 4.6 (A) The extraction time profile for three compounds sampled by the cooling membrane device with membrane temperature at 21 ± 0.5 ℃. (B) Comparison of the extraction time profile of limonene at different membrane temperatures. The concentrations of the target compounds in the sampling gas are 635 ng/L, 132 ng/L, 80 ng/L for limonene, cinnamaldehyde and 2-pentadecanone respectively. GC injector, solvent vent/split, 20 mL/min.

4.3.3 Effect of membrane size and temperature

According to Equation 1.1, when the sample volume (V_s) is sufficiently large and $V_s \gg K_{es}V_{es}$, the equation can be simplified to $n=K_{es}V_{es}C_s$. Thus, extraction amount (n) is assumed to be linearly proportional to the membrane volume (V_e) or the surface area (A) (based on Equation 1.3). In order to demonstrate this principle, three membranes with a thickness of 102 µm and different diameters were used. The surface areas of these membranes were 113 mm^2, 283 mm^2 and 491 mm^2. Triplicate experiments for each size membrane were performed for a 30 min extraction period with membrane temperatures kept at 23 ± 0.5 ℃. The average amount of three extractions for each membrane was plotted versus the membrane surface area, as displayed in Figure 4.7. All the curves show a linearity correlation (R-square) higher than 0.9949. Results confirm that the cooling membrane sampling follows the extraction principle, while demonstrating that the sensitivity of the cooling membrane can be further improved by using a larger diameter membrane.

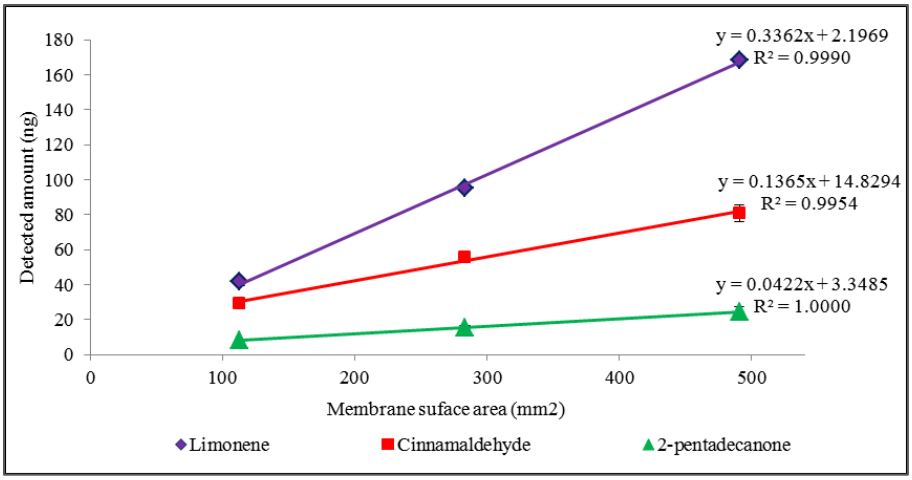

Figure 4.7 The membrane size effect. The concentrations of the target compounds in the sampling gas are 635 ng/L, 132 ng/L, 80 ng/L for limonene, cinnamaldehyde and 2-pentadecanone respectively. GC injector, solvent vent/split, 20 mL/min.

Membrane temperature profiles for three target compounds were completed in order to investigate if there is a statistically significant membrane temperature effect. The profiles were obtained by 30 min sampling with varying membrane temperatures ranging from -4.8 ± 0.5 ^{o}C to 23 ± 0.5 ^{o}C at a linear sampling gas velocity towards the membrane of 1.3 cm/s. Figure 4.8 shows that for the volatile compound limonene, the extracted amount increased approximately 40 times when the membrane temperature was decreased from 23 ℃ to -4.8 ℃. This result can be attributed to low temperatures increasing the distribution coefficient. Conversely, extracted amounts did not vary significantly for the semi-volatile compounds cinnamaldehyde and 2-pentadecanone when the membrane temperature was decreased. This phenomenon is in agreement with the concept previously described in Equation 1.2. As can be observed from their extraction time profile, cinnamaldehyde and 2-pentadecanone did not reach equilibrium during the 30 min sampling time (Figure 4.6). According to Equation 1.2, the initial extraction amount would not be influenced by the distribution coefficient; therefore, decreasing the membrane temperature would have no significant effect on the pre-equilibrium extraction amount.

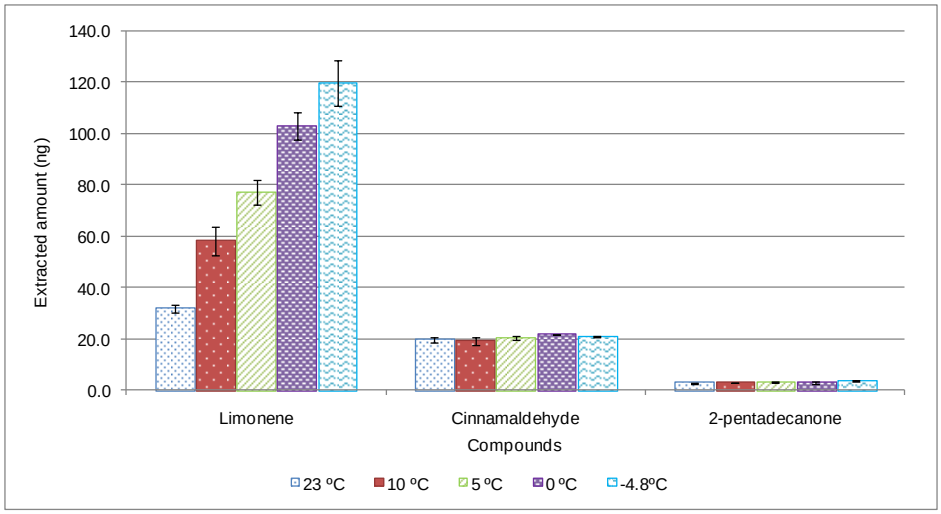

Figure 4.8 The effect of the membrane temperature. The concentrations of the target compounds in the sampling gas are 635 ng/L, 132 ng/L, 80 ng/L for limonene, cinnamaldehyde and 2-pentadecanone respectively. GC injector, solvent vent/split, 50 mL/min

The results of the membrane size effect and temperature profiles demonstrate the advantages of the cooling membrane device for trace gas sampling. In order to improve sampling method sensitivity, strategies of either increasing the membrane surface area or decreasing the membrane temperature can be used for pre-equilibrium or equilibrium sampling.

4.3.4 Effect of sampling flow rate

Gas velocity is an important sampling parameter that affects the extraction efficiency due to its influence on the thickness of the boundary layer. In this experiment, the effect of sampling gas velocity was evaluated by monitoring the extraction efficiency using different gas velocities. The gas was sampled for 30 min from the standard gas generator at room temperature (23 ± 0.5 ^{o}C). Results showed that gas velocity did not significantly affect the extraction amount of limonene when the flow rate was higher than 0.83 cm/s (Figure 4.9). In contrast, the extraction amount of cinnamaldehyde and 2-pentadecanone was significantly influenced by the sampling flow rate, and the extraction efficiency was dramatically increased as the flow rate increased. Additionally, the flow rate effect was found to be more significant for 2-pentadecanone than for

cinnamaldehyde. Extracted amounts of cinnamaldehyde and 2-pentadecanone were enhanced by more than 3 and 9 times respectively when the gas flow rate increased from 0.41 cm/s to 3.7 cm/s. The effect of the small fan inside the sampling chamber was also evaluated. Results showed that when sampling gas velocity was slow (0.41 cm/s), the small fan facilitated extraction efficiency. Conversely, when gas velocity was fast (3.7 cm/s), the small fan had no significant effect on the extraction amount.

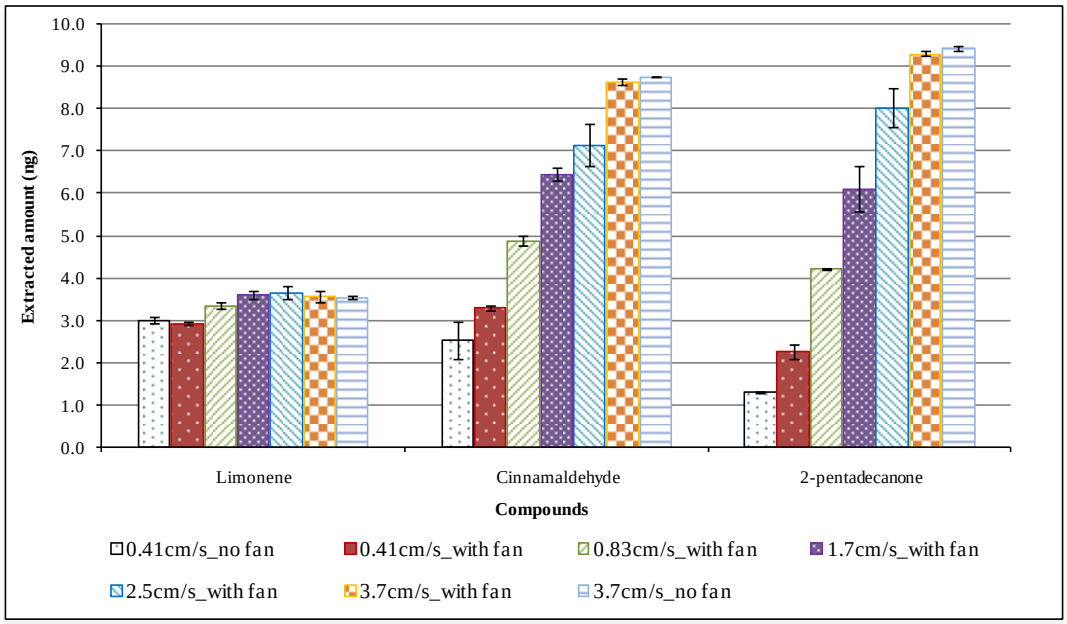

Figure 4.9 The gas velocity effect. The concentrations of the target compounds in the sampling gas are 374 ng/L, 27 ng/L, 23 ng/L for limonene, cinnamaldehyde and 2-pentadecanone respectively. GC injector, solvent vent/split, 50 mL/min.

According to Equation 1.2, the initial extraction rate is inversely proportional to the thickness of the boundary layer: an increase in flow rate decreased the thickness of the boundary layer (δ), therefore enhancing the initial extraction amounts for cinnaldehyde and 2-pentadecanone. In contrast, for an equilibrium extraction, the extracted amount is determined by the thermodynamic parameters instead of the kinetic parameters. The extraction time profile (Figure 4.6) shows that limonene reached equilibrium within 30 min when the gas velocity was

1.3 cm/s. Thus, not finding a significant difference in the extraction amount when the gas velocity was higher than 1.7 cm/s (Figure 4.9) for limonene is consistent with the theory. In other words, it is important to have precise flow rate control when determining pre-equilibrium sampling quantification data.

4.3.5 Effect of sampling gas humidity

Humidity is an inevitable factor in air sampling, and may also influence extraction efficiency. Jacek *et al*. found that for solid coatings such as DVB/PDMS fibers [18], extraction amounts decreased as sampled gas humidity increased, especially when the sampling time was approaching the equilibrium time. This occurrence is explicated as being caused by water molecules occupying the active sites on the solid coating surface. In this experiment, since the membrane is a liquid coating PDMS, theoretically, extraction amounts should not be influenced by humidity. A validation experiment was conducted by comparing the extraction amount of the model compounds in three gases with different relative humidity (19%, 32%, 66%). The gas velocity was set at 2.5 cm/s while the membrane temperature was 4.5 ℃. Comparative results (in Figure 4.10) showed no significant difference on extraction efficiency for gas samples with different humidity. This result was consistent with the prediction, and also demonstrated the advantages of using the liquid coating. A lack of variation in extraction efficiency for gases with different humidity simplified the calibration process for the real sample analysis.

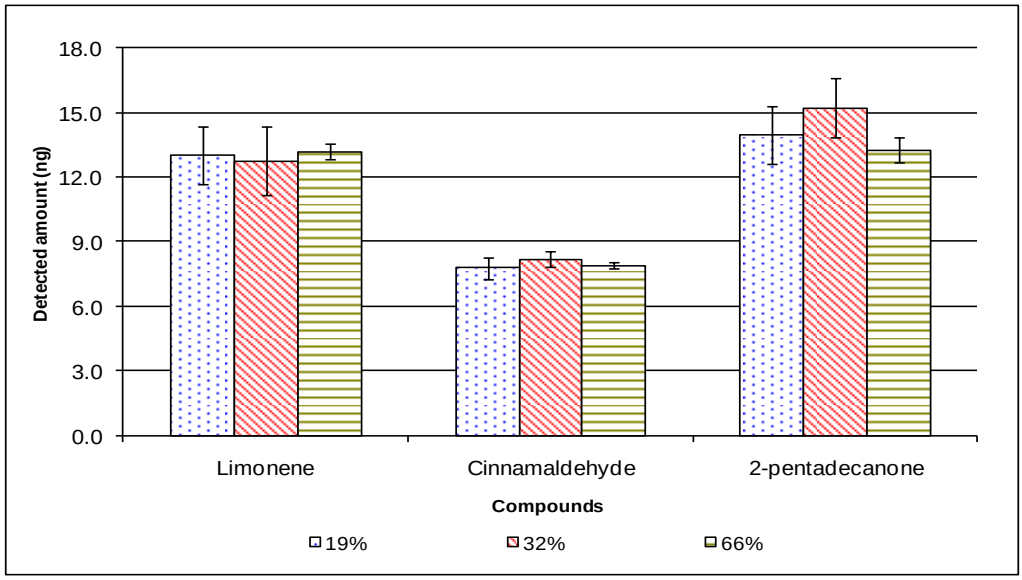

Figure 4.10 The effect of gas humidity. The concentrations of the target compounds in the sampling gas are 442 ng/L, 32 ng/L, 41 ng/L for limonene, cinnamaldehyde and 2-pentadecanone respectively. GC injector, solvent vent/split, 50 mL/min.

4.3.6 The limit of detection

In this experiment, the temperature of the permeation chamber was set at 25 ℃ with a constant nitrogen flow of 150 SCCM (standard cubic centimeter per minute). Different diluted gases, ranging from 3800 SCCM to 9000 SCCM, were used to obtain the standard gases with various concentrations. A calibration curve was first generated by sampling from these gases for 30 min at room temperature. Then, the LOD for the proposed cooling membrane device was determined by 7 samplings of the standard gas with lowest concentration. Here, the standard deviation times three equals the signal of the LOD. By plotting the signal into the calibration curve, the LOD (shown in Table 4.2) for limonene, cinnamaldehyde and 2-pentadecanone were 9.2 ng/L, 0.12 ng/L, and 0.10 ng/L, respectively. It is worth mentioning that the LOD for this experiment was obtained by a standard size membrane with a diameter of 19 mm, and no membrane cooling during the sampling. Lower LODs can be achieved by utilizing larger membranes and/or cooling the membranes.

4.3.7 Real sample analysis

The developed cooling membrane device was used to sample air in an analytical chemistry lab (Room 162, Department of Chemistry, University of Waterloo). Six membranes were used in this experiment. Three of them were used in cooling samplings (4.5 ℃) while the other three were used in non-cooling samplings (23 ℃). The samplings were conducted at the same time and lasted 3 hours in total. Since only one cooling device was developed, for the non-cooling sampling, the membrane was simply placed on a stainless steel desk of the same height as the cooling membrane device. The sampling chamber was removed from the cooling membrane device, and the three pieces of membrane were placed on top of the cooler without cover. Next, the cooling device and the stainless steel desk were placed inside a home-made sampling device (See Figure 5.4, Chapter 5) with a sampling velocity of 3.2 m/s. Figure 4.11 displays chromatograms obtained from the cooling and non-cooling samplings. As observed, it is clear that membrane cooling significantly enhanced the sampling efficiency for the volatile compounds. Highly volatile compounds such as trichloroethylene and toluene could not be detected by the non-cooling membrane. As the volatility decreased, the difference in the extraction efficiency between the cooling and non-cooling membranes decreased.

4.4 Summary

In this Chapter, a novel sample preparation approach which combined the advantages of TFME and cold fiber SPME to further improve the sensitivity of the SPME method was investigated. A detailed procedure for manufacturing this cooling membrane was described, and the device was evaluated by three fragrance compounds representing different volatilities. The results demonstrated that the extraction performance of this device has good agreement with the fundamental theories of SPME and cold fiber SPME. Higher sensitivity sampling for volatile

compounds can be accomplished by decreasing the membrane temperature and/or using large volume extraction phase, while for semi-volatiles, larger and thinner membranes are recommended. Next, the proposed cooling membrane was used for sampling air in the laboratory, and significant improvement in the extraction efficiency was observed when using the membrane with cooling effect.

Last, we review the example raised in the introduction part: for benzene present in air with a concentration of 0.12 ng/mL (detection limit of OSHA-12 standard method), using the proposed cooling membrane device with a membrane diameter of 19 mm and sampling temperature at 5 ℃, the equilibrium extraction amount is around 3.4 ng, which is 3 times higher than the instrument detection limit, 1.2 ng in OSHA-12 standard method. This preliminary study indicated that the cooling membrane device can potentially become a powerful tool in the determination of trace compounds found in air.

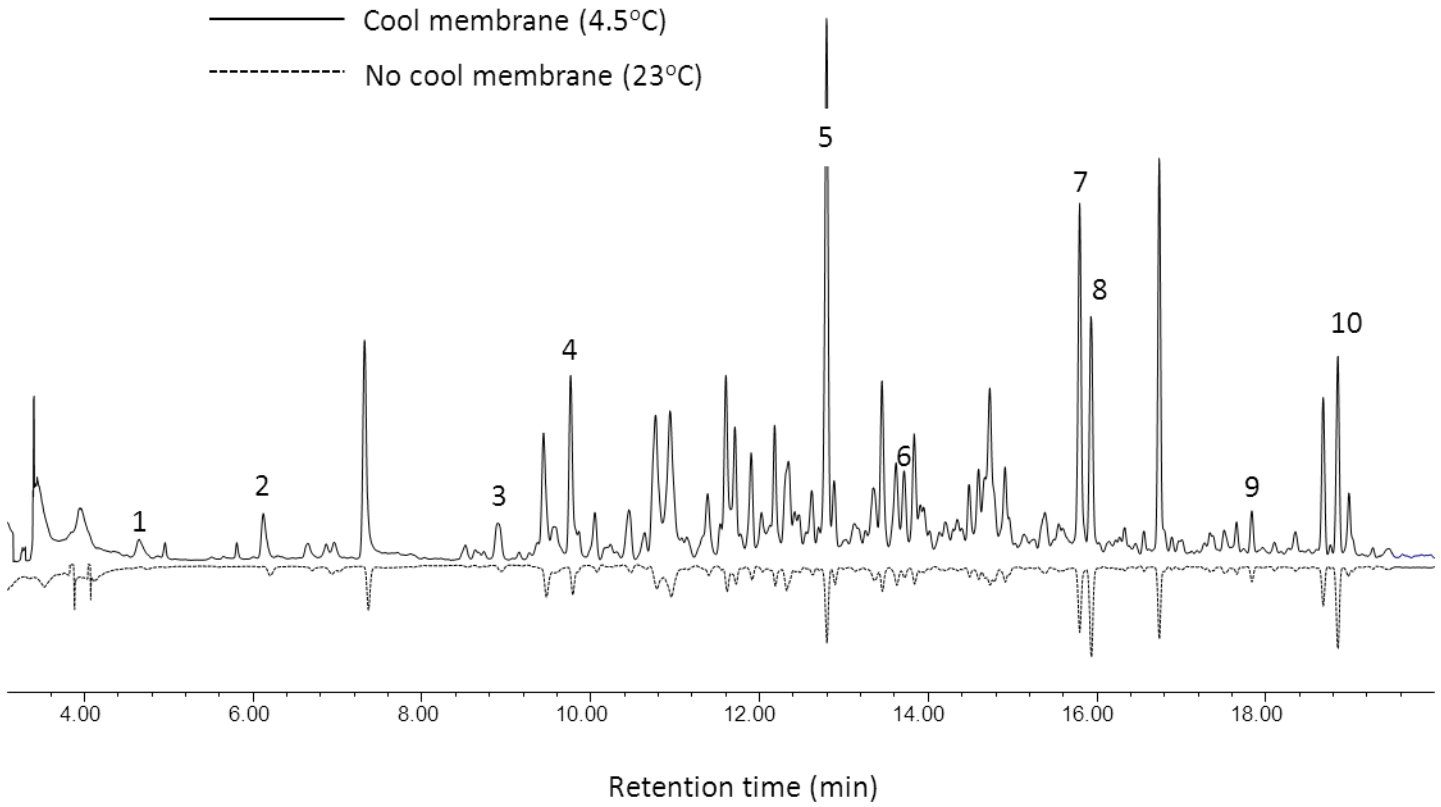

Figure 4.11 Comparison of extraction efficiency of cooling and without cooling for real sample analysis using the cooling membrane device. The sampling time, 3 hours. 1. trichloroethylene; 2. toluene; 3. o-xylene; 4. nonane; 5. decane; 6. limonene; 7. undecane; 8. nonanal; 9. decanal ; 10. undecanal.

Chapter 5 **Preparation of a Particle Loading Membrane for Trace Gas Sampling**

5.1 Introduction

As mentioned in Chapter 1, the introduction of solid sorbents is an alternative approach to improve the capacity of the extraction phase; this is particularly applicable in the sampling of highly volatile compounds. Figure 1.6 in Chapter 1 shows an example of using commercial DVB/PDMS and PDMS fiber for sampling toluene in air sample. The comparison result clearly demonstrated that the DVB/PDMS fiber possesses much higher extraction capacity than the pure PDMS fiber. Here, a membrane loaded with solid sorbent is proposed as an alternative approach to improve the extraction efficiency of the TFME.

Different than absorption phenomenon in liquid coating which is based on analytes permeating or dissolving in the whole volume of the sorbent, adsorption mechanism for solid coating is a consequence of surface energy. Analytes interact with the solid sorbent via $\pi - \pi$ bonding, hydrogen bonding or van der Waals force. Since the adsorption mechanism is different from absorption, the equation used to express the equilibrium extraction amount cannot be directly used for solid coating sampling. Gorecki *et al*. utilized the Langmuir isotherm model to describe the absorption isotherm of analytes on the solid coating [168], and derived the equation for the equilibrium extraction (Equation 5.1).

$$n = \frac{KC_s V_s V_e (C_{e\,max} - C_e)}{V_s + KV_e (C_{e\,max} - C_e)} \qquad \text{Equation 5.1}$$

Where $C_{e\,max}$ is the maximum concentration of the active sites on the coating; C_e is the equilibrium concentration of the analyte on the solid coating; K is the adsorption equilibrium

constant (affinity constant) of the analyte, and C_s is the initial concentration of the analyte in the sample.

Equation 5.1 is similar to the equation described for the liquid coating equilibrium extraction amount, with the exception of the presence of a fiber concentration term, $(C_{e\,max} - C_e)$, in both numerator and denominator. This term results in a non-linear dependence of the extracted amount related to the sample concentration due to a coating saturation effect. In addition, the K is different from the K_{es}, which is the distribution coefficient, whereas K is the adsorption equilibrium constant and expressed as follows:

$$[S] + [A] \rightarrow [SA] \qquad \text{Equation 5.2}$$

$$K = \frac{[SA]}{[S][A]} \qquad \text{Equation 5.3}$$

When the analyte concentration in the sample is low, the equilibrium concentration on the coating, C_e, is negligible compared to the total number of active sites, $C_{e\,max} \gg C_e$. Equation 5.1 can be reduced to Equation 5.4 in this case, which indicates that the extraction amount is linearly proportional to the concentration of the sample matrix (C_s).

$$n = \frac{KC_sV_sV_eC_{e\,max}}{V_s + KV_eC_{e\,max}} \qquad \text{Equation 5.4}$$

In fact, when $V_s \gg KV_eC_{e\,max}$, such as on-site air/water sampling, Equation 5.4 can be further simplified into Equation 5.5. Here, the $KV_eC_{e\,max}$ term is constant for a specific solid coating, and has been defined as fiber constant previously in the literature [169].

$$n = KC_sV_eC_{e\,max} \qquad \text{Equation 5.5}$$

In practice, it is very rare that only one analyte or compound with affinity for the coating is present in a sample. Therefore, due to the limited amount of active sites, the presence of another

compound (B) may significantly affect the extracted amount of analytes (A). In this case, the equilibrium extracted amount of compound A can be expressed as Equation 5.6.

$$n_A = \frac{K_A C_s^A V_s V_e (C_{e\,max} - C_e^A)}{(1 + K_B C_s^B) V_s + K_A V_e (C_{e\,max} - C_e^A)} \qquad \text{Equation 5.6}$$

In this equation, K_A and K_B are the adsorption equilibrium constants for compounds A and B, respectively, and C_e^A and C_s^B are the equilibrium concentrations of A in the coating, and B in the sample matrix, respectively. Thus, the equilibrium amount of analyte A in the presence of compound B must be lower than an amount present in a situation where no competing compounds exist. However, when the interfering compounds are present at a very low concentration, or have low affinity for the extraction phase, the term, $K_B C_s^B$, can be eliminated, and Equation 5.6 can be simplified to Equation 5.1. When the concentrations of components in the sample matrix are at trace levels, Equation 5.4 can be applied. The practical application of outdoor air sampling is that of a sample characterized as having low concentrations and a large volume, and thus the equilibrium calibration method discussed can be used for this solid sorbent quantification by determining the K value.

The solid sorbent chosen in this research is DVB particles which are a commonly used solid sorbent especially in air monitoring [170]. This material has a high degree of mesopores as well as some micropores (Table 1.2, Chapter 1), and it is primarily used for the extraction of semi-volatile and large size volatile analytes. The DVB has a temperature limit of 270 ℃. Above this temperature, the pores could begin to collapse, which would change the property of the adsorbent. In addition, DVB coating can be exposed to solutions within a pH range of 2-11.

The preparation method for the commercial DVB/PDMS fiber begins by suspending the particles inside the PDMS polymer, and layering the mixture over the fiber support until a

desired thickness is obtained. The PDMS polymer rapidly cross-links and serves as an adhesive to retain the particles. Since this PDMS layer is very thin, it does not interfere with the uptake behavior of the analytes onto the adsorbent.

Reported methods for thin film preparation include dipping [171-173], spreading [64, 67, 87], spraying [174], and spinning [88]. In the dipping method, a piece of substrate such as glass or stainless steel is immersed into the coating preparation solution several times until the design thickness is obtained. After curing, the support substrate can be removed or used together with the membrane during sampling. In a paper published by Sekine *et al*.[85], the authors proposed a novel method to prepare a derivatization reagent loaded membrane by first dipping a commercially available cellulose filter paper into the derivatization reagent, then subsequently drying it in the vacuum desiccators. However, this method is not suitable for large size membrane preparation. As well, it is difficult to prepare a reproducible coating with the same thickness.

Spreading coating, also known as bar coating, is the most common technique for wet film preparation. In this method, the thin film is simply prepared by manual or automated spreading of the solution with a film applicator. This method was used to prepare single phase smooth and frosted PDMS thin film [64] and mixed phase PDMS / β-cyclodextrin thin film [67]. Spread coating has been widely applied to commercial membrane preparation. This method provides a simple preparation procedure and can be used in the preparation of large sheets of membrane with a uniform thickness. Furthermore, this method makes preparation of a variety of membranes with different thicknesses very easy and convenient.

The spraying approach is also a traditional method for coating preparation. In a paper published by Mirnaghi *et al*. [174], the authors developed a spray coating method for preparation

of C18-PAN (octadecyl-polyacrylonitrile) 96-blade format thin film, and compared its stability to those prepared by dipping and brush painting. Results found that spray coating provided much better reproducibility and a longer lifetime for the coating. However, this method cannot be used in the preparation of large sheets of membrane. Also, removing the coating from the substrate after preparation is very difficult, and therefore, not suitable for non-support membrane preparation.

Spin coating has been used in the preparation of thin film for several decades. A typical process involves depositing a small puddle of coating solution onto the center of a substrate and then spinning the substrate at high speed (typically higher than 1000 revolutions per minute). Centripetal acceleration causes the solution to spread to the edge of the substrate, and leaves a thin film on the surface. In our laboratory, a spin coating method was developed to prepare the DVB and Carboxen particles-loaded thin film. In order to improve the stiffness of this particle loaded thin film, the membrane preparation solution was deposited on a piece of fiberglass fabric. These thin films were applied in the sampling of low concentration nitrosamines in drinking water, and the detection limits for nitrosamines were several orders of magnitude lower than the pure PDMS membranes. Furthermore, these thin films improved the stiffness of the membrane and facilitated direct extraction in an aqueous matrix with high agitation rate without folding [45]. Spin coating is suitable for preparation of this membrane with a thickness smaller than 10 μm. However, it is difficult to prepare a uniform coating thicker than 10 μm. Moreover, the size of the membrane is limited by the silica wafer, and a large quantity of membrane is difficult to prepare at once.

In this research, A DVB impregnated PDMS membrane was prepared using the bar coating method. The prepared membrane was fully evaluated and applied for semi-quantitative and quantitative sampling of indoor and outdoor air respectively.

5.2 Experimental

5.2.1 Reagents and supplies

Benzene and naphthalene were purchased from Sigma-Aldrich (Mississauga, ON, CA). The HPLC grade methanol used to prepare the standard solution was from Caledon Laboratories Ltd. (Georgetown, ON, CA). A SYLGARD® 184 silicone elastomer kit was purchased from Dow Corning (Midland, MI, USA). DVB particles with a diameter of 3-5 µm were provided by Supelco. Teflon tubes with wall thickness of 483 µm and 279 µm were purchased from Weico Wire & Cable, INC. (Edgewood, NY, USA). A sheet of PDMS membrane with a thickness of 254 µm was obtained from Specialty Silicone product (Ballston Spa, NY, USA). The membrane was cut into round shape with diameter of 6 mm and 17 mm and preconditioned in GERSTEL® thermal desorption system with a constant nitrogen purging flow for 4 hours at 200 ^{o}C, and 5 hours at 250 ^{o}C before use. Ultra-pure helium and nitrogen were purchased from Praxair (Waterloo, ON, Canada). Stainless steel wire with a diameter of 215 µm was purchased from Vita Needle (Needham, MA, USA).

5.2.2 Instrumentation

The analytical instrument used for separation and quantification was an Agilent 6890 GC and 5973 quadrupole MS (Agilent Technologies, CA, USA) coupled with the GERSTEL® CIS 4 and TDU for membrane analysis (GERSTEL, Mülheim an der Ruhr, GE). A GERSTEL® MPS2

autosampler was utilized to achieve the automatic injection. Detailed information regarding the operation of thin film TDU injection can be found in Section 3.2.2, Chapter 3.

The TDU desorption temperature program: 30 ℃ (2 min), 700 ℃ /min ramped to 250 ℃ (5 min). The desorbed solutes were cryofocused in the CIS 4 at -120 ℃. After membrane desorption, the CIS was heated up to 280 ℃ at 10 ℃/s ramping rate, and held for the whole GC run. Two types of injection modes for CIS including solvent vent/split and solvent vent/splitless were selected for different experiments.

Chromatographic separation was performed by a 30 m × 0.25 mm I.D × 0.25 μm thickness SLB^{TM}-5 fused silica column (Sigma-Aldrich, Mississauga, ON, CA). Helium of purity 5.0 was used as a carrier gas at the flow rate of 1mL/min. The column temperature was initially held at 40 ℃ for 2 min and then increased to 200 ℃ at a rate of 5 ℃/min, ramped to 250 ℃ at 10 ℃/min, then kept for 11 min. The MS detector transfer line temperature, MS quadrupole and MS source temperature were set at 300 ℃, 150 ℃ and 230 ℃, respectively. The MS system was operated in the electron ionization mode and mass fragments were collected at a mass-to-charge ratio of 35-300 range.

Both the bar coating machine and a film applicator (with an adjustable gap ranged from 0 - 250 μm) were from Elcometer (Rochester Hills, MI, USA). An anemometer purchased from Omega was utilized to measure the air velocity and temperature (Laval, QC, CA).

5.2.3 Standard gas generator

The evaluation experiments were done by sampling from the standard gas generator, which was composed of a permeation chamber, a mixing (dilution) chamber and a sampling chamber (Figure 5.1). Two permeation tubes containing benzene and naphthalene were prepared. Detailed

description of the preparation of the permeation tubes and construction of the standard gas generator can be found in Section 4.2.3, Chapter 4.

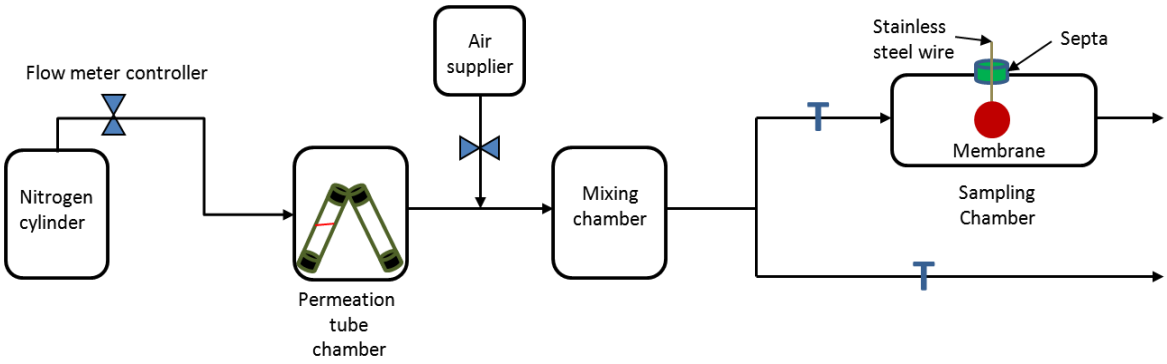

Figure 5.1 The configuration of the standard gas generator

The concentration of the target compounds from the permeation chamber was determined by using sorbent trap active sampling. A 22 gauge needle packed with 1 cm DVB particle (100 mesh) was connected to the downstream of the permeation chamber and a specific volume of standard gas was withdrawn through the needle trap with a pre-determined flow rate. The sampled needle trap was then injected into the GC/MS for desorption, separation and quantification. The sampled amount was determined by a liquid injection calibration curve, and the concentration of the standard gas from the permeation chamber was calculated by dividing the sampled amount by the sampled volume. In order to obtain different concentrations of standard gases, a dilution gas line was connected to the downstream of the permeation chamber, and both gases were passed through the mixing chamber, then separated into two gases after vacating the mixing chamber. The flow rate was regulated by two flow-limiting valves and determined by a soap bubble flow meter.

The stability of the standard gas generator was monitored by a daily QC test. The test was performed by sampling directly from the permeation chamber with a specific membrane for 30

min at room temperature. Any deviation in peak area counts greater than 15% required a direct liquid injection QC test to confirm the source of error. If the instrument signal performed normal, the conditions of the permeation chamber would be checked to ensure the constant emission rate. The absolute extraction amount was determined by a liquid injection calibration curve.

5.2.4 Particle loading membrane preparation

Since the diameters of the DVB particle are very small (3-5 μm), it is difficult to dissolve them directly in the high viscosity PDMS bulk. The organic solvent hexane was used to dissolve the particles first. 20/100, w/w, particle/hexane mixture was weighted into the 10 mL vial and sonicated for at least half an hour. Sonication would run for a longer period if there was a large amount of particles to be handled.

Other agitation methods such as stirring and shaking were investigated and compared. Results showed that the most effective method for this experiment would be sonication. It took a longer time to obtain a uniform solution by stirring and shaking because the particles tended to cluster due to their small diameter. It was concluded that if the particles in this step did not distribute uniformly in hexane, it would be difficult to disperse them evenly in a PDMS base, since the viscosity of PDMS is much higher than hexane.

The effect of sonication on particle structure was investigated: the morphology of the DVB particle before and after sonicating for 1 hour was taken by scan electron microscope (SEM). Figure 5.2 shows no significant difference on the particle appearance, which confirmed that the sonication process did not destroy the DVB particles. Another organic solvent, methylene chloride, was tested as well. However, the low boiling point of this solvent made it evaporate too fast, and caused a non-uniform surface during spreading.

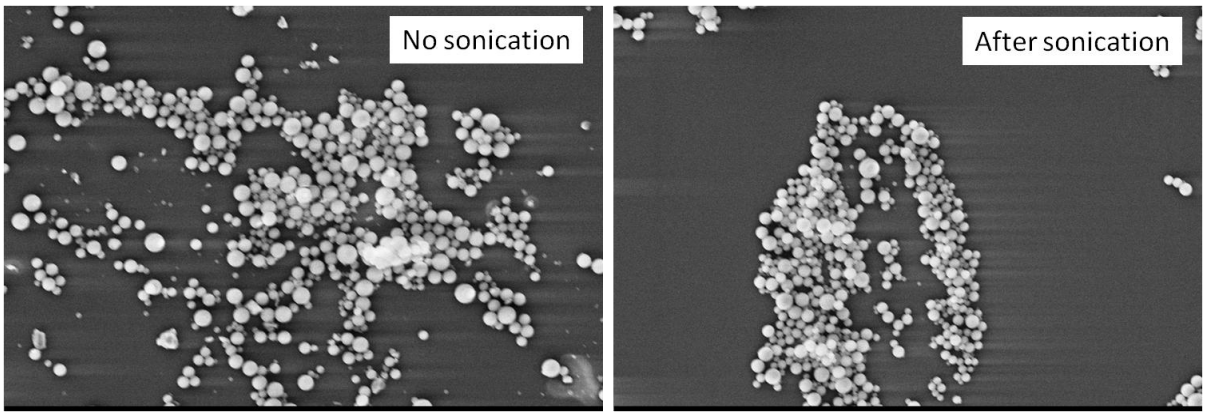

Figure 5.2 Comparison of the particle morphology before and after sonication

After thoroughly dispersing the particle in the hexane, the PDMS base was added. The mixture was then sonicated for another 1 hour in order to evenly blend the PDMS base with the particle solution. Next, a 10/100, w/w, curing reagent/PDMS base of curing reagent was added into the obtained mixture, and again thoroughly mixed for 30 min. At this point, the mixture in the vial should be uniform, without any layers. To test this, a small drop of the solution was taken and spread on a glass surface: if properly prepared, one should observe a glue-like solution without any visible particles in it.

In this optimization experiment, another type of PDMS with higher viscosity provided by Supelco was tested. However, the GC blank of the prepared membrane observed more siloxane peaks and a higher response than the membrane prepared using low viscosity PDMS purchased from Dow Corning (Figure 5.3). Therefore, the Dow Corning PDMS base and curing reagent kits were chosen for the following preparation experiment.

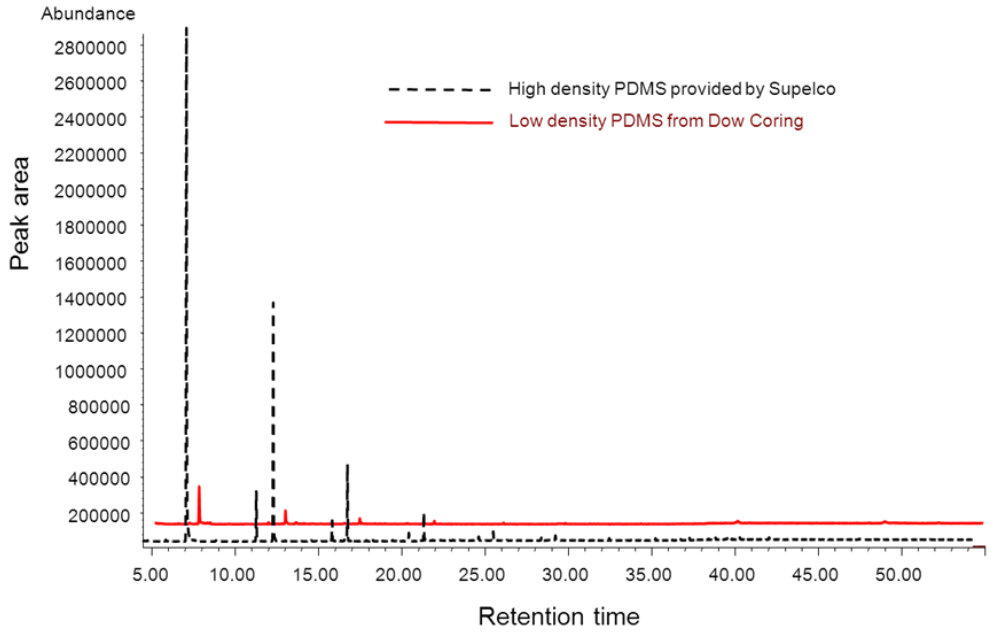

Figure 5.3 Chromatograms of the membrane blanks prepared by different PDMS

Before spreading, the viscosity of the obtained solution should be optimized, since lower viscosity results in thinner coating. To adjust the viscosity, the excess hexane can be purged away by using nitrogen gas till a suitable viscosity spreading solution was obtained. Higher viscosity can also be obtained after cross-linking of the PDMS starts.

In addition to viscosity, the thickness of the coating is also influenced by the height of the film applicator and the spreading speed. In order to obtain a uniform membrane, all experimental parameters, including the amount of solvent, sonication time and spreading speed should be constant for each preparation process. For these experiments, the thickness of the coating was measured by a digimatic micrometer from Mitutoyo (Mississauga, ON, CA).

After spreading, the prepared membrane was cured inside the oven with a temperature of 80 ℃ for 5 hours. Following, the temperature was increased to 120 ℃ under -15 mmHg vacuum for 3 hours. After curing, the membranes were cut into a round shape with two different diameters: 6

mm for lab applications and 17 mm for on-site analysis. Next, membranes were placed inside the GERTEL thermal condition tube for conditioning; they were baked under nitrogen flow at 200 ℃ for 5 hours and at 250 ℃ for 5 hours to ensure no significant bleeding and contamination in GC analysis. The membranes were also conditioned for 4 hours in a TDU injector with a split flow of 100:1 before sampling to obtain a reasonable membrane blank. A small amount of siloxane bleeding occurring in the prepared membrane is unavoidable; thus, in the membrane blank chromatography, some siloxane peaks were always detected (Figure 5.3).

5.2.5 Experimental procedure

Evaluation experiments for the particle loading membrane were conducted by sampling from the standard gas generator with an experimental set-up shown in Figure 5.1. A piece of DVB/PDMS membrane with diameter of 6 mm was attached to a stainless steel wire (215 μm diameter, 4 cm length). The wire was pierced through a piece of green septa and exposed inside the sampling chamber during sampling. After sampling, the septa with the membrane was removed from the sampling chamber, and the membrane with the wire was quickly inserted inside a TDU tube, which was capped with Teflon caps and cooled by dry ice immediately before injecting into the GC/MS for analysis.

For on-site air sampling, the membrane was cut into a round shape with a diameter of 17 mm and conditioned according to the procedure described in Section 5.2.4. A stainless steel cotter pin was used to hold the membrane during sampling. In order to maintain a constant flow rate, a home-made device (Figure 5.4) was used for sampling. The device was made of a paper cylinder: one end of the cylinder was connected to a fan to withdraw the air passing through the cylinder. The membranes were placed inside the box with a surface parallel to the air flow direction.

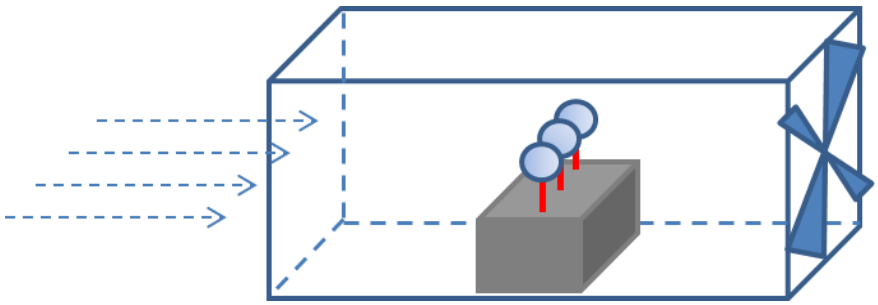

Figure 5.4 The home-made air sampling device

5.3 Results and discussion

5.3.1 Evaluation of the prepared DVB/PDMS membrane

5.3.1.1 Morphology of the prepared membrane

The first course of analysis was evaluating the morphology of the prepared particle loading membrane by SEM. Figure 5.5 shows images taken from both the cross section and the surface of the membrane (one side). The DVB particles were uniformly distributed in the PDMS bulk, with no separation layers or clustering observed. This result can be attributed to sufficient agitation during the membrane preparation process. The surface morphology shown in Figure 5.5 was taken from the side that faces the air during spreading. For membranes with different particle ratios, the densities of the particles can be easily distinguished from the SEM image.

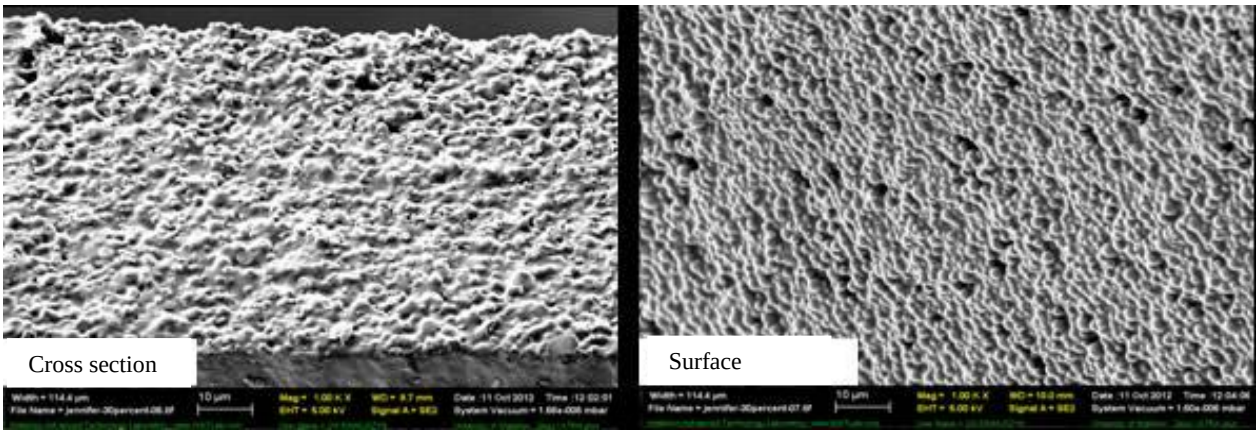

Figure 5.5 The morphology of the prepared particle loading membrane (DVB/PDMS, w/w, 30/100)

5.3.1.2 Effect of particle ratio on extraction efficiency

To evaluate the effect of particle ratio on the extraction efficiency of the prepared membrane, four membranes with particle ratios of 0/100, 10/100, 20/100, 30/100, w/w, DVB/PDMS, were prepared and applied for benzene sampling. The membranes all had the same diameter of 6 mm and different thicknesses of 152 µm, 142 µm, 105 µm and 102 µm for 0/100, 10/100, 20/100, 30/100, w/w, DVB/PDMS membranes, respectively. Each sampling was conducted in the standard gas generator with a benzene flow rate of 4.8 cm/s and concentration of 33 ng/mL for 30 min. Each membrane was sampled three times and the average extraction amount was shown in Figure 5.6. Comparison results demonstrate that membranes with higher particle ratios provided higher capacity for analyte extraction. The extraction amount of benzene increased more than 100 times when the particle ratio increased from 0/100 to 30/100.

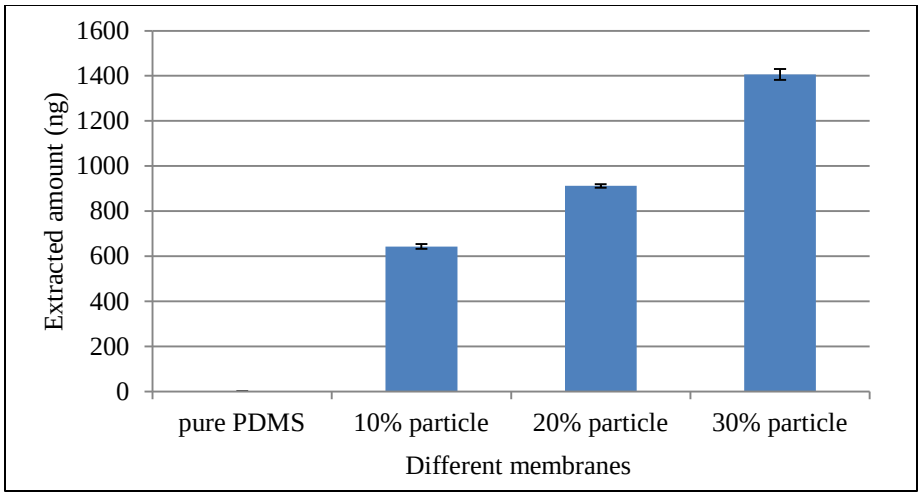

Figure 5.6 Comparison of the extraction amount of benzene for different particle ratio membranes

5.3.1.3 The analytical figures of merit

The analytical figures of merit for different particle ratio membranes were evaluated by sampling from the standard gas generator containing benzene. The diameter of the sampling membranes was 6 mm with different thicknesses (listed in Table 5.1). Three calibration curves with concentration ranging from 15 ng/mL to 165 ng/mL were plotted by three particle ratio membranes. The sampling time was 30 min while the sampling temperature was 23±0.5 ℃.

The linear range of the calibration curve is around 15 ng/mL to 99 ng/mL for all three membranes with a linearity coefficient higher than 0.9899. The plotted lines for all membranes started to curve when the concentrations of analyte were higher than 99 ng/mL. This result was expected since the extraction mechanism of the particle loading membrane is based on adsorption: when the active sites of the DVB particles tend to be saturated, the calibration curve losses its linearity. Furthermore, the linearity coefficient of the calibration curve decreased as the particle ratio increased. These results were predicted from Górecki's publication [168], where he concluded that an extraction phase with a lower K value possesses a broader linear concentration

range. On the other hand, the slope of the calibration curve increased as the particle ratio increased, which indicated that higher particle ratios result in higher sampling sensitivity.

The membrane constant for benzene can be determined from the slope of the calibration curve. According to Equation 5.5, if the volume of the extraction phase is known, then $KC_{e\,max}$ can be calculated by dividing the slope of the concentration profile over the volume of the extraction phase. From the results obtained in this experiment, the $KC_{e\,max}$ increased around 3 times when the particle ratio increased from 10% to 30%. The capacity of the particle loading membrane was mainly determined by the amount of particles, and can be further improved by increasing the particle ratio. However, the particle ratio cannot be increased past a certain extent for the self-supporting membrane. The PDMS functions as glue in the membrane, and when the amount of the PDMS decreases as particles ratio increase, the PDMS cannot strongly hold the particles, and the final membrane become very fragile. As previously stated, when higher particle ratio membranes need to be prepared, an external support such as glass fiber fabric can be used. This type of membrane was reported in paper published by Riazi Kermani *et al*. [68]. In his research, glass fiber fabric support carboxen/PDMS membrane was prepared for sampling nitroamines in water. Because of the additional support of fabric, the prepared membrane was very stiff and could be successfully used in water direct immersion sampling under 250 rpm agitation.

The detection limit for the three particle ratio membranes were around 0.03 ng/mL, which is lower than the OSHA-12 standard method indicated in Chapter 4 (0.12 ng/mL). The LOD was determined from the calibration curves: three times the standard deviation of the calibration curve was used as the signal for the detection limit. By dividing the signal by the slope of the calibration curve, the concentration of the detection limit can be obtained.

No significant difference in the LOD was observed for the different particle ratio membranes. This is because the volume of the 10% DVB membrane was bigger than the other two membranes, which increased the capacity of the membrane. In fact, the LOD can be further improved by using a larger membrane.

Table 5.1 The analytical figures of merit for DVB/PDMS membrane benzene air sampling

Membranes	Thickness	ID	LogK	Linear range (ng/mL)	Slope	R square	LOD (ng/mL)
10% particle	142		3.68		0.44	0.9937	0.0374
20% particle	105	6mm	3.96	15 -99	0.60	0.9918	0.0349
30% particle	102		4.16		0.91	0.9899	0.0317

5.3.1.4 Effect of membrane size

An experiment was conducted to verify the extraction theory of the home made DVB/PDMS membrane. According to Equation 5.5, when the analyte concentration is constant and the volume of the sample matrix is large enough, the equilibrium extraction amount is linearly proportional to the volume of the extraction phase. In this experiment, three pieces of 20/100, w/w, DVB/PDMS membranes with same thickness but different diameters (3.4 mm, 6 mm, 8 mm) were selected as the extraction phase. The sampling was conducted from the standard gas generator with a known benzene concentration of 7.2 ng/mL at a gas flow rate of 4.8 cm/s, and lasted for 30 min. Triplicate experiments for each membrane were conducted, and average extraction amount versus volume of the membranes was plotted in Figure 5.7. Good linearity between the extraction amount and the membrane size was obtained, which demonstrated that the extraction mechanism of the prepared DVB/PDMS membrane was in agreement with adsorption fundamental theory.

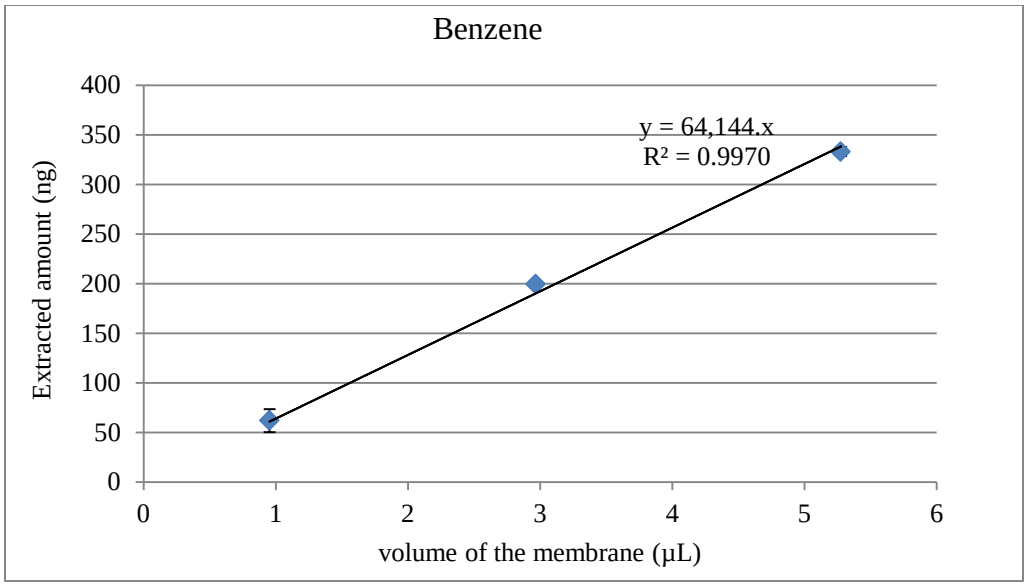

Figure 5.7 The effect of membrane size on the particle loading membrane

5.3.1.5 Comparison of the extraction efficiency of the DVB/PDMS membrane with PDMS membrane and DVB/PDMS fiber

In this experiment, the extraction efficiency of the DVB/PDMS membrane was compared with the commercial PDMS membrane and the commercial DVB/PDMS fiber for outdoor air sampling. The sampling lasted for 6 hours (9:30 am to 3:30 pm), and was conducted in the balcony of the chemistry department lounge room at University of Waterloo. Three pieces of 20% particles DVB/PDMS membranes (105 μm), three pieces of PDMS membranes (254 μm) and three DVB/PDMS fibers (65 μm) were used and sampled at the same time in a close area. The sampling was conducted in the home-made device shown in Figure 5.4. To compensate for errors due to differences in sampling spots, the positions of the extraction phase were randomized. After sampling, membranes were stored inside the TDU tube and capped with Teflon caps and fibers were retracted back into the needle and capped with home-made Teflon caps (made by Science machine shop, University of Waterloo). All the extraction phases were stored in dry ice before GC analysis to prevent analyte loss. The PDMS membranes were analyzed first, followed

by DVB/PDMS membranes and DVB/PDMS fibers, respectively. The chromatograms obtained from each injection were processed using the NISTEPA.MSL library by AMDIS software. Compounds appearing in all triplicate chromatograms were recognized as the sampled compounds for that specific extraction phase

The average extraction amounts of each compound for the three extraction phases are compared in Figure 5.8. Results show that the prepared DVB/PDMS membrane had a higher affinity towards a large range of compounds with different volatilities. This is particularly true for volatile compounds such as BTEX, 2-heptanone and cyclohexanone. These compounds cannot be detected by the pure PDMS membrane, and have a low response for the commercial DVB/PDMS fiber. Results further revealed that the particle addition membrane not only increased the volume of the extraction phase but also high affinity towards a range of compounds. In addition, the small error bar of the three membranes sampling demonstrates the applicability of this new membrane towards comparison analysis and quantification application. This result was expected due to the spreading preparation procedure. Three membranes were cut from the same sheet of a large membrane, guaranteeing the reproducibility of the inter-membrane sampling. Additionally, the prepared DVB/PDMS membrane also showed higher affinity towards polar compounds such as dimethylamine, benzaldehyde and 1,2-dichlorobenzene when compared to the pure PDMS membrane. In contrast, the DVB/PDMS membrane showed no significant improvement on the extraction of large compounds such as dodecane, tridecane, 1-undecanol and pentadecane when compared to PDMS membrane. This result may due to the large size of the analytes that cannot retain by the DVB particle pore. As introduced in Chapter 1, the adsorbent can retained analytes that are around half the size of particle pores. This conclusion can be also illustrated by the extraction amount of decane (14), undecane (20), dodecane (24),

tridecane (25) and pentadecane (28) with DVB/PDMS membrane and PDMS membrane. Comparison results showed that as the carbon number increased, the DVB/PDMS extracted amount compared to the PDMS membrane extracted amount became smaller.

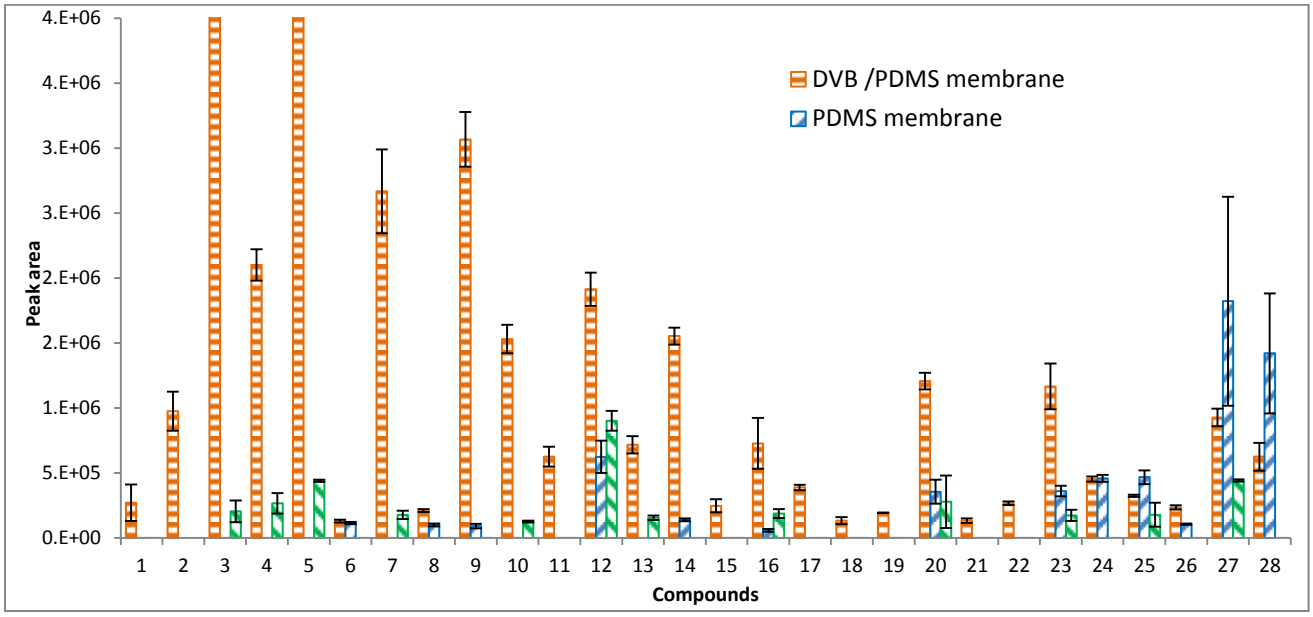

Figure 5.8 Comparison of the extraction efficiency for three types of extraction phase for outdoor air sampling. (Compounds shown in Table 5.2)

Table 5.2 Compounds detected from the outdoor air

#	Compounds	CAS #	Ref. index	Cal. Index
1	Dimethylamine	124-40-3	434	441
2	Benzene	71-43-2	629	617
3	Toluene	108-88-3	755	755
4	Ethylbenzene	100-41-4	850	862
5	m-Xylene	95-47-6	875	872
6	2-Heptanone	110-43-0	889	893
7	o-Xylene	95-47-6	893	898
8	Cyclohexanone	108-94-1	874	901
9	alpha.-Pinene	80-56-8	939	939
10	Camphene	79-92-5	953	955
11	Benzene, propyl-	103-65-1	962	957
12	Benzaldehyde	100-52-7	970	966
13	Benzene, 1,2,4-trimethyl-	95-63-6	976	972
14	Decane	124-18-5	1000	1000
15	Benzene, 1,2-dichloro-	95-50-1	1013	1017

16	Limonene	138-86-3	1031	1031
17	Benzene, 1-methyl-2-propyl-	1074-17-5	1050	1052
18	Decane, 4-methyl-	2847-72-5	1060	1060
19	Benzene, 1-ethyl-2,4-dimethyl-	874-41-9	1077	1077
20	Undecane	1120-21-4	1100	1100
21	Benzene, 1,2,3,5-tetramethyl-	527-53-7	1118	1110
22	Benzene, 1,2,4,5-tetramethyl-	95-93-2	1123	1121
23	Naphthalene	91-20-3	1185	1187
24	Dodecane	112-40-3	1200	1198
25	Tridecane	629-50-5	1300	1300
26	Naphthalene, 2-methyl-	91-57-6	1300	1300
27	1-Undecanol	112-42-5	1347	1307
28	Pentadecane	629-62-9	1500	1498

5.3.2 Semi-quantitative air sampling

The previous evaluation results show that the prepared DVB/PDMS membrane provided higher extraction capacity towards a large range of compounds with different volatilities when compared to the pure PDMS membrane and the fiber SPME. This feature demonstrates that the prepared membrane is a suitable extraction medium for global screening of air pollutants in working places. The detected compounds can be semi-quantified by searching the obtained mass spectra in the NIST02 library, and further confirmed by Kovats index. The Kovats index was determined by injecting the alkane standards containing C5 - C20 into the GC with the same conditions as the real sample analysis. The Kovats index was calculated according to Equation 5.7, and compared to the literature values were obtained from NIST webbook [175].

$$I = 100 \times [n + (N - n)\frac{t_{r(unknown)} - t_{r(n)}}{t_{r(N)} - t_{r(n)}}] \qquad \text{Equation 5.7}$$

Where n is the number of carbon atoms in the smaller n-alkane; N is the number of carbon atoms in the larger n-alkane; t_r is the retention time.

The first sampling place chosen was the chemical storage room in the chemistry department, where chemicals, including inorganic and organic compounds, are stored. Three pieces of 20% DVB/PDMS membranes with a diameter of 17 mm and a thickness of 140 μm were placed in the home-made sampling device shown in Figure 5.4. However, since electronic devices are not allowed in the chemical storage room, the fan was removed and the cylinder was attached to the venting system in the room. The sampling lasted 7 hours, from 9:30 am to 4:30 pm. After sampling, the membranes were stored in the TDU tube and cooled by dry ice before GC/MS analysis. The obtained chromatograms were processed by the AMDIS software with a library that composes organic compounds stored in the storage room. Table 5.3 shows the compounds detected from the three chromatograms. Among them, peaks for trichloromethane, heptane, toluene, and 1,3-dimethyl benzene were much higher than the others. Later investigation in the Chemstore led to the discovery that these four compounds were being stored in a big jar with an ineffective seal.

Table 5.3 Compounds detected from the chemical storage room

Comp. #	Name	CAS	Ref. index	Cal. Index
1	Pentane	67-66-3	500	500
2	Hexane	110-54-3	600	600
3	Ethyl Acetate	141-78-6	618	616
4	Ammonium acetate	631-61-8	ND	623
5	Trichloromethane	67-66-3	621	623
6	Benzene	71-43-2	657	657
7	Pentane, 2,2,4-trimethyl-	540-84-1	689	685
8	Heptane	142-82-5	700	699
9	Acetic acid	64-19-7	660	711
10	Triethylamine	121-44-8	727	760
11	Toluene	108-88-3	776	775
12	Acetic acid, butyl ester	123-86-4	800	825
13	Benzene, chloro-	108-90-7	859	858
14	Benzene,1,3-dimethyl-	108-38-3	885	883
15	o-Xylene	95-47-6	908	906
16	Cyclohexanone	108-94-1	894	907
17	Aniline	62-53-3	945	945
18	Phenol	108-95-2	967	981
19	Benzoic acid	65-85-0	1160	1152
20	Benzophenone	119-61-9	1611	1615

Ref. Index: Kovats index from literature

Cal. Index: Kovats index from experimental result calculation

Another semi-quantification application of the prepared particle loading membrane was conducted for screening featured fragrance compounds from a specific perfume. As we known, for a specific perfume, it contains three notes, top notes, middle notes, and base notes. Usually, top notes contain compounds with high volatility while base notes contain the ones with less volatility. For compounds from different notes, different sampling procedures are usually required. In this experiment, we used the prepared DVB/PDMS membrane as the extraction phase to sampling the air impregnated with perfume. The sampling was conducted in a 10 m^2 room where the air condition system was operating normally. A person wearing the perfume entered the room 40 min after spraying, and the sampling started 20 min after entrance to the room. Three membranes were placed inside the home-made sampling device (Figure 5.4), and

the fan was used to force the air flow through the membrane. This sampling lasted for 8 hours. After sampling, the membranes were analyzed by GC/MS and the chromatograms were processed by AMDIS software with library containing fragrance compounds. The selected fragrance compounds have been reported for the notes in the perfume. The detected compounds was confirmed using Kovats index.

One of the perfumes used for this experiment was Tresor Midnight Rose for women. For this fragrance, the reported top notes are raspberry and blackcurrant; middle notes are rose absolute, jasmine, peony; base notes are virginian cedar, musk and vanilla. Another perfumes used in this experiment was Mon Jasmine Noir. The top notes for this perfume are citruses and lily of valley; middle note is jasmine, and base notes are musk, patchouli, virginian cedar and nougat. The detected compounds from the chromatogram were listed in Table 5.4 as well as the possible sources of the compounds. From the identified compounds, we can detect the compounds from the three notes.

Table 5.4 Fragrance compounds detected from the indoor air

Compound Name	CAS	Ref. index	Cal. Index	Source
Propylene Glycol	57-55-6	753	795	Vanilla
beta.-Pinene	127-91-3	956	951	Raspberry, black currant,rose,
beta.-Phellandrene	555-10-2	1005	988	Raspberry
Limonene	138-86-3	1036	1042	Citrus
Benzyl Alcohol	100-51-6	1046	1043	Rose
Benzenepropanal	104-53-0	1109	1064	Rose
1,6-Octadien-3-ol, 3,7-dimethyl-	78-70-6	1103	1104	Rose, Jasmine, citrus
Nonanal	124-19-6	1094	1108	Black currant
Acetic acid, phenylmethyl ester	140-11-4	1165	1164	Jasmine
6-Octen-1-ol, 3,7-dimethyl- (beta-citronellol)	106-22-9	1209	1181	Citrus
Dihydro iso-jasmone			1186	Jasmine
Formic acid, 2-phenylethyl ester	104-62-1	1178	1253	Rose
Benzaldehyde, 4-methoxy-	123-11-5	1258	1255	Vanilla
2,6-Octadienal, 3,7-dimethyl-, (Z)- **(Cirial)**	106-26-3	1249	1266	Citrus
2,6-Octadien-1-ol, 3,7-dimethyl -, acetate, (Z)- (neryl acetate)	141-12-8	1375	1374	Rose
Vanillin	121-33-5	1394	1392	Vanilla
Caryophyllene	87-44-5	1418	1414	Rose
3-Buten-2-one, 4-(2,6,6-trimethyl-1-cyclohexen-1-yl)- **(beta-ionone)**	14901-07-6	1486	1477	Rose
3-Buten-2-one, 4-(2,6,6-trimethyl-2-cyclohexen-1-yl)- **(alpha-ionone)**	6901-97-9		1662	Raspberry
Patchouli alcohol	5986-55-0	1695	1723	Patchouli
Benzyl Benzoate	120-51-4	1803	1811	solvent for musk
Cyclopentadecanone, 3-methyl- **(Muscone)**	541-91-3	1831	1857	Musk
Ethanone, 1-(5,6,7,8-tetrahydro-3,5,5,6,8,8-hexamethyl-2-naphthal enyl)-	21145-77-7	1850	1869	Musk

5.3.3 Quantitative air sampling

Benzene and naphthalene were the two compounds chosen for the quantitative study. Benzene has been classified as carcinogenic compound by EPA (Environmental Protection Agency). Chronic inhalation of certain levels of benzene can cause disorders in the blood, affect bone marrow and cause both structural and numerical chromosomal aberrations in humans [176-178]. Naphthalene is defined as a potential human carcinogen by EPA. Short term human exposure to naphthalene by inhalation, ingestion, and dermal contact is associated with hemolytic anemia, damage to the liver and neurological damage. Long term exposure has been reported to cause cataracts and retinal hemorrhage [179, 180].

Both compounds are ubiquitous air pollutants that are mainly found in emissions from burning coal and oil, motor vehicle exhaust, evaporation from gasoline service stations and cigarette smoking [181-183]. It is important to evaluate the concentration of both compounds in outdoor air, especially traffic air, since some drivers spent most of their time on the road. Long exposures in this environment may threaten their health.

5.3.3.1 Loss and storage evaluation

Before using the DVB/PDMS membrane for quantitative sampling of air pollutants, a loss evaluation of the membrane after sampling should be done to ensure the accuracy of the quantification results. Here, the loss evaluation experiment was presented as the desorption time profile of the deuterated target compounds d6-benzene and d8-naphthalene. The membrane was preloaded with these two compounds and placed in the air flow system with a flow rate of 10.6 cm/s for different periods of time. After desorption, the membrane was injected into the GC/MS in order to obtain the amount of analyte left on the membrane. The desorption time profile is shown in Figure 5.9a. For the volatile compound benzene, the desorption amount dropped dramatically as the exposure time increased. Within 10 min, 50% of the benzene was desorbed from the membrane. This result indicated the membrane sampled with benzene should be stored at a low temperature. An ideal storage method for sampled PDMS membrane was discussed in Section 3.2.4, Chapter 3; results showed that dry ice was the best coolant to store the volatile compounds. To evaluate optimized conditions for membrane handling after sampling, a shorter desorption time was investigated. The shortest time required to remove the membrane from the sample matrix and place it in the TDU tube is 5 s. As the operation time increased to 20 s, the extracted amount decreased around 5% (Figure 5.9b), which is within the experimental error for the sampling. Therefore, if the membrane handling time falls within 20 s after sampling, analyte

loss can be neglected; a 20 s moving period should not be an issue for quantitative analysis. However, 20 s are rarely needed for membrane transportation.

In contrast, there were no significant changes for the desorption amount of naphthalene during the selected desorption time. This demonstrates that the DVB/PDMS membrane has a strong affinity towards naphthalene and can be stored at room temperature after sampling.

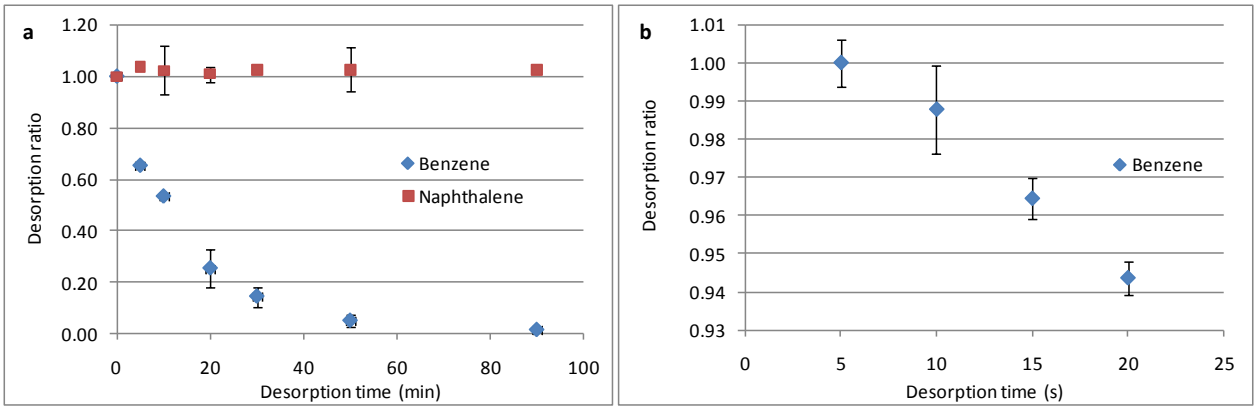

Figure 5.9 The desorption profile of benzene and naphthalene. (a) desorbed in standard gas generator with flow rate of 10.6 cm/s; (b) exposed in the environmental air.

5.3.3.2 The extraction time profiles for the target compounds

The extraction time profiles of the two target compounds, benzene and naphthalene, were obtained by sampling from the standard gas generator. To avoid a displacement effect, both of the extraction time profiles were done by sampling from a standard gas with only one compound present at a time when conducting the extraction time profile. The experimental set-up is shown in Figure 5.1: the concentrations were 33 ng/mL and 0.0033 ng/mL for benzene and naphthalene, respectively. The membrane used for this sampling was a 20/100, w/w, DVB/PDMS membrane with a diameter of 6 mm and a thickness of 105 µm.

The obtained extraction time profiles for benzene and naphthalene are shown in Figure 5.10; while benzene reached equilibrium within 20 min, naphthalene was still in the linear increase

region after 540 min of extraction. These results indicated that the equilibrium calibration method can be used for benzene sampling while the pre-equilibrium calibration method should be considered for naphthalene due to its long equilibrium time.

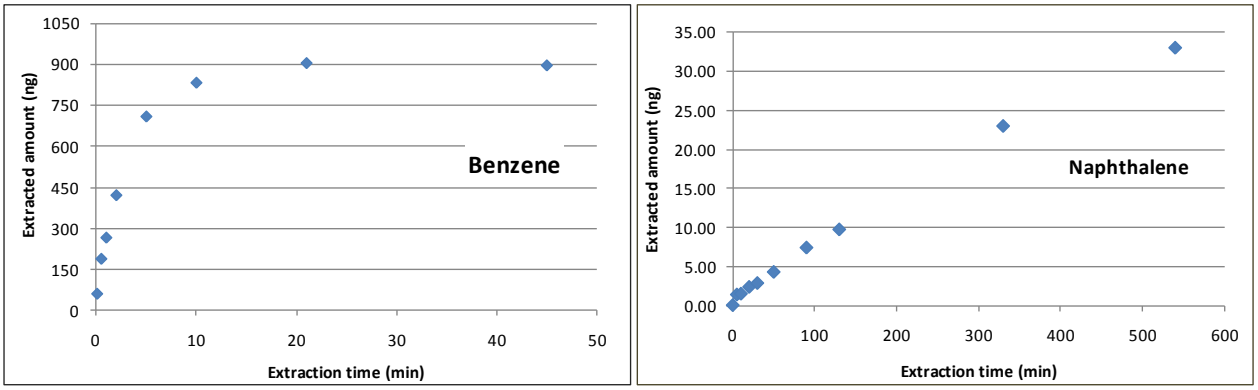

Figure 5.10 Extraction time profiles for benzene and naphthalene from standard gas generator

5.3.3.3 The equilibrium calibration method for volatile compounds

For equilibrium calibration, according to Equation 5.4, the value of $KC_{e\,max}$ should be determined. When using a single compound standard gas, based on Equation 5.4, the $KC_{e\,max}$ can be calculated from the equilibrium extraction amount if the concentration and the volume of the extraction phase are known. From the benzene extraction time profile, we can determine the $KC_{e\,max}$ for the 20% DVB/PDMS membrane (shown in Table 5.1).

However, the obtained $KC_{e\,max}$ cannot be used in air sampling quantification without ensuring that displacement effect from the interference compounds in the sample matrix has no taken place. Here, a displacement effect may not happen because of the high capacity of the DVB/PDMS membrane and the low level characteristic of organic compounds in the outdoor air sample. In order to demonstrate this effect, three matrices with different concentration of interference compounds (toluene, naphthalene) were used to determine the $KC_{e\,max}$ value for benzene. The equilibrium extraction amount was determined by sampling from each matrix for

60 min. The log $KC_{e\,max}$ value for each matrix was calculated and results are shown in Table 5.5. As predicted, no significant difference was observed on the $KC_{e\,max}$ value from different matrices. This observation demonstrated that the prepared particle loading membrane can be used for equilibrium calibration method for benzene sampling in low concentration air, such as outdoor air sampling.

Table 5.5 The log$KC_{e\,max}$ of benzene on 20% DVB/PDMS membrane obtained from different matrices.

	B (single)	**B (0.74 ng/mL) T (3.9 ng/mL)**	**B (2.4 ng/mL) T (0.26 ng/mL)**	**B (1.4 ng/mL) N (0.0017 ng/mL)**
log $KC_{e\,max}$	3.96	3.97	3.96	3.97

B=benzene, T=toluene, N=Naphthalene

5.3.3.4 The Pre-equilibrium calibration methods for semi-volatile compounds

5.3.3.4.1 On-fiber standard calibration

The on-fiber standard calibration method is suitable for on-site air sampling. The on-membrane standard calibration method has been applied to determine the TWA concentrations of PAHs in Hamilton Harbor using PDMS membranes [60, 61]. Experimental results were compared to those obtained from both fiber exposed and fiber retracted SPME formats. Furthermore, this method observed a much higher sampling rate compared to the fiber geometry.

Before using this method, the symmetric relationship between the adsorption and desorption process should be investigated since the membrane used here is a solid coating. A loading method using the standard gas system described in Section 3.2.4, Chapter 3 was used in this experiment to preload the deuterated compounds d6-benzene and d8-naphthalene. The deuterated compounds were spiked into a 40 mL vial containing pump oil and DVB particles mixture. The membrane attached to a piece of stainless steel wire was exposed inside the vial where deuterated compounds released from the mixture of pump oil and DVB particle were headspace

sampled for a pre-determined time. After loading the compounds, the membrane was exposed in the standard gas containing benzene and naphthalene. The non-deuterated analytes from the standard gas generator were adsorbed onto the membrane while the deuterated compounds were desorbed from the membrane. The extraction time profiles and desorption time profiles for the non-deuterated and deuterated benzene and naphthalene are shown in Figure 5.11. From these figures we can see that, for benzene, the symmetric relationship is clear. However, naphthalene did not provide the same relationship between the adsorption and desorption; the d8-naphthalene cannot desorb from the membrane at room temperature. Therefore, we cannot use an on-membrane standard calibration method for naphthalene. It is important to note that the equilibrium time for benzene shown in Figure 5.11 is much longer (90 min) than the one observed in Figure 5.10 (20 min). This phenomenon may be due to limited active sites on the membrane surface. The membrane was preloaded with deuterated compounds before exposing it in the sample matrix; during the exposition time, the occupied active sites were gradually released, providing space for the non-deuterated compounds to be extracted. Therefore, the equilibrium time was extended.

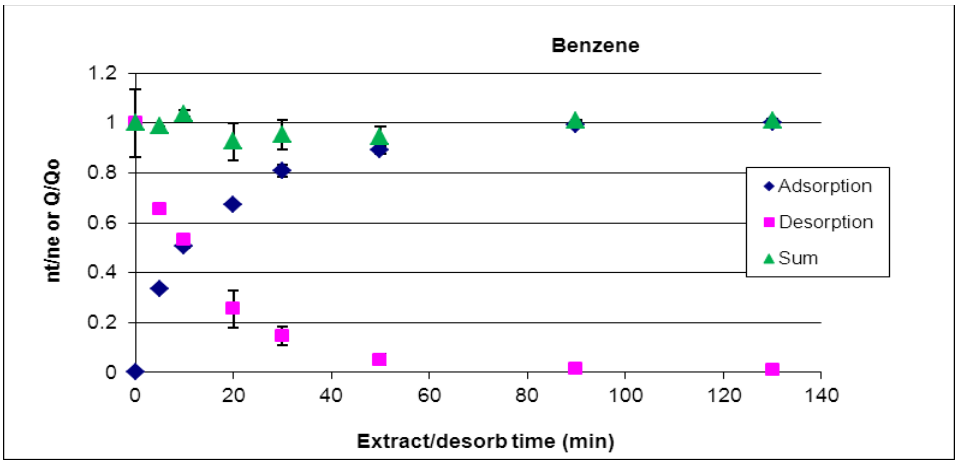

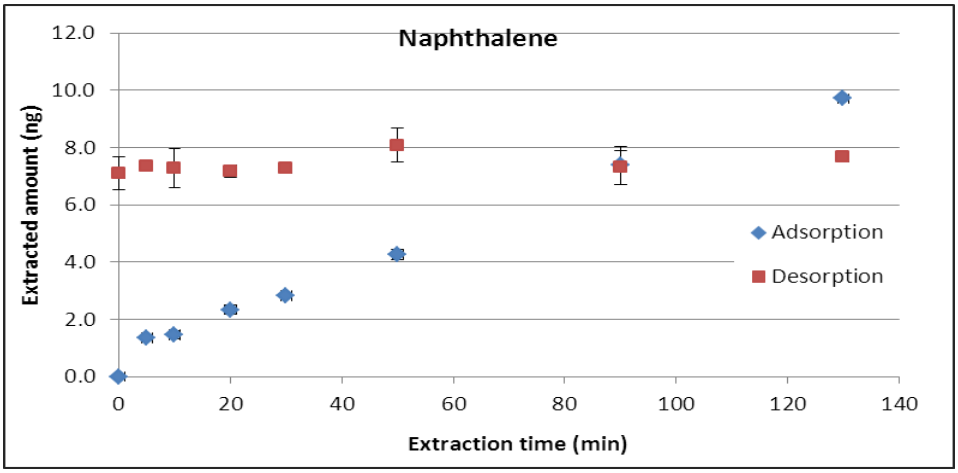

Figure 5.11 The relationship of the adsorption and desorption profiles of benzene and naphthalene

5.3.3.4.2 The diffusion-based calibration method

As previously introduced, diffusion-based calibration utilizes the linear range of an extraction process. The extraction kinetic can be expressed as $\frac{dn}{dt} = R_s C_s$ where R_s is the sampling rate that can be determined by experiments or by calculation when a proper model is used (a detailed introduction can be found in Section 1.3.5, Chapter 1).

The R_s can be experimentally determined from the slope of the initial linear range of an extraction time profile. If the concentration of the sample matrix is known, the R_s can be determined by dividing the slope over the sample matrix concentration. Two extraction time profiles were determined by sampling from the standard gases with different concentrations and sampling flow rates. The sampling rates were calculated and are shown in Table 5.6.

By calculation, a sampling model should be utilized. In this experiment, we utilized the cross-flow model proposed by Chen to determine the sampling rate [33].

The membrane in the air flow can be considered as the flow over a parallel plate with a two-dimensional, incompressible steady flow. According to the heat transfer theory, average Nusselt number, $\overline{Nu}$, in this case can be expressed as Equation 5.8 [184].

$$\overline{N_u} = 0.664 R_e^{1/2} P_r^{1/3} = \frac{\bar{h} b}{D_g} \qquad \text{Equation 5.8}$$

Where D_g is the gas-phase molecular diffusion coefficient which can be found in the literature or be estimated from the empirical equations; b is the radius of the membrane; $\bar{h}$ is the average mass-transfer coefficient; R_e is the Reynolds number ($R_e = ub/v$), u is the linear air velocity, v is the kinetic viscosity for air; P_r is the Prandtl number ($P_r = v/D_g$). The extraction amount and the concentration can be expressed as $\frac{n}{t} = \bar{h}AC_s$, in which $\bar{h}$A is the sampling rate. When sampling conditions such as air flow rate, diffusion coefficient, and sampling time are known, the sampling rate can be calculated.

In the above two naphthalene extraction time profiles, the experimental parameters are as follows: u=1.3 cm/s and 11.4 cm/s, v=0.1548 cm^2/s, b=0.6 cm, D_g=0.059 cm^2/s, so R_e= 5.04 and 44.2, P_r =2.62, $\overline{N_u} = 2.06$ and 6.09, $\bar{h} = 0.2021$ cm/s and 0.5989 cm/s, respectively. The calculated and experimental sampling rates are shown in Table 5.6. The calculated results were consistent with the experimental ones, which demonstrated that the cross-flow model can be used for the membrane air sampling quantification.

Table 5.6 Comparison of calculations with experimental results

Naphthalene	Theoritical calculation, Rs (cm^3/min)	Experimental result, Rs (cm^3/min)
Matrix #1	6.85	7.00±0.3
Matrix #2	20.3	20.6±0.5

Matrix #1: Naphthalene, 0.0018 ng/mL; sampling flow rate , 1.3 cm/s

Matrix #2: Naphthalene, 0.0033 ng/mL; sampling flow rate, 11.4 cm/s

5.3.3.5 Real sample anlaysis

The developed DVB/PDMS membrane was applied to monitor the concentration of benzene and naphthalene in traffic air. The membranes used in this experiment are 20% DVB particle membranes with a diameter of 17 mm. The samplings were conducted on a near-road site in the Waterloo region, Ontario, Canada from 7:22 am to 6:10 pm on November 7th 2012. The home-made sampling device (Figure 5.4) without the fan was used to house the membranes during sampling. Two pieces of membrane were sampled from 7:22 am to 6:10 pm. During this 11 hours sampling period, spot sampling at different time points was also conducted, and each spot sampling lasted for 1 hour. Since the GC running time was also 1 hour, only one sample per each sampling point was conducted in this experiment. The sampling temperature and air velocity were monitored using an anemometer for every 30 min. The average of three velocities and temperatures in 1 hour period was used for calculation. The equilibrium calibration method was applied for benzene sampling, and the fiber constant ($KC_{e\,max}$) was obtained from the standard gas generator using the same type of membrane at room temperature. The calibration of fiber constant at different temperatures was carried out by the following equation [4].

$$K_{T2} = K_{T1}\exp[-\frac{\Delta H}{R}\left(\frac{1}{T_2}-\frac{1}{T_1}\right)] \quad \text{Equation 5.9}$$

where K_{T1} is the fiber constant when sampling temperature is at T_1 (in degrees Kelvin), ΔH is the molar change in enthalpy of the analyte when it moves from sample to fiber coating, and R is the gas constant. The enthalpy change, ΔH, is considered constant over temperature. For volatile compounds, ΔH is approximated by the heat of vaporization of the pure compound, ΔH_{vf}.

Diffusion-based calibration was applied for naphthalene sampling. The sampling rate was calculated based on the average velocity from measurements and diffusion coefficient from literature. The diffusion coefficient is temperature dependent and can be calibrated using the following relationship [18].

$$D_T \propto T^{1.75}$$

The experimental results for both benzene and naphthalene sampling were shown in Figure 5.12. For benzene, two peak concentrations were detected during rush hours 7:22 am to 8:22 am, and 4:30 pm to 6:10 pm. Similarly, naphthalene also observed a high concentration after 4:30 pm. However, the detected concentration in the morning rush hour is not high, which may be due to the high binding efficiency of naphthalene on the air particulate, or it is an experimental error. More experiments need to be conducted to have the statistically conclusion.

Besides the spot concentration, the TWA concentration was also evaluated. Two methods were utilized for determining the TWA concentration. The first method was by averaging the spot sampling concentration. Results show that the benzene TWA concentration is 11.78 ng/L. The reported annual mean concentration of benzene in Canadian urban environmental is 0.6 to 5.5 ng/L (2003) [185]. However, the obtained concentration was much higher than the reported one, which may be due to the sampling location and the sampling time in this experiment. While the reported annual average concentration considers the whole year instead of a specific time slot, the sampling was conducted on a busy street close to a traffic light area, and on a weekday during daytime hours, when the traffic at its busiest.

For naphthalene, the TWA concentration is 0.21 ng/L using the averaging method, which is close to the reported values for outdoor air in Ontario urban area ranged from 0.008 - 0.18 ng/L [186]. Furthermore, another method for determining the TWA concentration was done by

exposing the membranes in the sampling matrix for the whole period of sampling time. The concentration was quantified base on the sampling amount and the calculated sampling rate using model described in the previous section. Result showed that both methods provide similar concentrations, which further proved the advantage of using this particle loading membrane for air sampling (Figure 5.12). By using one type of membrane, we can monitor the spot concentration and the TWA concentration at the same time.

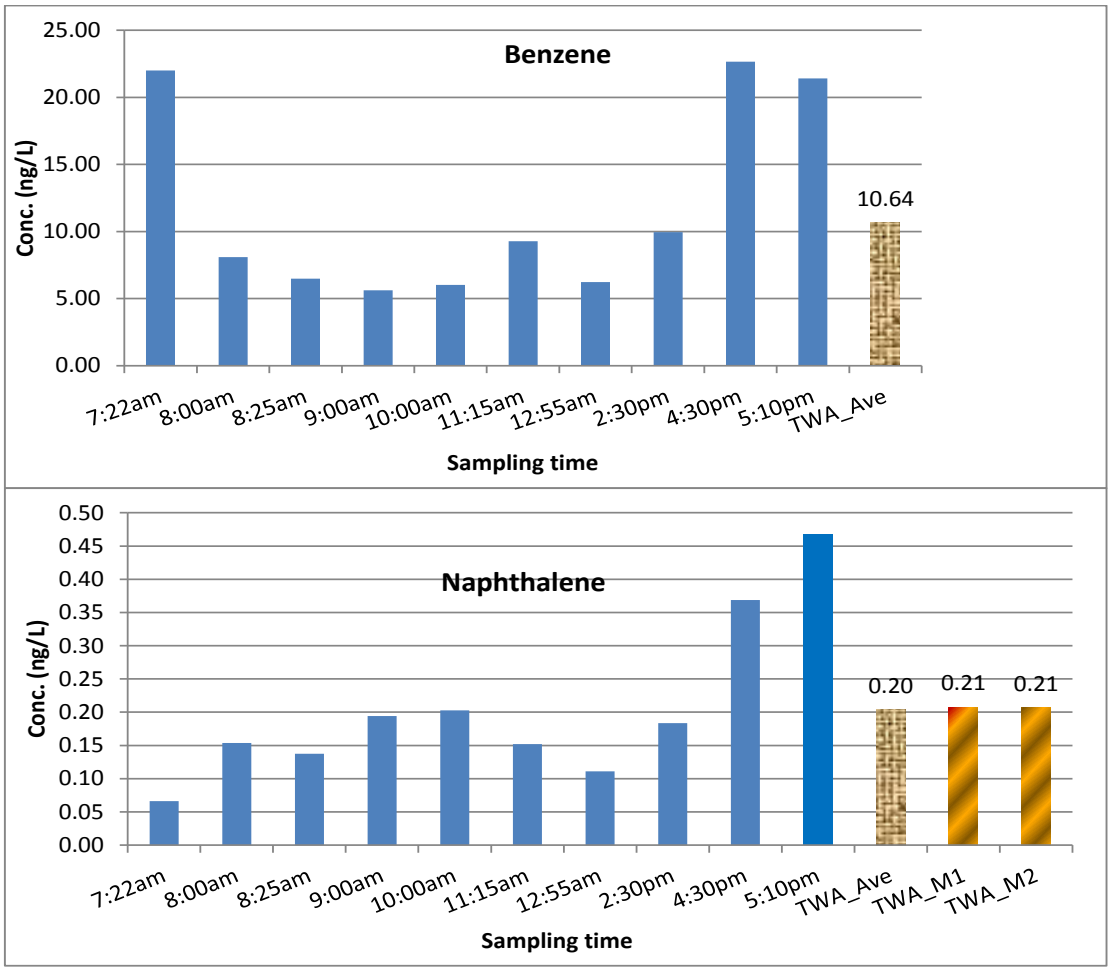

Figure 5.12 Monitoring the benzene and naphthalene concentration in traffic air.

5.4 Summary

In this project, a DVB particle loading membrane was prepared using the spread coating method. The performance of the prepared membrane was evaluated in terms of morphology, particle ratio, extraction efficiency and reproducibility. First, the SEM images of the surface and cross section of the particle loading membrane were studied, and the result showed that the DVB particles were uniformly distributed in the PDMS base, which ensured the reproducibility of this membrane sampling. Next, the extraction efficiency of the particle loading membrane for benzene sampling was improved as the particle ratio increased. However, experimental results also demonstrated that the particle ratio cannot be higher than 30%, as the PDMS cannot support the particles anymore. Following, the extraction efficiency of the DVB/PDMS membrane for outdoor air sampling was compared to a pure PDMS membrane and DVB/PDMS fiber, where enhancement on the extraction efficiency of volatile and polar compounds was observed. In addition, the high reproducibility of the DVB/PDMS membrane sampling demonstrated the advantages of the spread coating method, which allowed for quantification sampling and provided comparison results. Additionally, the proposed membrane was applied for indoor and outdoor air semi-quantification and quantification sampling. Equilibrium and diffusion-based quantification methods were proposed for sampling of the volatile and semi-volatile compounds. Results showed that the equilibrium calibration method can be used for low level air pollutant sampling when using this high capacity membrane, without a displacement effect occurring. Conversely, a diffusion-based model can be used for quantification the semi-volatile compounds. Good agreement between experimental results and theoretical calculations were observed by using this model. The proposed sampling approach can be used for monitoring the spot concentration and the TWA concentration of the outdoor air pollutants.

Chapter 6 **Summary and Future Perspectives**

In this thesis, development and investigation of four sample preparation techniques were conducted in order to further improve the sensitivity of the SPME technique based on its fundamental principles. Results showed that all the developed methods observed higher extraction capacity when compared to traditional SPME fiber sampling methods.

First, a fully automated cold fiber device coupled to the GERSTEL® MPS 2 autosampler was developed. For the first time, high throughput analysis was achieved with the use of a septumless injector, and a large number of samples (more than 200) could be analyzed without human intervention. Evaluation of the device revealed a robust and reliable automated device. The device was successfully applied in the analysis of both volatiles and semi-volatiles with varying polarities, and from different sample matrices (aqueous and solid samples). Extraction efficiency of this automated cold fiber device was much higher than the commercial PDMS fiber and cold fiber without cooling. Particularly, the cold fiber observed a unique advantage during sampling of solid samples that required high temperatures to release analytes into the headspace. Future applications of this device can be focused on the sampling of thermal stable compounds in high boiling point systems such as pollutants in sea sand, sediment, toys, clothes and crude oil, among other uses. Further improvement of the device setup is possible by completely integrating the temperature controller into the autosampler device. As well, application of the current cold fiber device configuration is limited to the types of coating that can be used; preparation of different coatings for cold fiber application is another possible approach for high affinity extraction.

Next, TFME was applied to facilitate the reproducibility and high sensitivity of skin emissions sampling. Due to the flexibility of the membrane geometry, the sampling set-up was simple and convenient. Likewise, the proposed headspace set-up minimized contamination of the fiber from the skin surface, and ensured the reproducibility of *in vivo* sampling. The stability of the samples under reasonable storage conditions and extended time periods allowed sampling and analysis to be performed in different locations. Additionally, the sampling sensitivity was found to be proportional to the size of the membrane. This result demonstrated that larger size membrane can be used to improve the extraction efficiency. Finally, the described method was applied in dietary biomarker monitoring after garlic and alcohol ingestion. The results indicated that the developed approach has potential in the clinical and forensic investigation fields, and can be applied in other skin samplings, such as plant and animal sampling.

Cooling membrane combines the advantages of TFME and cold fiber SPME to further improve the sensitivity of SPME. A detailed procedure for manufacturing this cooling membrane device was described, and the device was evaluated by three fragrance compounds representing different volatilities. The extraction mechanism of this proposed sampling device was demonstrated and proven to be consistent with the cold fiber sampling mechanism. As predicted, cooling membrane sampling obtained higher extraction efficiency for the volatile compounds when compared to thin film without cooling. However, no significant enhancement was observed on the pre-equilibrium extraction when only the extraction phase temperature was decreased. Though, a higher flow rate observed significant improvement on the pre-equilibrium extraction amount. Furthermore, humidity showed no influence on the extraction amount of both equilibrium and pre-equilibrium extraction due to the liquid property of the coating. These preliminary results indicated that the cooling membrane gas sampling approach can be used in

some circumstances where temperatures are relatively high and the analytes are found in trace level.

Following, a particle-loading membrane was prepared for high sensitivity sampling of volatile and polar compounds. This membrane provided a high extraction capacity based on the presence of solid sorbent and thin film geometry. Experimental results showed that the extraction efficiency of benzene improved more than 100 times as the DVB particle addition increased from 0% to 30%. Extraction efficiency comparisons of DVB/PDMS membrane with the DVB/PDMS fiber indicated that increasing the volume of the extraction phase dramatically improved the extraction efficiency. The proven reproducibility of the DVB/PDMS membrane sampling demonstrated the advantages of the applied membrane preparation method, and facilitated quantification sampling and comparison analysis. Furthermore, the prepared particle loading membrane was applied in indoor and outdoor air semi-quantitative and quantitative sampling. Results confirmed that the membrane can be applied for trace pollutant monitoring. Good agreement between the experimental results and theoretical calculation data confirmed the proficiency of equilibrium calibration and diffusion-based calibration methods for quantitative air sampling using the particle-loading membrane. Recommendations for future development of this technique include preparation of supported particle loading membranes and other sorbent impregnated membranes. Available results have indicated that when the particle ratio was higher than 30%, the PDMS base could not support the DVB particle, and the membrane became fragile. To overcome this issue, supported materials, such as fiber glass fabric, can be utilized to prepare a higher particle ratio membrane. Also, other solid sorbents, such as carbon materials, can be used. Above all, future applications of this high capacity particle-loading membrane are not

restricted to use in gas sampling, but may also be applied in the sampling of other sample matrices.

References

[1] G. Vas, K. Vekey, J. Mass Spectrom. 39 (2004) 233.

[2] M.D. Alpendurada, J. Chromatogr. A 889 (2000) 3.

[3] R.M. Smith, J. Chromatogr. A 1000 (2003) 3.

[4] J. Pawliszyn, Handbook of Solid Phase Microextraction. Chemical Industry Press of China, Beijing, 2009, p. 406.

[5] E. Baltussen, C. Cramers, P. Sandra, Anal. Bioanal. Chem. 373 (2002) 3.

[6] K. Demeestere, J. Dewulf, B. De Witte, H. Van Langenhove, J. Chromatogr. A 1153 (2007) 130.

[7] L. Berrueta, B. Gallo, F. Vicente, Chromatographia 40 (1995) 474.

[8] L. Ramos, J. Ramos, U.A.T. Brinkman, Anal. Bioanal. Chem. 381 (2005) 119.

[9] N.H. Snow, G.C. Slack, TrAC Trends Anal.Chem. 21 (2002) 608.

[10] M.A. Jeannot, F.F. Cantwell, Anal. Chem. 68 (1996) 2236.

[11] H. Liu, P.K. Dasgupta, Anal. Chem. 68 (1996) 1817.

[12] C.L. Arthur, J. Pawliszyn, Anal. Chem. 62 (1990) 2145.

[13] E. Psillakis, N. Kalogerakis, TrAC Trends Anal.Chem. 22 (2003) 565.

[14] S. Pedersen-Bjergaard, K.E. Rasmussen, Anal. Chem. 71 (1999) 2650.

[15] M. Rezaee, Y. Assadi, M.R. Milani Hosseini, E. Aghaee, F. Ahmadi, S. Berijani, J. Chromatogr. A 1116 (2006) 1.

[16] H. Lord, J. Pawliszyn, J. Chromatogr. A 885 (2000) 153.

[17] Z. Zhang, J. Pawliszyn, Anal. Chem. 65 (1993) 1843.

[18] J. Koziel, M. Jia, J. Pawliszyn, Anal. Chem. 72 (2000) 5178.

[19] D. Louch, S. Motlagh, J. Pawliszyn, Anal. Chem. 64 (1992) 1187.

[20] J. Pawliszyn, Solid Phase Microextraction: Theory and Practice. Wiley-Vch New York, 1997, p. 264.

[21] F. Augusto, J. Koziel, J. Pawliszyn, Anal. Chem. 73 (2001) 481.

[22] M. Chai, C.L. Arthur, J. Pawliszyn, R.P. Belardi, K.F. Pratt, Analyst 118 (1993) 1501.

[23] J.A. Koziel, M. Odziemkowski, J. Pawliszyn, Anal. Chem. 73 (2001) 47.

[24] J.A. Koziel, I. Novak, TrAC Trends Anal. Chem. 21 (2002) 840.

[25] R. Eisert, K. Levsen, J. Chromatogr. A 733 (1996) 143.

[26] G. Ouyang, J. Pawliszyn, TrAC Trends Anal. Chem. 25 (2006) 692.

[27] G. Ouyang, W. Zhao, M. Alaee, J. Pawliszyn, J. Chromatogr. A 1138 (2007) 42.
[28] G. Ouyang, J. Pawliszyn, Anal. Bioanal. Chem. 386 (2006) 1059.
[29] G. Ouyang, D. Vuckovic, J. Pawliszyn, Chem. Rev. 111 (2011) 2784.
[30] A.R. Ghiasvand, S. Hosseinzadeh, J. Pawliszyn, J. Chromatogr. A 1124 (2006) 35.
[31] J.R. Dean, S.L. Cresswell, Compr. Anal. Chem. 37 (2002) 559.
[32] M. Jia, J. Koziel, J. Pawliszyn, Field Anal. Chem. Tech. 4 (2000) 73.
[33] Y. Chen, J.A. Koziel, J. Pawliszyn, Anal. Chem. 75 (2003) 6485.
[34] M. Chai, J. Pawliszyn, Environ. Sci. Technol. 29 (1995) 693.
[35] P.A. Martos, J. Pawliszyn, Anal. Chem. 69 (1997) 206.
[36] J. Koziel, M. Jia, A. Khaled, J. Noah, J. Pawliszyn, Anal. Chim. Acta 400 (1999) 153.
[37] J. Wang, L. Tuduri, M. Mercury, M. Millet, O. Briand, M. Montury, Environ. Pollut. 157 (2009) 365.
[38] L. Van der Wal, T. Jager, R.H.L.J. Fleuren, A. Barendregt, T.L. Sinnige, C.A.M. Van Gestel, J.L.M. Hermens, Environ. Sci. Technol. 38 (2004) 4842.
[39] A.A. Boyd-Boland, J.B. Pawliszyn, J. Chromatogr. A 704 (1995) 163.
[40] V. Pino, J.H. Ayala, A.M. Afonso, V. González, Anal. Chim. Acta 477 (2003) 81.
[41] J. Carpinteiro, I. Rodriguez, R. Cela, Anal. Bioanal. Chem. 380 (2004) 853.
[42] P. Rearden, P.B. Harrington, Anal. Chim. Acta 545 (2005) 13.
[43] M.C. Wei, W.T. Chang, J.F. Jen, Anal. Bioanal. Chem. 387 (2007) 999.
[44] Z. Zhang, J. Pawliszyn, Anal. Chem. 67 (1995) 34.
[45] F. Riazi Kermani, Optimization of Solid Phase Microextraction for Determination of Disinfection By-products in Water. PhD Thesis, University of Waterloo, 2012.
[46] E.H.M. Koster, C. Crescenzi, W. den Hoedt, K. Ensing, G.J. de Jong, Anal. Chem. 73 (2001) 3140.
[47] V. Pichon, J. Chromatogr. A 1152 (2007) 41.
[48] E. Turiel, J. Tadeo, A. Martin-Esteban, Anal. Chem. 79 (2007) 3099.
[49] W.M. Mullett, P. Martin, J. Pawliszyn, Anal. Chem. 73 (2001) 2383.
[50] H. Lord, M. Rajabi, S. Safari, J. Pawliszyn, J. Pharm. Biomed. Anal. 40 (2006) 769.
[51] H.L. Lord, M. Rajabi, S. Safari, J. Pawliszyn, J. Pharm. Biomed. Anal. 44 (2007) 506.
[52] F.M. Musteata, M. Walles, J. Pawliszyn, Anal. Chim. Acta 537 (2005) 231.
[53] E. Carasek, J. Pawliszyn, J. Agric. Food Chem. 54 (2006) 8688.

[54] Y. Chen, J. Pawliszyn, Anal. Chem. 78 (2006) 5222.
[55] S.H. Haddadi, J. Pawliszyn, J. Chromatogr. A 1216 (2009) 2783.
[56] S. Gura, P. Guerra-Diaz, H. Lai, J.R. Almirall, Drug Test Anal. 1 (2009) 355.
[57] P. Guerra-Diaz, S. Gura, J.R. Almirall, Anal. Chem. 82 (2010) 2826.
[58] I. Eom, S. Risticevic, J. Pawliszyn, Anal. Chim. Acta 716 (2012) 2.
[59] Z. Qin, Thin Film Microextraction. PhD Thesis, University of Waterloo, 2010, .
[60] L. Bragg, Z. Qin, M. Alaee, J. Pawliszyn, J. Chromatogr. Sci. 44 (2006) 317.
[61] G. Ouyang, W. Zhao, L. Bragg, Z. Qin, M. Alaee, J. Pawliszyn, Environ. Sci. Technol. 41 (2007) 4026.
[62] Z. Qin, L. Bragg, G. Ouyang, J. Pawliszyn, J. Chromatogr. A 1196 (2008) 89.
[63] Z. Qin, S. Mok, G. Ouyang, D.G. Dixon, J. Pawliszyn, Anal. Chim. Acta 667 (2010) 71.
[64] F. Wei, F. Zhang, H. Liao, X. Dong, Y. Li, H. Chen, J. Sep. Sci. 34 (2011) 331.
[65] X. Li, H. Wang, W. Sun, L. Ding, Anal. Chem. 82 (2010) 9188.
[66] T.A. Sergeyeva, H. Matuschewski, S.A. Piletsky, J. Bendig, U. Schedler, M. Ulbricht, J. Chromatogr. A 907 (2001) 89.
[67] Y.L. Hu, Y.Y. Yang, J.X. Huang, G.K. Li, Anal. Chim. Acta 543 (2005) 17.
[68] F. Riazi Kermani, J. Pawliszyn, Anal. Chem. 84 (2012) 8990.
[69] Z. Qin, L. Bragg, G. Ouyang, V.H. Niri, J. Pawliszyn, J. Chromatogr. A 1216 (2009) 6979.
[70] I. Bruheim, X. Liu, J. Pawliszyn, Anal. Chem. 75 (2003) 1002.
[71] F. Sánchez-Rojas, C. Bosch-Ojeda, J.M. Cano-Pavón, Chromatographia 69 (2009) 79.
[72] J.B. Wilcockson, F.A.P.C. Gobas, Environ. Sci. Technol. 35 (2001) 1425.
[73] C.J. Golding, F.A.P.C. Gobas, G.F. Birch, Environ. Toxicol. Chem. 26 (2007) 829.
[74] L.M. Meloche, A.M.H. Debruyn, S. Otton, M.G. Ikonomou, F.A.P.C. Gobas, Environ. Toxicol. Chem. 28 (2009) 247.
[75] S. Sisalli, A. Adao, M. Lebel, I. Le Fur, P. Sandra, LC-GC Europe 19 (2006) 33.
[76] S. Riazanskaia, G. Blackburn, M. Harker, D. Taylor, C. Thomas, Analyst 133 (2008) 1020.
[77] A.N. Thomas, S. Riazanskaia, W. Cheung, Y. Xu, R. Goodacre, C. Thomas, M.S. Baguneid, A. Bayat, Wound Repair Regen. 18 (2010) 391.
[78] R. Jiang, J. Pawliszyn, Trends Anal. Chem. 39 (2012) 245.
[79] S.A. Merschman, S.H. Lubbad, D.C. Tilotta, J. Chromatogr. A 829 (1998) 377.
[80] D.L. Heglund, D.C. Tilotta, Environ. Sci. Technol. 30 (1996) 1212.

[81] B.L. Wittkamp, S.B. Hawthorne, D.C. Tilotta, Anal. Chem. 69 (1997) 1197.

[82] H. Bagheri, A. Aghakhani, M. Akbari, Z. Ayazi, Anal. Bioanal. Chem.(2011) 1.

[83] H. Bagheri, A. Aghakhani, Anal. Chim. Acta 713 (2012) 63.

[84] C. Bicchi, C. Cordero, E. Liberto, P. Rubiolo, B. Sgorbini, P. Sandra, J. Chromatogr. A 1148 (2007) 137.

[85] Y. Sekine, S. Toyooka, S.F. Watts, J. Chromatogr. B 859 (2007) 201.

[86] A. Jahnke, P. Mayer, D. Broman, M.S. McLachlan, Chemosphere 77 (2009) 764.

[87] F. Wei, J. Cheng, S. Liu, J. Huang, Z. Wang, X. Dong, P. Li, F. Kong, Y. Wu, Y. Li, Phytochem. Anal. 21 (2010) 290.

[88] P. Guerra, H. Lai, J.R. Almirall, J. Sep. Sci. 31 (2008) 2891.

[89] M. Mattarozzi, F. Bianchi, F. Bisceglie, M. Careri, A. Mangia, G. Mori, A. Gregori, Anal. Bioanal. Chem. 399 (2011) 2741.

[90] G. Ouyang, J. Pawliszyn, Anal. Chim. Acta 627 (2008) 184.

[91] L.M. Ravelo-Pérez, J. Hernández-Borges, T.M. Borges-Miquel, M.Á Rodríguez-Delgado, Electrophoresis 28 (2007) 4072.

[92] K. Saito, K. Okamura, H. Kataoka, J. Chromatogr. A 1186 (2008) 434.

[93] K. Mitani, M. Fujioka, A. Uchida, H. Kataoka, J. Chromatogr. A 1146 (2007) 61.

[94] N.C. Bouvier-Brown, R. Holzinger, K. Palitzsch, A.H. Goldstein, J. Chromatogr. A 1161 (2007) 113.

[95] S.N. Zhou, G. Ouyang, J. Pawliszyn, J. Chromatogr. A 1196 (2008) 46.

[96] L.S. De Jager, G.A. Perfetti, G.W. Diachenko, J. Chromatogr. A 1192 (2008) 36.

[97] L. Carrasco, S. Díez, J.M. Bayona, J. Chromatogr. A 1174 (2007) 2.

[98] N. Campillo, R. Peñalver, M. Hernández-Córdoba, J. Chromatogr. A 1125 (2006) 31.

[99] J. Iglesias, I. Medina, J. Chromatogr. A 1192 (2008) 9.

[100] L.K. Silva, C.R. Wilburn, M.A. Bonin, M.M. Smith, K.A. Reese, D.L. Ashley, B.C. Blount, J. Anal. Toxicol. 32 (2008) 273.

[101] B. Plutowska, W. Wardencki, Anal. Chim. Acta 613 (2008) 64.

[102] A. Sánchez, S. Millán, M.C. Sampedro, N. Unceta, E. Rodríguez, M.A. Goicolea, R.J. Barrio, J. Chromatogr. A 1177 (2008) 170.

[103] P.A. Martos, A. Saraullo, J. Pawliszyn, Anal. Chem. 69 (1997) 402.

[104] S. Isetun, U. Nilsson, A. Colmsjö, Anal. Bioanal. Chem. 380 (2004) 319.

[105] S. Isetun, U. Nilsson, Analyst 130 (2004) 94.
[106] J. Zeng, J. Chen, Z. Lin, W. Chen, X. Chen, X. Wang, Anal. Chim. Acta 619 (2008) 59.
[107] B. Shurmer, J. Pawliszyn, Anal. Chem. 72 (2000) 3660.
[108] P. Mayer, W.H.J. Vaes, J.L.M. Hermens, Anal. Chem. 72 (2000) 459.
[109] M. Polo, V. Casas, M. Llompart, C. García-Jares, R. Cela, J. Chromatogr. A 1124 (2006) 121.
[110] T. Zimmermann, W.J. Ensinger, T.C. Schmidt, J. Chromatogr. A 1102 (2006) 51.
[111] U. Kotowska, K. Garbowska, V.A. Isidorov, Anal. Chim. Acta 560 (2006) 110.
[112] P.A. Martos, J. Pawliszyn, Anal. Chem. 71 (1999) 1513.
[113] Y. Chen, J. Pawliszyn, Anal. Chem. 75 (2003) 2004.
[114] A. Khaled, J. Pawliszyn, J. Chromatogr. A 892 (2000) 455.
[115] Y. Chen, J. O'Reilly, Y. Wang, J. Pawliszyn, Analyst 129 (2004) 702.
[116] Y. Chen, J. Pawliszyn, Anal. Chem. 76 (2004) 5807.
[117] S.N. Zhou, W. Zhao, J. Pawliszyn, Anal. Chem. 80 (2008) 481.
[118] X. Zhang, A. Es-haghi, F.M. Musteata, G. Ouyang, J. Pawliszyn, Anal. Chem. 79 (2007) 4507.
[119] X. Zhang, A. Es-haghi, J. Cai, J. Pawliszyn, J. Chromatogr. A 1216 (2009) 7664.
[120] W. Zhao, G. Ouyang, M. Alaee, J. Pawliszyn, J. Chromatogr. A 1124 (2006) 112.
[121] G. Ouyang, W. Zhao, J. Pawliszyn, Anal. Chem. 77 (2005) 8122.
[122] A.R. Ghiasvand, L. Setkova, J. Pawliszyn, Flavour Frag. J 22 (2007) 377.
[123] S.H. Haddadi, V.H. Niri, J. Pawliszyn, Anal. Chim. Acta 652 (2009) 224.
[124] E. Carasek, E. Cudjoe, J. Pawliszyn, J. Chromatogr. A 1138 (2007) 10.
[125] F. Kanda, E. Yagi, M. Fukuda, K. Nakajima, T. Ohta, O. Nakata, Br. J. Dermatol. 122 (1990) 771.
[126] S. Haze, Y. Gozu, S. Nakamura, Y. Kohno, K. Sawano, H. Ohta, K. Yamazaki, J. Invest. Dermatol. 116 (2001) 520.
[127] N. Yamane, T. Tsuda, K. Nose, A. Yamamoto, H. Ishiguro, T. Kondo, Clinica Chimica Acta 365 (2006) 325.
[128] K. Yamai, T. Funada, T. Ohkuwa, H. Itoh, T. Tsuda, Clin. Chim. Acta 28 (2012) 511.
[129] U.R. Bernier, M.M. Booth, R.A. Yost, Anal. Chem. 71 (1999) 1.

[130] U.R. Bernier, D.L. Kline, D.R. Barnard, C.E. Schreck, R.A. Yost, Anal. Chem. 72 (2000) 747.

[131] Z.M. Zhang, J.J. Cai, G.H. Ruan, G.K. Li, J. Chromatogr. B 822 (2005) 244.

[132] B.D. Mookherjee, S. Patel, R.W. Trenkle, R.A. Wilson, Perfum. Flavor. 23 (1998) 1.

[133] C. Zouboulis, W.C. Chen, M. Thornton, K. Qin, R. Rosenfield, Hormone Metabol. Res. 39 (2007) 85.

[134] T. Abaffy, R. Duncan, D.D. Riemer, O. Tietje, G. Elgart, C. Milikowski, R.A. DeFazio, PloS One 5 (2010) e13813.

[135] T. Abaffy, M. Möller, D.D. Riemer, C. Milikowski, R.A. DeFazio, J. Cancer Res. 3 (2011) 140.

[136] S.K. Pandey, K.H. Kim, TrAC Trends Anal. Chem. 30 (2011) 784.

[137] M. Gallagher, C. Wysocki, J. Leyden, A. Spielman, X. Sun, G. Preti, Br. J. Dermatol. 159 (2008) 780.

[138] X. Zeng, J.J. Leyden, H.J. Lawley, K. Sawano, I. Nohara, G. Preti, J. Chem. Ecol. 17 (1991) 1469.

[139] A. Natsch, S. Derrer, F. Flachsmann, J. Schmid, Chem. Biodivers. 3 (2006) 1.

[140] A.M. Curran, C.F. Ramirez, A.A. Schoon, K.G. Furton, J. Chromatogr. B 846 (2007) 86.

[141] U.R. Bernier, D.L. Kline, S.A. Allan, D.R. Barnard, J. Am. Mosq. Control Assoc. 23 (2007) 288.

[142] H.A. Soini, K.E. Bruce, I. Klouckova, R.G. Brereton, D.J. Penn, M.V. Novotny, Anal. Chem. 78 (2006) 7161.

[143] H.A. Soini, K.E. Bruce, D. Wiesler, F. David, P. Sandra, M.V. Novotny, J. Chem. Ecol. 31 (2005) 377.

[144] A.M. Curran, S.I. Rabin, P.A. Prada, K.G. Furton, J. Chem. Ecol. 31 (2005) 1607.

[145] S. Riazanskaia, G. Blackburn, M. Harker, D. Taylor, C. Thomas, Analyst 133 (2008) 1020.

[146] C. Bicchi, C. Cordero, E. Liberto, P. Rubiolo, B. Sgorbini, P. Sandra, J. Chromatogr. A 1148 (2007) 137.

[147] W. Zhao, G. Ouyang, J. Pawliszyn, Analyst 132 (2007) 256.

[148] S. Sisalli, A. Adao, M. Lebel, I. Le Fur, P. Sandra, LCGC EUROPE 19 (2006) .

[149] P. Lenochova, S.C. Roberts, J. Havlicek, Chem. Senses 34 (2009) 127.

[150] D.K. Singh, V.K. Singh, Annu Rev Biomed Sci 10 (2008) 6.

[151] D.L. Layman, S.W. Jacob, Life Sci. 37 (1985) 2431.

[152] E. Germain, J. Auger, C. Ginies, M.H. Siess, C. Teyssier, Xenobiotica 32 (2002) 1127.

[153] H. Winning, E. Roldán-Marín, L.O. Dragsted, N. Viereck, M. Poulsen, C. Sánchez-Moreno, M.P. Cano, S.B. Engelsen, Analyst 134 (2009) 2344.

[154] F. Freeman, Y. Kodera, J. Agric. Food Chem. 43 (1995) 2332.

[155] T. Minami, T. Boku, K. Inada, M. Morita, Y. Okazaki, J. Food Sci. 54 (1989) 763.

[156] P.K. Wilkinson, A.J. Sedman, E. Sakmar, D.R. Kay, J.G. Wagner, J. Pharmacokinet. Biopharm. 5 (1977) 207.

[157] M. Gallagher, C. Wysocki, J. Leyden, A. Spielman, X. Sun, G. Preti, Br. J. Dermatol. 159 (2008) 780.

[158] S. Krol, B. Zabiegala, J. Namiesnik, TrAC Trends Anal. Chem. 29 (2010) 1092.

[159] E. Woolfenden, J. Chromatogr. A 1217 (2010) 2674.

[160] E. Woolfenden, J. Chromatogr. A 1217 (2010) 2685.

[161] M. Harper, J. Chromatogr. A 885 (2000) 129.

[162] http://www.osha.gov/dts/sltc/methods/organic/org012/org012.html, .

[163] M. Rosa Ras, F. Borrull, R. Maria Marce, TrAC Trends Anal. Chem. 28 (2009) 347.

[164] C.Y. Peng, S. Batterman, J. Environ. Monitor. 2 (2000) 313.

[165] V. Camel, M. Caude, J. Chromatogr. A 710 (1995) 3.

[166] K.H. Kim, D. Kim, Microchem. J. 91 (2009) 16.

[167] J.A. Koziel, P.A. Martos, J. Pawliszyn, J. Chromatogr. A 1025 (2004) 3.

[168] T. Górecki, X. Yu, J. Pawliszyn, Analyst 124 (1999) 643.

[169] F.M. Musteata, J. Pawliszyn, J. Proteome Res. 4 (2005) 789.

[170] I. Liska, J. Krupcik, P.A. Leclercq, Hrc-J. High, Res. Chrom. 12 (1989) 577.

[171] A. Jomekian, M. Pakizeh, A.R. Shafiee, S.A.A. Mansoori, Sep. Purif. Technol. 80 (2011) 556.

[172] E. Cudjoe, D. Vuckovic, D. Hein, J. Pawliszyn, Anal. Chem. 81 (2009) 4226.

[173] F.S. Mirnaghi, M.R.N. Monton, J. Pawliszyn, J. Chromatogr. A(2011) .

[174] F.S. Mirnaghi, Y. Chen, L.M. Sidisky, J. Pawliszyn, Anal. Chem. 83 (2011) 6018.

[175] http://webbook.nist.gov/chemistry/, .

[176] M. Aksoy, Am. J. Ind. Med. 7 (1985) 395.

[177] D.C. Glass, C.N. Gray, D.J. Jolley, C. Gibbons, M.R. Sim, L. Fritschi, G.G. Adams, J.A. Bisby, R. Manuell, Epidemiology 14 (2003) 569.

[178] N.J. Vianna, A. Polan, Lancet 1 (1979) 1394.

[179] S.J. Stohs, S. Ohia, D. Bagchi, Toxicology 180 (2002) 97.

[180] K.M. Abdo, S. Grumbein, B.J. Chou, R. Herbert, Inhal. Toxicol. 13 (2001) 931.

[181] M.M. Rhead, R.D. Pemberton, Energ. Fuel. 10 (1996) 837.

[182] J.M. Dasch, R.L. Williams, Environ. Sci. Technol. 25 (1991) 853.

[183] G.J. Nebel, J. Air Pollut. Control Assoc. 29 (1979) 391.

[184] C.P. Kothandaraman, Fundamentals Of Heat And Mass Transfer. New Age International (P) Ltd., 2006, .

[185] http://www.ccme.ca/assets/pdf/ambient_air_benzene03.pdf, .

[186] C. Jia, S. Batterman, Int. J. Environ. Res. Publ. Health 7 (2010) 2903.

Appendix

Reproduce permission for two published papers in this thesis:

ELSEVIER LICENSE
TERMS AND CONDITIONS

Mar 03, 2013

This is a License Agreement between Ruifen Jiang ("You") and Elsevier ("Elsevier") provided by Copyright Clearance Center ("CCC"). The license consists of your order details, the terms and conditions provided by Elsevier, and the payment terms and conditions.

All payments must be made in full to CCC. For payment instructions, please see information listed at the bottom of this form.

Supplier	Elsevier Limited The Boulevard,Langford Lane Kidlington,Oxford,OX5 1GB,UK
Registered Company Number	1982084
Customer name	Ruifen Jiang
Customer address	1-161 University Avenue East Waterloo, ON N2J2W4
License number	3101400822393
License date	Mar 03, 2013
Licensed content publisher	Elsevier
Licensed content publication	Analytica Chimica Acta
Licensed content title	Evaluation of a completely automated cold fiber device using compounds with varying volatility and polarity
Licensed content author	Ruifen Jiang,Eduardo Carasek,Sanja Risticevic,Erasmus Cudjoe,Jamie Warren,Janusz Pawliszyn
Licensed content date	12 September 2012
Licensed content volume number	742
Licensed content issue number	
Number of pages	8
Start Page	22
End Page	29
Type of Use	reuse in a thesis/dissertation
Portion	full article
Format	both print and electronic
Are you the author of this Elsevier article?	Yes
Will you be translating?	No
Order reference number	

ELSEVIER LICENSE
TERMS AND CONDITIONS

Mar 03, 2013

This is a License Agreement between Ruifen Jiang ("You") and Elsevier ("Elsevier") provided by Copyright Clearance Center ("CCC"). The license consists of your order details, the terms and conditions provided by Elsevier, and the payment terms and conditions.

All payments must be made in full to CCC. For payment instructions, please see information listed at the bottom of this form.

Supplier	Elsevier Limited The Boulevard,Langford Lane Kidlington,Oxford,OX5 1GB,UK
Registered Company Number	1982084
Customer name	Ruifen Jiang
Customer address	1-161 University Avenue East Waterloo, ON N2J2W4
License number	3101401188073
License date	Mar 03, 2013
Licensed content publisher	Elsevier
Licensed content publication	TrAC Trends in Analytical Chemistry
Licensed content title	Thin-film microextraction offers another geometry for solid-phase microextraction
Licensed content author	Ruifen Jiang,Janusz Pawliszyn
Licensed content date	October 2012
Licensed content volume number	39
Licensed content issue number	
Number of pages	9
Start Page	245
End Page	253
Type of Use	reuse in a thesis/dissertation
Intended publisher of new work	other
Portion	full article
Format	both print and electronic
Are you the author of this Elsevier article?	Yes
Will you be translating?	No

Reprinted permission for figure 1.3:

ELSEVIER LICENSE
TERMS AND CONDITIONS

Apr 16, 2013

This is a License Agreement between Ruifen Jiang ("You") and Elsevier ("Elsevier") provided by Copyright Clearance Center ("CCC"). The license consists of your order details, the terms and conditions provided by Elsevier, and the payment terms and conditions.

All payments must be made in full to CCC. For payment instructions, please see information listed at the bottom of this form.

Supplier	Elsevier Limited The Boulevard,Langford Lane Kidlington,Oxford,OX5 1GB,UK
Registered Company Number	1982084
Customer name	Ruifen Jiang
Customer address	1-161 University Avenue East Waterloo, ON N2J2W4
License number	3130961000425
License date	Apr 16, 2013
Licensed content publisher	Elsevier
Licensed content publication	Journal of Chromatography A
Licensed content title	Evolution of solid-phase microextraction technology
Licensed content author	Heather Lord,Janusz Pawliszyn
Licensed content date	14 July 2000
Licensed content volume number	885
Licensed content issue number	1–2
Number of pages	41
Start Page	153
End Page	193
Type of Use	reuse in a thesis/dissertation
Intended publisher of new work	other
Portion	figures/tables/illustrations
Number of figures/tables /illustrations	1
Format	both print and electronic
Are you the author of this Elsevier article?	No
Will you be translating?	No
Order reference number	

Reproduce permission for figure 1.5:

ELSEVIER LICENSE
TERMS AND CONDITIONS

Apr 16, 2013

This is a License Agreement between Ruifen Jiang ("You") and Elsevier ("Elsevier") provided by Copyright Clearance Center ("CCC"). The license consists of your order details, the terms and conditions provided by Elsevier, and the payment terms and conditions.

All payments must be made in full to CCC. For payment instructions, please see information listed at the bottom of this form.

Supplier	Elsevier Limited The Boulevard,Langford Lane Kidlington,Oxford,OX5 1GB,UK
Registered Company Number	1982084
Customer name	Ruifen Jiang
Customer address	1-161 University Avenue East Waterloo, ON N2J2W4
License number	3130930226264
License date	Apr 16, 2013
Licensed content publisher	Elsevier
Licensed content publication	TrAC Trends in Analytical Chemistry
Licensed content title	Sampling and sample-preparation strategies based on solid-phase microextraction for analysis of indoor air
Licensed content author	Jacek A. Koziel,Inman Novak
Licensed content date	December 2002
Licensed content volume number	21
Licensed content issue number	12
Number of pages	11
Start Page	840
End Page	850
Type of Use	reuse in a thesis/dissertation
Intended publisher of new work	other
Portion	figures/tables/illustrations
Number of figures/tables /illustrations	1
Format	both print and electronic
Are you the author of this Elsevier article?	No
Will you be translating?	No
Order reference number	

Reproduce permission for figure 1.6

JOHN WILEY AND SONS LICENSE TERMS AND CONDITIONS

Apr 16, 2013

This is a License Agreement between Ruifen Jiang ("You") and John Wiley and Sons ("John Wiley and Sons") provided by Copyright Clearance Center ("CCC"). The license consists of your order details, the terms and conditions provided by John Wiley and Sons, and the payment terms and conditions.

All payments must be made in full to CCC. For payment instructions, please see information listed at the bottom of this form.

License Number	3130940292840
License date	Apr 16, 2013
Licensed content publisher	John Wiley and Sons
Licensed content publication	Field Analytical Chemistry and Technology
Licensed content title	Fast field sampling/sample preparation and quantification of volatile organic compounds in indoor air by solid-phase microextraction and portable gas chromatography
Licensed copyright line	Copyright © 2000 John Wiley & Sons, Inc.
Licensed content author	Mingyu Jia,Jacek Koziel,Janusz Pawliszyn
Licensed content date	Sep 18, 2000
Start page	73
End page	84
Type of use	Dissertation/Thesis
Requestor type	University/Academic
Format	Print and electronic
Portion	Figure/table
Number of figures/tables	1
Original Wiley figure/table number(s)	Figure 2
Will you be translating?	No
Total	0.00 USD
Terms and Conditions	

Reproduce permission for figure 1.10:

ELSEVIER LICENSE
TERMS AND CONDITIONS

Apr 16, 2013

This is a License Agreement between Ruifen Jiang ("You") and Elsevier ("Elsevier") provided by Copyright Clearance Center ("CCC"). The license consists of your order details, the terms and conditions provided by Elsevier, and the payment terms and conditions.

All payments must be made in full to CCC. For payment instructions, please see information listed at the bottom of this form.

Supplier	Elsevier Limited The Boulevard,Langford Lane Kidlington,Oxford,OX5 1GB,UK
Registered Company Number	1982084
Customer name	Ruifen Jiang
Customer address	1-161 University Avenue East Waterloo, ON N2J2W4
License number	3130940880072
License date	Apr 16, 2013
Licensed content publisher	Elsevier
Licensed content publication	Journal of Chromatography A
Licensed content title	Comparison of thin-film microextraction and stir bar sorptive extraction for the analysis of polycyclic aromatic hydrocarbons in aqueous samples with controlled agitation conditions
Licensed content author	Zhipei Qin,Leslie Bragg,Gangfeng Ouyang,Janusz Pawliszyn
Licensed content date	4 July 2008
Licensed content volume number	1196–1197
Licensed content issue number	
Number of pages	7
Start Page	89
End Page	95
Type of Use	reuse in a thesis/dissertation
Intended publisher of new work	other
Portion	figures/tables/illustrations
Number of figures/tables /illustrations	1
Format	both print and electronic
Are you the author of this Elsevier article?	No
Will you be translating?	No

Reproduce permission for figure 1.9 and figure 2,1

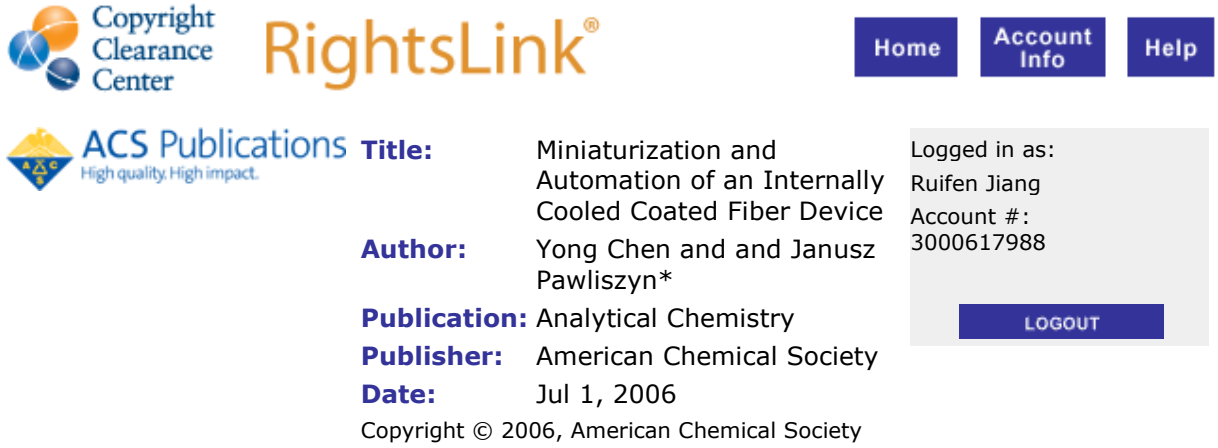

PERMISSION/LICENSE IS GRANTED FOR YOUR ORDER AT NO CHARGE

This type of permission/license, instead of the standard Terms & Conditions, is sent to you because no fee is being charged for your order. Please note the following:

- Permission is granted for your request in both print and electronic formats, and translations.
- If figures and/or tables were requested, they may be adapted or used in part.
- Please print this page for your records and send a copy of it to your publisher/graduate school.
- Appropriate credit for the requested material should be given as follows: "Reprinted (adapted) with permission from (COMPLETE REFERENCE CITATION). Copyright (YEAR) American Chemical Society." Insert appropriate information in place of the capitalized words.
- One-time permission is granted only for the use specified in your request. No additional uses are granted (such as derivative works or other editions). For any other uses, please submit a new request.

If credit is given to another source for the material you requested, permission must be obtained from that source.

BACK CLOSE WINDOW

Reproduce permission for figure 2,2:

ELSEVIER LICENSE
TERMS AND CONDITIONS

Apr 16, 2013

This is a License Agreement between Ruifen Jiang ("You") and Elsevier ("Elsevier") provided by Copyright Clearance Center ("CCC"). The license consists of your order details, the terms and conditions provided by Elsevier, and the payment terms and conditions.

All payments must be made in full to CCC. For payment instructions, please see information listed at the bottom of this form.

Supplier	Elsevier Limited The Boulevard,Langford Lane Kidlington,Oxford,OX5 1GB,UK
Registered Company Number	1982084
Customer name	Ruifen Jiang
Customer address	1-161 University Avenue East Waterloo, ON N2J2W4
License number	3130941114020
License date	Apr 16, 2013
Licensed content publisher	Elsevier
Licensed content publication	Journal of Chromatography A
Licensed content title	New cold-fiber headspace solid-phase microextraction device for quantitative extraction of polycyclic aromatic hydrocarbons in sediment
Licensed content author	Ali Reza Ghiasvand,Shokouh Hosseinzadeh,Janusz Pawliszyn
Licensed content date	18 August 2006
Licensed content volume number	1124
Licensed content issue number	1–2
Number of pages	8
Start Page	35
End Page	42
Type of Use	reuse in a thesis/dissertation
Intended publisher of new work	other
Portion	figures/tables/illustrations
Number of figures/tables /illustrations	1
Format	both print and electronic
Are you the author of this Elsevier article?	No
Will you be translating?	No

Reproduce permission for figure 3.1:

ELSEVIER LICENSE
TERMS AND CONDITIONS

Apr 16, 2013

This is a License Agreement between Ruifen Jiang ("You") and Elsevier ("Elsevier") provided by Copyright Clearance Center ("CCC"). The license consists of your order details, the terms and conditions provided by Elsevier, and the payment terms and conditions.

All payments must be made in full to CCC. For payment instructions, please see information listed at the bottom of this form.

Supplier	Elsevier Limited The Boulevard,Langford Lane Kidlington,Oxford,OX5 1GB,UK
Registered Company Number	1982084
Customer name	Ruifen Jiang
Customer address	1-161 University Avenue East Waterloo, ON N2J2W4
License number	3130920020669
License date	Apr 16, 2013
Licensed content publisher	Elsevier
Licensed content publication	Journal of Chromatography B
Licensed content title	Determination of acetaldehyde and acetone emanating from human skin using a passive flux sampler—HPLC system
Licensed content author	Yoshika Sekine,Satomi Toyooka,Simon F. Watts
Licensed content date	15 November 2007
Licensed content volume number	859
Licensed content issue number	2
Number of pages	7
Start Page	201
End Page	207
Type of Use	reuse in a thesis/dissertation
Intended publisher of new work	other
Portion	figures/tables/illustrations
Number of figures/tables /illustrations	1
Format	both print and electronic
Are you the author of this Elsevier article?	No
Will you be translating?	No
Order reference number	

ELSEVIER LICENSE
TERMS AND CONDITIONS

Apr 16, 2013

This is a License Agreement between Ruifen Jiang ("You") and Elsevier ("Elsevier") provided by Copyright Clearance Center ("CCC"). The license consists of your order details, the terms and conditions provided by Elsevier, and the payment terms and conditions.

All payments must be made in full to CCC. For payment instructions, please see information listed at the bottom of this form.

Supplier	Elsevier Limited The Boulevard,Langford Lane Kidlington,Oxford,OX5 1GB,UK
Registered Company Number	1982084
Customer name	Ruifen Jiang
Customer address	1-161 University Avenue East Waterloo, ON N2J2W4
License number	3130911373331
License date	Apr 16, 2013
Licensed content publisher	Elsevier
Licensed content publication	Journal of Chromatography A
Licensed content title	Sorptive tape extraction in the analysis of the volatile fraction emitted from biological solid matrices
Licensed content author	C. Bicchi,C. Cordero,E. Liberto,P. Rubiolo,B. Sgorbini,P. Sandra
Licensed content date	4 May 2007
Licensed content volume number	1148
Licensed content issue number	2
Number of pages	8
Start Page	137
End Page	144
Type of Use	reuse in a thesis/dissertation
Intended publisher of new work	other
Portion	figures/tables/illustrations
Number of figures/tables /illustrations	1
Format	both print and electronic
Are you the author of this Elsevier article?	No
Will you be translating?	No
Order reference number	